

**Hanford 200 Areas Spectral Gamma
Baseline Characterization Project**

**216-B-5 Injection Well and
216-B-9 Crib & Tile Field
Waste Site Summary Report**

November 2002



**U.S. Department
of Energy**

GRAND JUNCTION OFFICE

**Hanford 200 Areas Spectral Gamma Baseline
Characterization Project**

**216-B-5 Injection Well and 216-B-9 Crib & Tile Field
Waste Site Summary Report**

November 2002

Prepared for
U.S. Department of Energy
Idaho Operations Office
Grand Junction Office
Grand Junction, Colorado

Prepared by
S.M. Stoller Corp.
Grand Junction Office
Grand Junction, Colorado

Approved for public release; distribution is unlimited.
Work performed under DOE Contract No. DE-AC13-02GJ79491.

Contents

	Page
Signature Page.....	vi
Executive Summary	vii
1.0 Introduction	1
1.1 Background.....	1
1.2 Purpose and Scope of Project	1
1.3 Project Objectives	2
2.0 Spectral Gamma-Ray Logging Methods.....	3
2.1 Field Methods	3
2.2 Technical Methods.....	4
3.0 Background and Physical Setting of the 216-B-5 Injection Well, 216-B-9 Crib & Tile Field, and Adjacent Sites	7
3.1 Background of the 200 Areas	7
3.2 Geologic Conditions	8
3.2.1 Stratigraphy.....	8
3.2.1.1 Columbia River Basalt Group.....	8
3.2.1.2 Ringold Formation.....	9
3.2.1.3 Plio-Pleistocene Sediments.....	9
3.2.1.4 Hanford Formation.....	9
3.2.1.5 Holocene Surficial Deposits	10
3.2.2 Structure.....	11
3.3 Hydrology	11
3.4 Description of the 216-B-5 Injection Well, 216-B-9 Crib & Tile Field, and Adjacent Sites.....	12
3.5 Operational History.....	14
3.6 Previous Investigations	15
4.0 Logging Results.....	18
4.1 Boreholes and Wells Logged	18
4.2 Radionuclides Detected	20
4.2.1 Cs-137	21
4.2.2 Co-60.....	21
4.2.3 U-235/238.....	21
5.0 Interpretation of Results.....	21
5.1 Geophysical Correlation	22
5.2 Development of the Visualizations.....	23
5.2.1 Development of the Interpreted Data Set.....	23

Contents (continued)

	Page
5.2.2 Visualizations.....	25
5.3 Distribution of Man-Made Radionuclides	26
5.3.1 216-B-5 Injection Well	26
5.3.2 216-B-9 Crib and Tile Field.....	27
5.3.3 Adjacent Waste Sites	29
5.3.4 ⁶⁰ Co Contamination Below Groundwater Level.....	29
5.4 Comparison to Prior Spectral Gamma Logging.....	30
5.5 Potential Uncertainties and Inaccuracies	30
6.0 Conclusions	30
7.0 Recommendations	32

List of Figures

Figure 1. Hanford Site and Area Designations	35
2. Map of B Plant Waste Disposal Sites Showing the Locations of the 216-B-5 Injection Well and 216-B-9 Crib & Tile Field	36
3. Map of the 216-B-5 Injection Well, 216-B-9 Crib & Tile Field, and Adjacent Waste Sites, Boreholes, and Cross Sections.....	37
4. General Stratigraphy of the 216-B-5 Injection Well and 216-B-9 Crib & Tile Field ...	38
5. View of the Ground Surface at the 216-B-5 Injection Well from the East	39
6. View of the Ground Surface at the 216-B-9 Crib and Tile Field from the South	40
7. Distribution of Radionuclides in Groundwater in the Vicinity of the 216-B-5 Injection Well	41
8. Distribution of ²³⁹⁻²⁴⁰ Pu near the 216-B-5 Injection Well	42
9. Distribution of ⁹⁰ Sr near the 216-B-5 Injection Well	43
10. Distribution of ¹³⁷ Cs in Groundwater near the 216-B-5 Injection Well	44
11. Visualization of the ¹³⁷ Cs Data Acquired near the 216-B-5 Injection Well and 216-B-9 Crib & Tile Field.....	45
12. Visualization of the ⁶⁰ Co Data Acquired near the 216-B-5 Injection Well and 216-B-9 Crib & Tile Field.....	46
13. Visualization of the ¹³⁷ Cs Data Acquired at the 216-B-9 Crib and Tile Field	47
14. Visualization of the ²³⁵ U (1001 keV) Data Acquired at the 216-B-9 Crib and Tile Field	48
15. Visualization of the ²³⁸ U (186 keV) Data Acquired at the 216-B-9 Crib and Tile Field	49

Contents (continued)

	Page
Figure 16. Northwest-Southeast Cross Section A-A' Showing Contamination and Interpreted Stratigraphy at the 216-B-5 Injection Well	50
17. Northeast-Southwest Cross Section B-B' Showing Contamination and Interpreted Stratigraphy at the 216-B-5 Injection Well	51
18. East-West Cross Section C-C' Showing Contamination and Interpreted Stratigraphy near the 216-B-9 Crib and Tile Field	52
19. North-South Cross Section D-D' Showing Contamination and Interpreted Stratigraphy at the 216-B-9 Crib and Tile Field	53
20. North-South Cross Section E-E' Showing Contamination and Interpreted Stratigraphy at the 216-B-9 Crib and Tile Field	54
21. Visualization of the ¹³⁷ Cs Distribution at the 216-B-5 Injection Well	55
22. Visualization of the ¹³⁷ Cs Distribution at the 216-B-9 Crib and Tile Field	56
23. Alternative Visualization of the ¹³⁷ Cs Distribution at the 216-B-9 Crib and Tile Field	57
24. Elevation of the Top of the Zone of Sediments with 100 pCi/g of ¹³⁷ Cs Activity or Greater at the 216-B-9 Crib and Tile Field	58
25. Isopach of Net Thickness of Sediments Containing 100 pCi/g of ¹³⁷ Cs Activity or Greater at the 216-B-9 Crib and Tile Field	59
26. Borehole 299-E28-25 SGLS/RLS Comparison Plot	60

List of Tables

Table 2-1. Logging Sondes and Vehicles (September 2002)	3
2-2. Naturally Occurring Gamma-Emitting Radionuclides	4
2-3. Man-Made Radionuclides	5
3-1. Summary of the Operational History for the 216-B-5 Injection Well, 216-B-9 Crib & Tile Field, and Adjacent Sites	15
3-2. Summary of Median Radionuclide Release Estimates for the 216-B-5 Injection Well, 216-B-9 Crib & Tile Field, and Adjacent Sites	15
4-1. Boreholes and Groundwater Monitoring Wells Logged with the SGLS and HRLS During the Investigation of the 216-B-5 Injection Well, 216-B-9 Crib & Tile Field, and Adjacent Sites	19
5-1. Summary of the Wells Edited Before Inclusion Into the Interpreted Data Set Used During the Investigation of the 216-B-5 Injection Well and 216-B-9 Crib and Tile Field	25
References	61

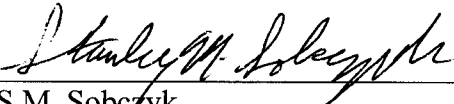
Project Documents Online: <http://www.gjo.doe.gov/programs/hanf/htfvz.html>

Contents (continued)

	Page
Appendix A. Spectral Gamma-Ray Logs for Boreholes and Wells in the Vicinity of the 216-B-5 Injection Well, 216-B-9 Crib & Tile Field, and Adjacent Waste Sites (accompanying CD-ROM)	
Appendix B. Spreadsheet Listing Boreholes and Wells used in this Study of the 216-B-5 Injection Well, 216-B-9 Crib & Tile Field, and Adjacent Waste Sites and Log Depths of the Main Geologic Units Identified on the Spectral Gamma-Ray Logs.....	B-2

**Hanford 200 Areas Spectral Gamma Baseline Characterization Project
216-B-5 Injection Well and 216-B-9 Crib & Tile Field
Waste Site Summary Report**

Prepared by:



S.M. Sobczyk
S.M. Stoller, Hanford

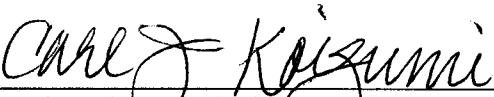
11/6/2002
Date

Concurrence:



R.G. McCain, Hanford Technical Lead
S.M. Stoller, Hanford

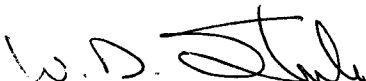
11/06/2002
Date



C.J. Koizumi, Technical Lead
S.M. Stoller, Grand Junction Office

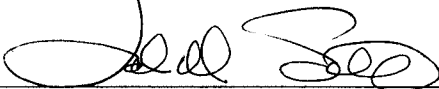
11/12/2002
Date

Approved by:



W.D. Steele, Project Manager
S.M. Stoller, Hanford

11/13/2002
Date



J.M. Silko, Project Manager
U.S. Department of Energy
Richland Operations Office

11.13.02
Date

Executive Summary

The U.S. Department of Energy Richland Office (DOE-RL) tasked the DOE Grand Junction Office (DOE-GJO) to conduct a baseline characterization of the gamma-ray-emitting radionuclides distributed in vadose zone sediments in the vicinity of waste sites in the Central Plateau (200 East and West Areas) of the Hanford Site.

The Spectral Gamma Logging System (SGLS) was used to collect data in existing boreholes and monitoring wells and to perform geophysical logging of new boreholes and wells drilled as part of ongoing site investigation projects. This system uses a high-purity germanium (HPGe) detector to acquire high-resolution, gamma-energy spectra for the detection, identification, and quantification of gamma-emitting radionuclides.

This report documents SGLS results obtained from 25 boreholes in the area surrounding the 216-B-5 Injection Well and 216-B-9 Crib and Tile Field. Gamma-emitting radionuclide concentration data were determined for naturally occurring and man-made radionuclides. Cesium-137 (^{137}Cs), cobalt-60 (^{60}Co), uranium-238 (^{238}U), and uranium-235 (^{235}U) were detected while logging in this study area. ^{137}Cs was the predominant contaminant detected at these waste sites. The maximum ^{137}Cs concentration detected near the 216-B-5 Injection Well was 3,300 picocuries per gram (pCi/g), and the maximum ^{137}Cs concentration detected near the 216-B-9 Crib was 84,000 pCi/g. $^{235/238}\text{U}$ were only detected at the 216-B-9 Crib and Tile Field at activities near their respective minimum detection levels (MDLs).

The distribution of ^{137}Cs near the 216-B-5 Injection Well, as determined from the SGLS logging data, appears consistent with previous studies. The SGLS was unable to log the interval below the groundwater near the 216-B-5 Injection Well because of waste management issues. According to previous studies, this 40-foot (ft) interval was highly contaminated with ^{137}Cs , strontium-90 (^{90}Sr), americium-241 (^{241}Am), and plutonium-239/240 ($^{239/240}\text{Pu}$). Acquiring log data below the groundwater is essential to fully characterize the area and provide data that are fundamental to assessing the mobility of ^{137}Cs and other radionuclides in groundwater under field conditions. Above the present groundwater level, ^{137}Cs concentrations appear to decrease with distance and are below the detection limit within 75 ft of the injection well. The H3 Silt, a member of the Hanford formation (see Section 3.2.1.4), appears to have influenced the distribution of ^{137}Cs near the injection well.

^{137}Cs contamination detected at the 216-B-5 Injection Well above the elevation of the perforations (446 ft) in boreholes 299-E28-7, 299-E28-23, 299-E28-24, and 299-E28-25 is believed to occur inside the casing; this contamination was probably “dragged-up” when these boreholes were drilled and/or deepened. The ^{137}Cs concentrations detected in boreholes 299-E28-14 and 299-E28-1 at elevations between 426 and 415 ft probably originated from the injection well and were transported by groundwater to their present location.

The logs from two boreholes located close to the 241-B-361 Settling Tank did not detect any gamma-emitting radionuclides that would indicate that the tank had leaked.

SGLS logs from boreholes in the area of the 216-B-9 Crib and Tile Field indicate that significant site-related contamination is generally not detected below approximately 60 ft from the ground

surface (elevation 682 ft). The zone of ^{137}Cs -contaminated soil appears to dip to the north-northwest. The maximum extents of the vadose zone contamination to the west and south of the crib and tile field are unknown. Depending upon the level of characterization required for future environmental activities, additional boreholes are recommended to the west of the 216-B-9 Crib and Tile Field. Evaluations of SGLS data and historical gross gamma logs collected in 1963 suggest that contamination is confined to the vadose zone and that contaminant breakthrough to the groundwater in the vicinity of the 216-B-9 Crib and Tile Field has not occurred.

In addition to contamination identified at the two major sites, an interval of ^{60}Co contamination was identified that does not appear to be directly associated with these sites. This contamination was detected within the groundwater in the wells that could be logged below groundwater level. The ^{60}Co is probably the result of historical groundwater contamination that may have originated from the BY Cribs. Historical gross gamma logs indicate that a radioactive front (interpreted as ^{60}Co based on the SGLS logs) migrated past well 299-E28-14 between 1968 and 1976.

A comparison of the profiles of historical gross gamma logs and current SGLS logs, as well as a more direct comparison of more recent RLS spectral logs with the SGLS, suggest contamination profiles appear to be relatively stable and concentration levels are not changing except by radioactive decay.

1.0 Introduction

The Hanford 200 Areas Spectral Gamma Baseline Characterization Project team deploys borehole geophysical logging equipment to measure naturally occurring and anthropogenic radionuclides in the subsurface in the vicinity of 200 Area waste sites. The following sections provide brief discussions of background, project purpose and scope, field and technical methods, and project objectives.

1.1 Background

The U.S. Department of Energy (DOE) Hanford Site encompasses approximately 1,450 square kilometers (km²) (560 square miles [mi²]) in the Columbia Basin of south central Washington State. Beginning in World War II, the Hanford Site was involved in production of plutonium to support the national nuclear weapons program. The Hanford Site is subdivided into a number of operational regions identified as the 100, 200, 300, and 1100 Areas (Figure 1). In 1989, the U.S. Environmental Protection Agency (EPA) placed these areas on the National Priorities List (NPL) pursuant to the *Comprehensive Environmental Response, Compensation, and Liability Act of 1980* (CERCLA). The 200 Areas are located on a plateau near the center of the Hanford Site. These areas consist of the 200 West Area and 200 East Area, which include waste management facilities and inactive irradiated-fuel reprocessing facilities, and the 200 North Area, which was formerly used for interim storage and staging of irradiated fuel.

1.2 Purpose and Scope of Project

The goal of the DOE Grand Junction Office (DOE-GJO) Hanford 200 Areas Spectral Gamma Baseline Characterization Project is to collect data from existing boreholes and determine the present nature and extent of contamination associated with gamma-ray-emitting radionuclides distributed in the subsurface in the vicinity of 200 Area waste sites. The investigation includes liquid effluent disposal sites (and their associated structures such as pipelines) resulting from the discharge of radioactive effluent from processing facilities to the ground (via ponds, cribs, and ditches), burial grounds, the peripheral regions of the single-shell waste storage tank farms where leakage of high-level radioactive waste constituents from specific tanks may have migrated, and unplanned releases. Most of the liquid waste sites and all of the burial grounds and unplanned release sites have been assigned to the Environmental Restoration (ER) Program. A small percentage of the soil waste sites and the peripheral regions of the tank farms have been assigned to the DOE Office of River Protection (DOE-ORP).

The purpose of the Hanford 200 Areas Spectral Gamma Baseline Characterization Project is to present spectral gamma data collected from existing boreholes in and adjacent to waste sites in the Hanford 200 Areas. High-resolution gamma-energy spectra are collected in these boreholes using consistent and defensible methodology. This work effectively extends the existing baseline data set developed for the Hanford single-shell tank farms into the surrounding areas. The baseline data are evaluated to determine the source(s) of the contamination, to develop a dataset that can be used to assess future changes, and to correlate the geophysical signatures of known and presumed geologic features that may affect radionuclide migration within the vadose zone. This information is needed to manage the sites and to make informed decisions regarding waste management, retrieval operations, environmental activities, and site closure.

The Spectral Gamma Logging System (SGLS) is used to acquire gamma-ray energy spectra from boreholes and wells related to the 200 Area waste sites. Intervals of high gamma-ray intensity are logged with the High Rate Logging System (HRLS).

Gamma spectra from each borehole are analyzed to determine concentrations of naturally occurring radionuclides potassium-40 (^{40}K), thorium-232 (^{232}Th), uranium-238 (^{238}U), and associated decay progeny, as well as, man-made gamma-emitting radionuclides such as cesium-137 (^{137}Cs), cobalt-60 (^{60}Co), and europium-152/154 ($^{152/154}\text{Eu}$). Variations in naturally occurring radionuclides are useful in stratigraphic correlation.

This project is limited in scope to passive spectral gamma-ray logging. Only radionuclides that decay with the emission of gamma-ray photons can be detected and quantified. Furthermore, only existing boreholes/wells and any new boreholes drilled for other projects are logged. No new borehole drilling is specified or planned as a part of this project, although recommendations for additional boreholes may be provided when appropriate. Additional details regarding the scope and general approach to this characterization program are included in the baseline characterization plan (DOE 2001c) and project management plan (DOE 2001b).

Specific activities under this project include preparation and maintenance of a database of existing boreholes and geophysical log data, logging existing boreholes with the SGLS and HRLS, analysis and plotting of log data, and preparation of reports. Because many waste sites are the subjects of site characterization efforts in Remedial Investigation/Feasibility Studies (RI/FS) work plans, well logging is performed in existing and new boreholes to support these activities, and data are provided for incorporation into the Remedial Investigation Reports.

1.3 Project Objectives

Specific project objectives are:

- To use passive spectral gamma logging to identify the activities of man-made radionuclide contaminants and to estimate current subsurface radionuclide contamination in the vicinity of 200 Area waste sites. Many areas of the subsurface have been contaminated by the disposal of liquid waste to the ground, and, in some cases, by surface spills.
- To identify probable contaminant migratory pathways and residual contamination by measuring the radionuclide contaminant activity in multiple boreholes and correlating data between those boreholes. It is possible, in many cases, to link detected subsurface contamination with probable sources.
- To provide a baseline dataset to help assess ongoing migration of the radionuclides through the vadose zone, and to provide data for the validation of initial or boundary conditions of contaminant transport models.
- To generate data that can be used for stratigraphic correlations in 200 Area waste sites. Migration of radionuclides through the vadose zone is affected by differences in vadose zone composition, porosity, density, and water content. Accurate stratigraphic characterization helps in identifying target-monitoring horizons and in delineating controlling factors in subsurface flow. Lithologic characterization data include vertical profiles of naturally occurring ^{40}K , ^{238}U , and ^{232}Th .

Although the primary focus of this project is collection and evaluation of spectral gamma log data, part of this project involves assessment of existing data, such as historical gross gamma data, spectral gamma and neutron logs, drilling logs, groundwater monitoring information, geology and hydrogeology information, construction details, and operational information. This information is compiled and evaluated with the newly acquired spectral gamma data to understand its significance in relation to the nature and extent of vadose zone contamination. The background and historical information helps to identify potential sources of contamination, the date of contamination, rate of contaminant migration (if it occurs), and to explain the nature of the contamination identified by the new spectral gamma log data.

2.0 Spectral Gamma-Ray Logging Methods

The following sections discuss field and technical methods used by the Hanford 200 Areas Spectral Gamma Baseline Characterization Project that have been specifically developed for high-resolution borehole measurements with a sensitivity and accuracy comparable to laboratory equipment.

2.1 Field Methods

Existing boreholes are logged by the SGLS, which uses a cryogenically cooled HPGe detector with an intrinsic efficiency of approximately 35 percent. The HRLS is used in zones of high gamma activity, where the SGLS detector can become “saturated” and no usable spectra can be acquired. Both detector systems are operated on the same logging vehicle. Each combination of sonde and logging vehicle represents a unique logging system. Two logging vehicles, three SGLS sondes, and one HRLS sonde are available. Table 2-1 lists currently available logging systems.

Table 2-1. Logging Sondes and Vehicles (September 2002)

Sonde	Type	Serial No.	Vehicle	
			Gamma 1 HO 68B-3574	Gamma 2 HO 68B-3572
A	SGLS	34TP20893A	N/A ¹	(11/01) ²
B	SGLS	36TP21095A	N/A	(11/01)
C	HRLS	39A314	(11/02)	N/A
D	SGLS	34TP11019B	(06/01)	N/A

¹ Not applicable

² Date of last calibration

SGLS and HRLS log data are collected in accordance with a logging procedure (DOE 2001a). Gamma energy spectra are collected in “move-stop-acquire” mode where the sonde is held stationary for measurement and then moved a specified depth increment to the next measurement point. The typical depth increment is 0.5 ft. System gain is adjusted as necessary to maintain a consistent channel relationship for a marker peak (typically the ⁴⁰K peak at 1461 keV). Measurement times are selected to detect prominent gamma peaks associated with natural radionuclides (⁴⁰K, ²³⁸U, and ²³²Th). Depending on casing thickness, typical count times are 100 or 200 seconds (s) for the SGLS and 300 s for the HRLS. This results in logging speeds of feet per hour instead of the feet per minute rates common in the petroleum and mineral industries. In deep boreholes where no contamination is expected, a depth increment of 1.0 ft may be used to expedite logging. This larger depth increment

generally is preferable to reducing count time, because the overall spectrum quality is not compromised. Verification spectra are collected at the beginning and end of each logging day to monitor system performance, and repeat sections are logged to demonstrate repeatability and consistency.

2.2 Technical Methods

Evaluation of gamma energy spectra provides identification and quantification of naturally occurring and man-made radionuclides based on characteristic energy emissions associated with their decay. Only gamma rays of sufficient energy to penetrate the steel borehole casing and sonde housing can be detected by the SGLS or HRLS. Radionuclides that emit one or more gamma rays at energies between about 150 and 2,800 keV are detectable with the SGLS. The minimum detectable concentration is dependent upon detector efficiency at the appropriate energy, background activity, and the yield (gamma rays emitted, on average, per decay). Factors such as casing, water, shielding, and the presence of other radionuclides also have an effect. Because waste disposal to the soil column has been discontinued, radionuclides with half lives of less than 1 year have not been detected on the spectral gamma logs and are presumed to have decayed to insignificant levels. Tables 2-2 and 2-3 summarize naturally occurring and man-made radionuclides that can be detected with the SGLS. The terms “primary gamma ray” and “secondary gamma ray” are used to differentiate between the more prominent gamma energy peaks and other, less prominent peaks that may be useful for confirmation. The values indicated in bold are those generally used to calculate concentrations.

Table 2-2. Naturally Occurring Gamma-Emitting Radionuclides

Radionuclide	Primary Gamma Rays			Secondary Gamma Rays		
	Daughter	E (keV)	Y (%)	Daughter	E (keV)	Y (%)
⁴⁰ K		1460.83	10.67			
²³² Th	²¹² Pb	238.63	43.30	²²⁸ Ac	911.21	26.60
	²⁰⁸ Tl	2614.53	35.64	²²⁸ Ac	968.97	16.17
	²⁰⁸ Tl	583.19	30.36	²²⁸ Ac	338.32	11.25
²³⁸ U ¹				²⁰⁸ Tl	510.77	8.06
	²¹⁴ Bi	609.31	44.79	²¹⁴ Pb	295.21	18.50
	²¹⁴ Pb	351.92	35.80	²¹⁴ Bi	1120.29	14.80
	²¹⁴ Bi	1764.49	15.36	²¹⁴ Pb	241.98	7.50
				²¹⁴ Bi	1238.11	5.86
				²¹⁴ Bi	2204.21	4.86
				²¹⁴ Bi	2447.86	1.50

¹ Attainment of secular equilibrium between ²³⁸U and bismuth-214/lead-214 (²¹⁴Bi/²¹⁴Pb) requires long time periods on the order of a million years. Activities of both ²¹⁴Bi and ²¹⁴Pb are commonly assumed to be equal to the activity of naturally occurring ²³⁸U. However, these radionuclides are short-term daughter products of radon-222 (²²²Rn), and accumulations of radon gas inside the casing may temporarily elevate the decay activities of ²¹⁴Bi/²¹⁴Pb relative to the decay activity of ²³⁸U.

Table 2-3. Man-Made Radionuclides

Radionuclide	Half Life (Years)	Primary Gamma Rays		Secondary Gamma Rays	
		E (keV)	Y (%)	E (keV)	Y (%)
⁶⁰ Co	5.2714	1332.50 1173.24	99.98 99.90		
¹⁰⁶ Ru	1.0238	511.86	20.40	621.93	9.93
¹²⁵ Sb	2.7582	427.88	29.60	600.60 635.95 463.37	17.86 11.31 10.49
¹²⁶ Sn	1.E+5	414.50	86.00	666.10 694.80	86.00 82.56
¹³⁴ Cs	2.062	604.70	97.56	795.85	85.44
¹³⁷ Cs	30.07	661.66	85.10		
¹⁵² Eu	13.542	1408.01	20.87	121.78 344.28 964.13 1112.12 778.90	28.42 26.58 14.34 13.54 12.96
¹⁵⁴ Eu	8.593	1274.44	35.19	123.07 723.31 1004.73 873.19	40.79 20.22 18.01 12.27
¹⁵⁵ Eu	4.7611	105.31	21.15		
²³⁵ U	7.038E+08	185.72	57.20	205.31	5.01
^{234m} Pa (²³⁸ U ¹)	4.47E+09	1001.03	0.84	811.00 766.36	0.51 0.29
²³⁷ Np	2.14E+06	312.17	38.60		
²³⁸ Pu	87.7	99.853	0.0074	43.498	0.04
²³⁹ Pu	24110	129.30 375.05 413.71	0.0063 0.0016 0.0015		
²⁴⁰ Pu	6563	104.234	0.007	45.244 160.308	0.045 0.0004
²⁴¹ Pu	14.35	148.567	0.0002	103.68	0.0001
²⁴¹ Am	432.2	59.54 ²	35.90	102.98 335.37 368.05 662.40 772.01	0.02 0.0005 0.0002 0.0004 0.0002

¹ ^{234m}Pa is a short-term daughter of ²³⁸U. Secular equilibrium is achieved relatively quickly. Because of the relatively low gamma yield, this peak is not observed when only background levels of naturally occurring ²³⁸U are present. Hence, the presence of gamma peaks associated with ^{234m}Pa without corresponding peaks associated with ²¹⁴Pb and ²¹⁴Bi indicates the presence of chemically processed uranium.

² The 59.54-keV gamma ray may not be detectable in thick casing.

Other radionuclides of interest, such as tritium (³H), strontium-90 (⁹⁰Sr), and technetium-99 (⁹⁹Tc), are “pure” beta emitters and do not emit any gamma rays that can be detected with the SGLS. However, experience has shown that the presence of ⁹⁰Sr at concentrations greater than 1,000 pCi/g can be inferred from the *bremsstrahlung* generated from interaction of the high-energy beta emissions from ⁹⁰Sr with the steel casing.

Field gamma spectra are processed and analyzed in accordance with a project-specific data analysis manual (DOE 2002b). Conventional gamma spectra analysis software is used to detect gamma

energy peaks, identify the source radionuclide, and determine the net count rate, counting error, and minimum detectable activity. From the net count rate (P_n , cps) for a specific energy peak, the apparent concentration of the source radionuclide (C_a , pCi/g) is determined by:

$$C_a = \frac{27.027}{Y} \times I(E) \times DTC \times K_c \times K_w \times K_s \times P_n,$$

where Y is the radionuclide yield, $I(E)$ is the logging system calibration function, DTC is the dead time correction, and K_c , K_w , and K_s are energy-dependent correction factors for casing, water, and shielding. The calibration function, $I(E)$, is unique for each combination of sonde and logging vehicle. Values of the calibration function are updated annually and documented in calibration certificates and a calibration report (Koizumi 2002). Concentration error and minimum detectable concentration are calculated using similar equations. The reported concentration error is based only on the estimated counting error. No effort is made to include the effects of errors in the calibration function or correction factors. These errors are discussed in the calibration report (Koizumi 2002). The term “apparent concentration” is used because the calibration model is based on an effectively infinite, homogeneous distribution uniformly distributed about the borehole axis, but the actual distribution of gamma-ray sources in the ground might be dissimilar.

The minimum detection level (MDL) of a radionuclide represents the lowest concentration at which the positive identification of a gamma-ray peak for that radionuclide is statistically defensible. A description of the MDL calculation is included in the data analysis manual (DOE 2002b).

For a counting time of 100 s, the MDL for ^{137}Cs is approximately 0.2 pCi/g. The MDL differs slightly for each spectrum depending upon count time, background activity and concentrations of other radionuclides at the data point, as well as casing thickness. In regions of higher man-made radionuclide concentrations, the Compton background continuum becomes elevated, increasing the MDL value.

The MDL for ^{60}Co is approximately 0.15 pCi/g; the MDL for ^{154}Eu is approximately 0.2 pCi/g; and the MDLs for ^{235}U and ^{238}U are approximately 1 and 10 pCi/g, respectively. These values are typical for a 100-s counting time, and an approximate casing thickness of 0.28 inch (in).

Natural and man-made radionuclide concentrations, total gamma count rate, and dead time are plotted as a function of depth. These plots are included in a Log Data Report that also summarizes borehole construction details, logging conditions, analysis notes, and log plot notes, as well as a brief discussion of results and interpretations. When appropriate, comparison plots with other available logs are also included. Log Data Reports for boreholes in the study area are included in the CD-ROM in Appendix A.

In accordance with conventional logging practice, log data are presented in terms of depth relative to a well-defined fixed point, such as top of casing in existing boreholes or wells. Where a fixed reference point is not available, depth relative to ground surface is used. In many cases, a reference elevation may not be available at the time log data are collected. When comparing features between boreholes or in stratigraphic correlation, elevation relative to a common reference datum (typically mean sea level) is used, which provides a better indication of the spatial position of the feature or bed and eliminates confusion resulting when boreholes are located at different ground surface elevations.

Log data and geological information from surrounding boreholes are assembled and correlated in an effort to identify contaminated zones and potential sources of contamination. Historical gross gamma, spectral gamma, and neutron log data are incorporated where available. Three-dimensional visualization software is used to interpolate data between boreholes.

A Waste Site Summary Report (WSSR) documents the results of the correlation and evaluation process for each group of waste sites. Waste site groups have been defined in terms of physical proximity and common configuration or operational history. Each WSSR provides a review of background information that includes a description and operational history of the waste sites, a summary of geologic and hydrogeologic conditions, a review of previous investigations, and any existing data such as gross gamma or spectral logs, geologic logs, or groundwater data. Assessments and interpretations of the spectral gamma-ray log information are also provided, along with conclusions and recommendations on future data needs or corrective action, where appropriate.

3.0 Background and Physical Setting of the 216-B-5 Injection Well, 216-B-9 Crib & Tile Field, and Adjacent Sites

The study area is located southeast of 241-B Farm and northeast of B Plant. Figure 2 is a map of the northwest-central 200 East Area that shows the general location of the 216-B-5 Injection Well and 216-B-9 Crib and Tile Field. Figure 3 is a more detailed map of the area. There are 25 existing boreholes available for evaluation that are associated with the 216-B-5 Injection Well, 216-B-9 Crib and Tile Field, 241-B-361 Settling Tank, 216-B-56 Crib, and UPR-200-E-112 (UPR = unplanned release). Other waste sites that do not have nearby boreholes are the 216-B-59 Trench, 216-B-59B Retention Basin, and UPR-200-E-7.

The information in the following sections was obtained from a variety of sources, including Waste Information Data System (WIDS), DOE (2000), DOE (1993a), Brodeur et al. (1993), and Smith (1980).

3.1 Background of the 200 Areas

Established in 1943, the Hanford Site was originally designed, built, and operated to produce plutonium for nuclear weapons. Uranium metal billets were received in the 300 Area and fabricated into jacketed fuel rods. The fuel rods were loaded into graphite-moderated reactors in the 100 Areas. With the exception of 100-N, which also provided steam to the Hanford Generating Project, these reactors were operated for the sole purpose of producing ^{239}Pu from neutron activation of ^{238}U . The fuel rods were then transported to the 200 Areas, where plutonium and uranium were separated from the residual activation and fission products using a variety of liquid chemical separation processes. The 600 Area includes portions of the Hanford Site not included in the 100, 200, or 300 Areas and served primarily as transportation corridors and buffer zones between the fabrication, irradiation, and chemical processing areas (DOE 1998).

Chemical separations process facilities were sited in both the 200 East and 200 West Areas. The 200 North Area temporarily stored irradiated fuel rods, allowing short-lived fission products to decay before being shipped to separations plants. With the startup of the separation plants, high-level

wastes containing the bulk of the fission products were discharged to large underground steel tanks, and large quantities of liquid wastes (primarily water) containing lesser concentrations of radionuclides and chemicals were discharged to the soil column and percolated into the vadose zone.

Depending on contaminant concentrations and a consequent need for isolation, liquid wastes were discharged either to surface ponds and ditches or to underground cribs, trenches, and French drains. Before 1950, injection wells and/or reverse wells were used to dispose of process waste directly to groundwater. Liquid wastes were divided into high (more than 100 microcuries [μCi] of beta emitters per milliliter), intermediate (more than $5 \times 10^{-5} \mu\text{Ci}$ and less than $100 \mu\text{Ci}$ of beta emitters per milliliter), and low-level (less than $5 \times 10^{-5} \mu\text{Ci}$ of beta emitters per milliliter) categories (Routson 1973). The high-level wastes were sent to the tanks for storage. The intermediate level wastes were disposed to cribs. "Cribs are underground structures from which the solution percolates through the sediment (soil) to the groundwater. ... Limited amounts of special intermediate wastes were disposed to the ground in trenches on a specific retention basis" (Routson 1973). These liquid disposal sites were located in the 200 Areas near the processing plants and in the nearby 600 Areas (DOE 1998).

3.2 Geologic Conditions

This section summarizes the geologic setting of the Hanford Site, 216-B-5 Injection Well, and 216-B-9 Crib and Tile Field. Figure 4 shows the general stratigraphy and geology for the study area. Lithologic information, used to develop stratigraphy, is obtained from field analysis of sediment samples retrieved during borehole drilling operations and from nearby outcrops. When available, gross gamma-ray logs have been used to support the geologic interpretation. Most of the boreholes were drilled with a cable tool drill rig, and the samples were obtained from bailings, core barrels, or as retained cuttings, generally from 5-ft intervals. Smith (1980), Lindsey et al. (1992), and DOE (1993a) presented detailed descriptions and interpretations of the geologic formations near the 216-B-5 Injection Well and 216-B-9 Crib and Tile Field.

3.2.1 Stratigraphy

Overlying the basalt flows of the Columbia River Basalt Group are the Ringold Formation, the unnamed Plio-Pleistocene unit, the informal Hanford formation, and Holocene-Age deposits. Rockwell (1979), Reidel et al. (1992), Delaney et al. (1991), Lindsey (1991), Lindsey et al. (1994), and Bjornstad et al. (2002) (draft report) have presented extensive descriptions and discussions of these formations. Bjornstad et al. (2002) currently are formalizing the stratigraphic nomenclature for post-Ringold sediments at the Hanford Site. When the nomenclature proposed by Bjornstad et al. (2002) is finalized, it will be used in subsequent reports.

3.2.1.1 Columbia River Basalt Group

The Columbia River Basalt Group consists of 174,000 cubic kilometers (km^3) of tholeiitic flood-basalt flows that erupted between 17 and 6 million years ago and cover approximately 164,000 km^2 of eastern Washington, Oregon, and western Idaho (Reidel et al. 1989). The distribution of the basalt flows reflects the tectonic history of the area (Reidel et al. 1989). The basalt is as much as 4,000 meters (m) thick in the vicinity of the Hanford Site (Reidel et al. 1989; Glover 1985). The uppermost basalt flow, the Elephant Mountain Member, is at an elevation of about 390 ft under the

waste sites. Reidel et al. (1989), Reidel and Fecht (1981), and Rockwell (1979) presented additional information about the Columbia River Basalt Group.

3.2.1.2 Ringold Formation

Ringold sediments predominantly consist of layers of fluvial sand, ancient soils (paleosols), and lacustrine sand, silt, and clay (Lindsey 1996). This formation, as much as 600 ft thick across the Hanford Site, consists of uncemented to locally well-cemented clay, silt, fine- to coarse-grained sand, and pebble to cobble conglomerate. Sediments of the Ringold Unit 'A' are underneath the study area (DOE 1993a).

3.2.1.3 Plio-Pleistocene Sediments

The Plio-Pleistocene unit sediments unconformably overlie the Ringold Formation. This unit is laterally discontinuous. Plio-Pleistocene sediments, which are absent in the vicinity of the study area (Williams et al. 2000), consist of locally derived basaltic alluvium and pedogenic calcium-carbonate-rich material. The basaltic material consists of weathered and unweathered locally derived basaltic gravel containing varying amounts of sand and silt. The carbonate-rich sediments consist of calcium carbonate cemented silt, sand, and gravel interfingering with carbonate-poor sediments. Both of these facies may be present at some locations. The Plio-Pleistocene unit generally dips to the south-southwest. Bjornstad et al. (2002) have proposed naming these sediments the Cold Creek Interval.

In the past, the Plio-Pleistocene was divided into an upper silty sand to sandy silt that was designated as early Palouse soil and a lower calcium carbonate-rich interval often referred to as the "caliche layer" (Lindsey et al. 2000). Numerous investigations conducted in the 1990s have observed that the upper unit contains stratified fine sand indicative of lacustrine deposition and not eolian conditions associated with the early Palouse soil (Lindsey et al. 2000). The Plio-Pleistocene unit also contains a series of paleosols with calcium carbonate development indicative of an arid environment (Slate 1996).

The pre-Missoula gravel, which consists of quartzose to gneissic clast-supported pebble to cobble gravel with quartzo-feldspathic sand matrix, underlies the Hanford formation in the east-central region of the Cold Creek syncline and at the east end of Gable Mountain anticline east and south of the 200 East Area (Williams et al. 2000).

A compact, massive loess-like silt with minor fine-grained sand unit may overlie the Plio-Pleistocene unit. This unit is designated the "Early Palouse soil," and it can range to tens of feet thick. The Early Palouse sediments can grade upward into sediments similar to those at the base of the overlying Hanford formation, making the contact between these two lithologic units difficult to distinguish. The Early Palouse soil is thickest in the southwest and southeast portions of the 200 West Area, where it reaches a maximum thickness of 65 ft. The Early Palouse soil is not present underneath the area containing the 216-B-5 Injection Well and 216-B-9 Crib and Tile Field (Williams et al. 2000).

3.2.1.4 Hanford Formation

A series of Pleistocene catastrophic flood deposits, informally known as the Hanford formation, overlies the Plio-Pleistocene and older sediments throughout the Hanford Site. The Hanford formation consists of gravel, sand, and silt. The sediments of the Hanford formation are

unconsolidated, uncemented, and highly transmissive for the flow of water. This formation is thickest in the central Hanford Site, where it thickens to 350 ft. The Hanford formation is divided into three facies (gravel-dominated, sand-dominated, and silt-dominated) that are gradational with each other. Bjornstad et al. (2002), Lindsey (1991), Reidel et al. (1992), and Wood et al. (2000) provided detailed discussions of the Hanford formation lithology. The Hanford Site is in the process of formalizing the stratigraphic nomenclature for the Hanford formation (Bjornstad et al. 2002).

Interpretations of sediment samples obtained from boreholes in the 200 Areas (Lindsey et al. 1992; and Reidel et al. 1992) have resulted in subdividing the Hanford formation into units (H1a, H1, H2, H2a, H3, and H4). Units H1a, H2a, H3, and H4 are laterally discontinuous, and H3 and H4 are locally identified at the base of the formation (Lindsey et al. 2000).

The rhythmite facies sediments (Hanford H4) were deposited under slack water conditions and in back-flooded areas remote from the main flood channel. These sediments consist of thinly bedded, plane-laminated and ripple cross-laminated silt and fine- to coarse-grained sand and commonly display normally graded rhythmites a few centimeters to several tens of centimeters thick (Baker et al. 1991; DOE 1988). This facies dominates the Hanford formation along the western, southern, and northern margins of the Pasco Basin, within and south of the 200 Areas.

In the study area, the Hanford H3 unit varies from 50 to 80 ft thick, and this lower coarse-grained unit consists of pebble and cobble gravel with interbedded sand. The H3 generally consists of coarse-grained basaltic sand and granule to boulder gravel, and ranges from well sorted to poorly sorted. In outcrop, these sediments display massive bedding, planar to low-angle bedding, and large-scale planar cross bedding. The gravel-dominated facies was deposited by high-energy floodwaters in or immediately adjacent to the main flood channel.

The Hanford H2 unit is about 180 to 190 ft thick in the area and consists of sand-dominated facies with interbedded silt lenses (Lindsey et al. 1992, 1994). Some laterally discontinuous silt-rich interbeds are reported in this area, and these high-silt zones may have higher moisture content and CaCO_3 content than the surrounding sand-dominated material. The depositional facies are discontinuous in both horizontal and vertical extents, and little correlation between boreholes has been possible in terms of the minor differences between such features as the silty sand and sandy silt layers (Lindsey et al. 1992, 1994).

Unit H1 is dominated by coarse to granule sand and lesser pebble gravel formed from a complex interfingering of gravel and sand-dominated facies (Lindsey and Law 1993; Lindsey et al. 1994). The relative abundance of gravelly facies decreases from the northwest to the south. As gravel content decreases, unit H1 interfingers with the more sand-rich strata of unit H2.

Clastic dikes that consist of layers of silt, sand, and granule gravel crosscut the Hanford formation. These clastic dikes generally crosscut the bedding as alternating vertical to subvertical dikes, although they may locally run parallel to bedding. Clastic dikes also occur in the older sediments (Fecht et al. 1999).

3.2.1.5 Holocene Surficial Deposits

Holocene surficial deposits consist of a mix of silt, sand, and gravel deposited by a combination of eolian and alluvial processes (DOE 1988).

3.2.2 Structure

The Hanford Site is located in the Pasco Basin, which is a physical and structural depression in the Columbia Plateau created by tectonic activity and folding of the Columbia River basalts. The structural framework of the Pasco Basin began developing before Columbia River Basalt Group volcanism (Reidel et al. 1994) and was an area of subsidence that accumulated thick deposits of sediments and volcanic rock. This pattern continued through Columbia River Basalt Group volcanism. Anticlinal ridges were growing under north-south compression. This compression resulted in a series of anticlinal ridges and synclinal valleys with a general east-west trend. The north-south compression and east-west extension have persisted from at least the middle Miocene to the present (Hooper and Camp 1981; Reidel 1984; Hooper and Conrey 1989; Reidel et al. 1989).

The geologic structure of the Pasco Basin area is dominated by a series of east-west-trending anticlines and synclines. Anticlines to the north and south create topographic high areas (Gable Mountain and Rattlesnake Mountain, respectively) with outcropping basalt flows. The Hanford Site 200 Areas are situated on the northern limb of the Cold Creek syncline where bedrock dips to the south at an angle of approximately 5 degrees. Approximately 320 ft of sediments overlie the dipping basalt bedrock in the vicinity of the site.

3.3 Hydrology

Hartman et al. (2002), Narbutovskih (1998), and Narbutovskih (2000) described the hydrology of the Hanford Site and the B-BX-BY Waste Management Area (WMA). The water table is nearly flat with a southerly flow in the vicinity of B Plant and the B-BX-BY WMA. The groundwater level has been declining since liquid discharges were curtailed in the 1980s. The top of the unconfined aquifer is currently at an elevation of approximately 402 ft (122.5 m) and within the H3 unit. The base of the unconfined aquifer is believed to be the top of the basalt. Aquifer thickness is about 40 ft in the area. The study area is located in a region of very low hydraulic gradient between the groundwater mound beneath B Pond, which is located east of the 200 East Area and the eastward-moving groundwater from the 200 West Area (Caggiano 1996).

The groundwater monitoring program has detected tritium, uranium, iodine-129 (^{129}I), ^{137}Cs , and ^{90}Sr above drinking water standards near the 216-B-5 Injection Well. Hartman et al. (2002) has described the current status of groundwater contamination in the study area. Plutonium has also been detected in the groundwater near the 216-B-5 Injection Well. Groundwater samples from well 299-E28-23, located approximately 4 ft east and slightly down gradient of the 216-B-5 Injection Well, generally have the highest reported concentrations in the study area. For example, maximum uranium concentrations are about seven times higher at borehole 299-E28-23 (220 micrograms/liter [$\mu\text{g/L}$]) than at borehole 299-E28-25 (30.3 $\mu\text{g/L}$), which is located about 20 ft northwest and slightly up gradient relative to the injection well. Groundwater samples from four wells (299-E28-2, 299-E28-23, 299-E28-24, and 299-E28-25, locations are shown on Figure 3) contained ^{90}Sr concentrations above 8.0 picocuries/liter (pCi/L) (drinking water standard). Only groundwater from borehole 299-E28-23 exceeded the drinking water standards for ^{137}Cs . Technetium-99 (^{99}Tc) concentrations are not above drinking water standards in this area.

3.4 Description of the 216-B-5 Injection Well, 216-B-9 Crib & Tile Field, and Adjacent Sites

Several facilities into which millions of gallons of liquid waste and wastewater were discharged to the soil column and groundwater are located in this study area. The major waste sites are the 216-B-5 Injection Well (Figure 5) and associated 241-B-361 Settling Tank and 216-B-9 Crib and Tile Field (Figure 6). Other facilities that had lesser impacts to the vadose zone are the 216-B-59 Trench and 216-B-59B Retention Basin. Unplanned releases designated 200-E-112 and UPR-200-E-7 also occurred within the area. There is no record of wastes being discharged to the 216-B-56 Crib. The boundaries of the study area were chosen to include the nearby groundwater monitoring wells in the vicinity of the 216-B-5 Injection Well (Figure 3). A brief discussion of each site or unplanned release is included in the following sections. Figure 3 provides the locations of each site.

The 216-B-5 Injection Well is the only facility at the Hanford Site that discharged waste directly to the water table (DOE 2000). The 216-B-5 Injection Well is an inactive waste management unit that was constructed in 1944. It is located in the 200 East Area about 1,000 ft (300 m) northeast of the 221-Building and east of Baltimore Road. Figure 5 is a photograph of the ground surface at the location of this injection well. From April 1945 until September 1946, the injection well received overflow waste from the 241-B-361 Settling Tank, which received lanthanum/fluoride process waste from the 224-B Concentration Facility and bismuth/phosphate process drainage from Cells 5 and 6 in the 221-B Building. The 241-B-361 Settling Tank removed the particulates. Between September 1946 and October 1947, drainage and other liquid waste from Cells 5 and 6 were directly injected into the well (Brown and Ruppert 1950). Approximately 31,000,000 L (8,100,000 gal) of liquid were discharged to the 216-B-5 Injection/Reverse Well, containing an estimated 4,275 g of plutonium and 3,800 Curies (Ci) of beta-gamma activity (Brown and Ruppert 1950).

A water sample collected in September 1947 from well 299-E33-18, north of B Tank Farm, revealed alpha contamination in the groundwater ($<20 \times 10^{-7}$ $\mu\text{Ci/L}$), which led to the cessation of waste discharge to the injection well (Brown and Ruppert 1950). Eleven additional wells were drilled in 1947 and 1948 to evaluate the contamination plume. The zone of groundwater contamination extended laterally 600 m (2,000 ft) from the injection well. The injection well was characterized again in 1979 (Smith 1980).

In 2001, the 216-B-5 Injection (Reverse) Well was given a well name (299-E28-29) and a well identification number (C3542) (DOE 2000). The 216-B-5 Injection Well consists of four casing strings: a 16-in. (40-cm) casing to 13 ft (4 m), a 12-in. (30-cm) casing to 102 ft (31 m), a 10-in. (25-cm) casing to 243 ft (74 m), and a 8-in. (20-cm) casing to 302 ft (92 m). The final casing string is perforated from a depth of 243 to 302 ft (74 to 92 m) (Brown and Ruppert 1950). Total depth of the injection well is 302 ft (92 m). The injection well received effluent from the 241-B-361 Settling Tank through a 2-in. (5-cm) stainless-steel inlet pipe located 13 ft (4 m) below grade. The 216-B-5 Injection Well was deactivated by blanking the pipeline inlet to the well, and 221-B Building (Cells 5 and 6) wastes were rerouted to the 216-B-7A and 216-B-7B Cribs (Maxfield 1979).

Smith (1980) suggested that the distribution of contamination at this site may be influenced in part by grain-sized distribution and the position of the water table. The presence of ^{137}Cs in the silt layer at an elevation of approximately 432 ft (132 m) is indicative of sediment control on the distribution of radionuclides. Peaks in ^{90}Sr , ^{137}Cs , and $^{239/240}\text{Pu}$ activities also correspond to the

position of the water table in 1948. Figures 7 through 9 show the distribution of $^{239/240}\text{Pu}$, ^{90}Sr , and ^{137}Cs in the vicinity of the 216-B-5 Injection Well in 1980.

According to WIDS, the 241-B-361 Settling Tank operated from April 1945 to September 1947 to precipitate solids from the waste that originated in B Plant and the 224-B Facility. The waste was routed first to the 241-B-154 Diversion Box before being transferred to the settling tank. After settling, the supernate from the tank was discharged to the 216-B-5 Injection Well. The tank sludge contains an estimated 2.4 kilograms (kg) of plutonium and 2 million Ci of ^{90}Sr . On June 5, 1985, the tank liquid was pumped to 244-BX. The liquid level in the settling tank was reduced from 118.25 in. to 113.75 in. When the tank was isolated and stabilized on 6/27/85 the liquid level was recorded as 115.50 in.

The 241-B-361 Settling Tank is constructed of 6-in. (15-cm) reinforced, prestressed concrete. The top of the unit is 6 ft (1.8 m) below grade. Eleven risers are visible above grade. One is equipped with a manual tape, a second contains two dip tubes, a third vents the unit, and the eight remaining risers are blanked off.

According to WIDS, the 216-B-9 Crib and Tile Field were built to replace the 216-B-5 Injection Well. The drainage waste from the B Plant 5-6W Cells was re-routed directly to the crib, by-passing the 241-B-361 Settling Tank. The 216-B-9 Crib carries an alias of 241-B-361 Crib. The unit is a wooden structure, 14 ft by 14 ft (4.3 m by 4.3 m bottom surface) by 8 ft (2.4 m) high, located in an excavation. The timbers are 6 by 6 in. (15.2 by 15.2 cm). The tile field, 180 ft by 84 ft (55.0 by 25.6 m), is 540 linear ft (165 m) of 6-in. (15.2-cm) clay tile pipe, with each leg in a trench 4 ft (1.2 m) wide at the bottom. Pipes are buried 12 ft (3.7 m) deep at head and 6 ft (1.8 m) at the other end. Above and below the pipes are 18 in. (45.7 cm) of gravel. Roofing felt covers the top side of the pipes. Three legs branch from each side of the distribution pipe, leaving at 45 degrees to the trunk. The slope of the excavation surface is 1:1.5. Figure 6 is a photograph of the ground surface area near the crib and tile field.

A total of 18,400,000 liters of waste were discharged to the crib between August 1948 and January 1950. The crib and tile field were deactivated by removal of the jumper in the 241-B-154 Diversion Box. The waste discharged contained approximately 95 grams (3.3 ounces) of plutonium and 2,050 Ci of fission products. Sludge in the waste plugged the crib and decreased its capacity. Acid was added to the crib to keep it in operation. The crib eventually became sealed with sludge and overflow into the tile field began in November 1948. The entire crib was covered with 2 ft (0.61 m) of clean fill in 1991. The unit was stabilized and revegetated in 1992.

UPR-200-E-7 was a cave-in on the process line from B-Plant. According to WIDS, the exact location of the cave-in on the process line cannot be determined from the available documentation. On the basis of coordinates from WIDS, the UPR-200-E-7 is shown as being approximately 165 ft (50 m) southwest of the 216-B-5 Injection Well (see Figure 3). An alternative location for the cave-in is very close to the southwest edge of the posted 216-B-9 Crib (DOE 1993a).

The original 216-B-59 designation was an unlined trench. The trench was upgraded in 1974 to a retention basin by adding a Hypalon[®] liner and changing its identification number to 216-B-59B. It held diverted cooling water for subsequent reprocessing. It was later upgraded again (in 1983) by replacing the hypalon liner with a concrete liner and cover. No visual features of the unlined trench currently remain.

The original trench (216-B-59) was designed as an emergency cooling water diversion for 221-B cooling water with allowable radionuclide concentrations above those for the existing ponds. The site was activated in 1967 and received only a single discharge of approximately 477,000 liters (126,000 gal) of waste in March 1968.

The 216-B-59B Retention Basin was designed to receive diverted 221-B Building cooling water that contained radionuclide concentrations above the limits allowed for disposal in the B Pond system. The diverted waste was pumped back into 221-B to be reprocessed.

The 216-B-56 Crib is 70 ft (21 m) long and 10 ft wide (3 m) and was filled with gravel during construction (DOE 1993a). The site was constructed to receive organic waste from 221-B (B Plant). The pipeline connection to the site was never installed because of a change in disposal practices, and this crib was never activated (DOE 1993a).

Site 200-E-112 is two process sewers that run underground from B Plant to the 207-B Retention Basin. The pipelines cross the northwest portion of the study area (Figure 3). The 2904-E-1 sewer line extends eastward from the south side of 221-B and turns north to connect to the west side of the 207-B Retention Basin. The 2904-E-2 sewer line runs from the north side of 221-B to the east side of the 207-B Retention Basin. The 2904-E-2 sewer could discharge directly to the 216-B-2 ditches. The pipelines are marked above ground with steel posts and marked as "Underground Radioactive Material/Pipeline."

According to WIDS, "Some pipeline leakage had been documented in the 1970's and 1980's. Corrosion, erosion and time contributed to the defects in the sewer system. After evidence of a leak was discovered while performing an excavation near the sewer line, leak tests were conducted. Two fire hoses were placed into the sewer line. The downstream flow was equivalent to the flow from only one fire hose. Later, a temporary dam was placed in the pipeline. It took 36 hours to overflow at the sampling station. Calculating a 222 gallon per minute flow rate, an estimated loss of 300,000 gallons per day could have been leaking into the ground from the pipeline. These results prompted the 1985 Chemical Sewer Upgrade project. A major portion of the vitrified clay pipes on the north side of 221-B were relined."

There are no existing boreholes associated with 200-E-112. Hence, the nature and extent of any subsurface contamination associated with this site are unknown.

3.5 Operational History

The B Plant complex generated the waste discharged in the area by a variety of major chemical processing operations (DOE 1993a). Table 3-1 provides a general summary of the sites and associated wastes and Table 3-2 presents an estimate of releases of various radionuclides.

Table 3-1. Summary of the Operational History for the 216-B-5 Injection Well, 216-B-9 Crib & Tile Field, and Adjacent Sites

Site	Time in Use	Mean Estimate of Volume (m ³)	Source	Type of Waste
216-B-5 Injection Well	04/1945-10/1945	30,600	221 B & 224-B	221-B facility wastes
216-B-9 Crib and Tile Field	08/1948-07/1951	36,000	221-B	221-B facility wastes
216-B-56 Crib	Not Used	0.001	ITS-1 Unit in the 241-BY Tank Farm	
216-B-59 Trench	3/1968-	480	221-B	Diverted cooling water from 221-B
200-E-112				
UPR-200-E-7				
References:	DOE (1993a)	Bergeron et al. (2001)	DOE (1993a)	DOE (1993a)

Table 3-2. Summary of Median Radionuclide Release Estimates for the 216-B-5 Injection Well, 216-B-9 Crib & Tile Field, and Adjacent Sites

Trench	¹³⁷ Cs (Median Estimate in Curies)	¹⁵⁴ Eu (Median Estimate in Curies)	⁶⁰ Co (Median Estimate in Curies)	U (total) (Median Estimate in kg)	⁹⁰ Sr (Median Estimate in Curies)	⁹⁹ Tc (Median Estimate in Curies)	²³⁹ Pu (Median Estimate in Curies)
216-B-5 Injection Well	1,520	0.102	0.006	1,860	1,140	0.137	0.436
216-B-9 Crib & Tile Field	82.7	0.056	0.003	2,040	72.7	0.076	0.007
216-B-59 Trench	0.009	0.0009	8 X 10 ⁻⁸	0.033	9 X 10 ⁻⁵	0.0003	0.002
200-E-112							
UPR-200-E-7							
Reference:	Simpson et al. (2001). Radionuclides are decayed to January 1, 1994.						

¹ N/A – not applicable

3.6 Previous Investigations

Previous investigators have provided assessments of the 216-B-5 Injection Well and 216-B-9 Crib & Tile Field. The 216-B-5 Injection Well was extensively evaluated by Brown and Ruppert (1950) and again by Smith (1980). In addition, geophysical logging of monitoring wells and boreholes was conducted as early as 1957 at the facilities related to B Plant operations. Several subsequent evaluations of the log data were performed, including Raymond and McGhan (1964) and Fecht et al. (1977), which are described in this section. DOE (1993a) provided comprehensive descriptions of these studies, a discussion of gross gamma logging methodology, and interpretations of the data. DOE (1993a) also presented an evaluation of individual waste units such as cribs, ponds, trenches, and ditches. Brodeur et al. (1993) provided summaries of several waste units that include waste discharge histories, plan views of the sites, and geophysical log data acquired in the monitoring

boreholes. Spectral gamma logs were acquired near the 216-B-5 Injection Well (borehole 299-E28-25) and the 216-B-9 Tile Field (borehole 299-E28-61) by Brodeur et al. (1993).

In the late 1940s, an exploration program was conducted to assess the impacts of the waste disposal practices at Hanford (Brown and Ruppert 1950). As a result, 11 groundwater wells were drilled to investigate the impacts of the 216-B-5 Injection Well, and 9 vadose zone boreholes were drilled at the 216-B-9 Crib and Tile Field. No contaminated sediments were encountered by any of the groundwater wells, including 299-E28-7, which is located approximately 50 ft (15 m) from the injection well. A body of contaminated water was discovered (Figures 7 through 10) and described as “a gigantic, elliptical lens, up to about 60 feet thick, 2500 feet long, and 1000 feet wide.” It was suggested that the top of the basalt was the lower limit of the contamination. The contamination initially appeared to be moving to the southeast at an average rate of 500 ft a year. Due to the increasing height of the groundwater mound to the east, the rate of contaminated groundwater movement decreased until it became stationary. Borehole 299-E28-53 (previously known as 361-B-13), installed near the 216-B-9 Crib, was drilled at an 85-degree angle toward the bottom of the center of this crib. The acid used to clear the crib caused the well casing to corrode and wash crib sediments into the borehole. The borehole was found to be filled with sludge and sediments to within 24 ft (7.3 m) of the ground surface. A sample of the sediments collected through the well casing in 1949 revealed 1830 $\mu\text{Ci/kg}$ fission products and 14,800,000 disintegrations per minute per kilogram of alpha contamination. Some waste liquids were concluded to have been introduced into the ground at a depth of 150 ft, because the well casing was filled with sediments. Test holes were placed in the tile field to investigate its drainage. In April 1949, 7 in. of liquid was measured in a borehole. Analysis of a sample of the liquid revealed 11.5 $\mu\text{Ci/L}$ of fission products and 9,000 disintegrations per minute per liter of alpha contamination. Sediment samples collected in October 1949 revealed 152 $\mu\text{Ci/kg}$ of fission products and 943,000 disintegrations per minute per kilogram of alpha contamination.

Conclusions of the investigation presented in Smith (1980) are summarized below. Contaminants near the 216-B-5 Injection Well were predominantly detected at elevations below 445 ft msl (136 m). The injection well is perforated from 243 to 302 ft (74 to 92 m). This zone represents points of release for the liquid waste discharged to the ground. This interval also represents the lower 43 ft (13 m) of the vadose zone and the upper portion of the water table. Contaminants detected in the soil samples at this site include ^{137}Cs , $^{239/240}\text{Pu}$, ^{90}Sr , and ^{241}Am . The activity of ^{137}Cs ranged from less than the detection limit to 51,300 pCi/g. The maximum activities of ^{90}Sr , $^{239/240}\text{Pu}$, and ^{241}Am were 60,000 pCi/g, 75,000 pCi/g, and 2,540 pCi/g, respectively. The highest activities were detected in soils in borehole 299-E28-23 located within several feet of the injection well.

During 1979 and 1980, three wells were drilled to basalt and another well was deepened to basalt around the injection well. Sediment samples were collected during drilling and analyzed to determine the spatial distribution of radionuclides sorbed on the sediments (Figures 7, 8, and 9). The sample data indicated that $^{239-240}\text{Pu}$ and ^{90}Sr levels exceeding 10,000 pCi/g were limited to within 20 ft (6 m) of the injection well and that ^{137}Cs migrated laterally away from the injection well in three zones: a silt layer in the unsaturated sediments, at the position of the 1948 water table, and at the basalt surface. By 1980, the concentrations of radionuclides in the groundwater near the injection well were less than the drinking water standards. It was concluded that the sorbed radionuclides were not contributing to contamination problems in groundwater. Gamma scintillation logging detected a widespread layer of contamination just above the basalt surface. The BY Cribs, which are located

2,950 ft (900 m) to the north of the injection well, may have been a possible source of this contamination. Two vadose zone boreholes drilled about 5 ft (1 m) away from the 241-B-361 Settling Tank did not encounter contaminated sediments, suggesting the tank did not leak.

Review and visual comparison of gross gamma log profiles over time have been useful to determine if contamination has moved downward or changed in intensity. Due to the poor spatial resolution of the data (1 ft) and depth registration errors, tabulation of the maximum spatial peak count rates and comparison of those count rates over time are not recommended. Small changes in the position of the borehole probe between loggings cause large variations in the spatial peak count rates. Only by qualitatively reviewing changing trends in the temporal data is it possible to identify actual changes in the formation contamination concentration. The frequency of gross gamma logging is variable in boreholes such that a statistical analysis of trends is not possible.

Raymond and McGhan (1964) provided gross gamma logs from a scintillation detector in “representative wells adjacent to waste disposal sites. Logs of wells that show no ground contamination are not included.” The lower detection limit of the scintillation detector system was reported as about 3 pCi/cc (Ru^{106} - Rh^{106}) in water. The maximum count rate was reported as approximately 5,000 pCi/g (Ru^{106} - Rh^{106}) in water. Log data between 1957 and 1964 were acquired with a similar detection system but with at least three modifications. These modifications generally were to improve system sensitivity and to reduce noise. Because the profile of the gamma count rate is not significantly changed by these modifications, comparisons over time may be made. Recorder chart data may have been transferred to logarithmic graph paper to account for required scale changes needed to accommodate wide variations in gamma activity encountered during logging, which made direct observation and interpretation somewhat difficult. A narrow band of contamination from 5 to 40 ft in borehole 299-E28-55 near the 216-B-9 Crib was detected.

Fecht et al. (1977) evaluated the historical gross gamma-ray logs acquired between 1954 and 1973 and compared these logs to data collected in 1976 with a new logging system. The original equipment was replaced in 1974 with a system that increased the lower limit sensitivity by approximately a factor of three over the former system. Data were normalized to adjust the background level of the pre-1976 logs to the 1976 values to allow easier, “direct” comparison of the various logs. At the 216-B-9 Crib and Tile Field, scintillation probe profiles collected between 1963 and 1976 found the maximum radiation intensity was located 1.5 ft (0.5 m) below the bottom of the crib and indicated that radioactive effluents primarily were discharged to the secondary lateral, immediately south of borehole 299-E28-57. In 1963, boreholes 299-E28-58 and 299-E28-59 showed radioactive contaminants at 50 ft (15.2 m) and 60 ft (18.3 m), respectively, below the distributor pipe. In 1976, the contamination peaks had decreased to near background levels, presumably due to radioactive decay. Only background activity was detected in boreholes 299-E28-56 and 299-E28-60. It was concluded that radioactive contaminants are held high in the soil column; no measureable migration of radionuclides beneath the 216-B-9 Crib and Tile Field occurred between 1963 and 1973, and breakthrough to groundwater did not occur. Near the 216-B-56 Crib, scintillation probe profiles from well 299-E28-14 were evaluated and only background activity was reported.

DOE (1993a) compiled the scintillation probe profiles from the boreholes located near the 216-B-5, 241-B-361, 216-B-9, 216-B-59, and 216-B-56 waste management units into cross sections by correlating the scintillation probe profiles with the lithologic section presented by Smith (1980) and the regional mapping of Lindsey et al. (1992). The features on the scintillation probe profiles correlated well with the local stratigraphy. Elevated gamma activity was observed below the

groundwater table in all of the groundwater wells in the area and the proposed source of this contamination was the 216-B-5 Injection Well. In the vicinity of the 216-B-5 Injection Well, it was concluded that the distributions of the radionuclides above the water table are probably controlled by the layering in the Hanford H3, which was interpreted to dip to the south-southwest. On the basis of the lack of elevated gamma readings in boreholes 299-E28-56, 299-E28-58, 299-E28-59, and 299-E28-60, no indications of lateral migration of radionuclides were evident.

4.0 Logging Results

This section details the results of recent logging in boreholes within the study area. Log plots and Log Data Reports for these boreholes were previously issued and are available in Appendix A on the accompanying CD-ROM and on the Internet at <http://www.gjo.doe.gov/programs/hanf/HTFVZ.html>.

4.1 Boreholes and Wells Logged

Fifteen vadose zone boreholes and 10 groundwater monitoring wells were logged with the SGLS. Five boreholes near and in the 216-B-9 Crib and Tile Field encountered high gamma flux and were logged with the HRLS. Table 4-1 lists the boreholes and groundwater wells that were logged with the SGLS and HRLS during this investigation. Figure 3 shows the boreholes and wells used in the vadose zone characterization efforts for the study area.

The boreholes and groundwater wells identified in Table 4-1 have been associated with specific liquid waste disposal sites based on their relative proximity to these sites. Groundwater wells that are not in close proximity to a waste site are grouped separately. Also included in the table are the dates the boreholes were drilled, previous logs reviewed for this characterization, the depth intervals (elevation) logged with the SGLS, and a general description of the depths at which specific radionuclides were detected. All boreholes were logged from ground surface to the total depth except for seven groundwater wells. Because of waste management issues, DOE-GJO was unable to log below the water table in the following groundwater wells: 299-E28-3, 299-E28-7, 299-E28-10, 299-E28-14, 299-E28-23, 299-E28-24, and 299-E28-25.

Table 4-1. Boreholes and Groundwater Monitoring Wells Logged with the SGLS and HRLS During the Investigation of the 216-B-5 Injection Well, 216-B-9 Crib & Tile Field, and Adjacent Sites

Borehole	Date Drilled TOC (ft)	Previous Logging Review	SGLS Interval Logged (Elevation, ft)	Elevation (ft) Radionuclides Detected	Maximum Concentration (pCi/g)
216-B-5 Injection Well					
299-E28-1	11/1947 688.5	^a 1959	685-365	685-684 – ¹³⁷ Cs 417-413 – ¹³⁷ Cs 404 – ⁶⁰ Co 372-365 – ⁶⁰ Co	<1 <1 <1 1.1
299-E28-3	1/1948 696.2	^a 1963, ^b 1979	697-416	697 – ¹³⁷ Cs 664 – ¹³⁷ Cs 592 – ¹³⁷ Cs 54 1 – ¹³⁷ Cs	1.5 <1 <1 <1
299-E28-7	4/1948 690.0	^a 1959, ^a 1963, ^b 1976	683-398	683 – ¹³⁷ Cs 575-571 – ¹³⁷ Cs 543 – ¹³⁷ Cs 444 – ¹³⁷ Cs	1 <1 <1 <1
299-E28-23	7/1979 689.5		688-403	688-423 – ¹³⁷ Cs 422-403 – ¹³⁷ Cs	<100 3,200
299-E28-24	2/1980 689.6	1986, ^b 1987	688-403	688-627 – ¹³⁷ Cs 612-605 – ¹³⁷ Cs 593-421 – ¹³⁷ Cs 420-403 – ¹³⁷ Cs	<1 24 1.4 3,300
299-E28-25	2/1980 689.1	^c 1992	688-402	688-672 – ¹³⁷ Cs 664-635 – ¹³⁷ Cs 509 – ¹³⁷ Cs 478 – ¹³⁷ Cs 443-402 – ¹³⁷ Cs	2.6 <1 <1 <1 400
241-B-361 Settling Tank					
299-E28-73	5/1979 689.0	^b 1987	689-650	None	None
299-E28-74	5/1979 689.4	^b 1987	689-648	688 – ¹³⁷ Cs	<1
216-B-9 Crib & Tile Field					
299-E28-53	7/1948 686.3	^a 1963, ^b 1976	684-661	684-661 – ¹³⁷ Cs	84,000
299-E28-54	7/1948 686.2	^a 1963, ^b 1976	684-536	682 – ¹³⁷ Cs 669-652 – ¹³⁷ Cs 611 – ¹³⁷ Cs 629 – ²³⁸ U 620 – ²³⁸ U	<1 4,000 <1 17 17
299-E28-55	7/1948 685.9	^a 1963, ^b 1976	683-535	683-684 – ¹³⁷ Cs 674-648 – ¹³⁷ Cs 643-626 – ^{235/238} U (intermittent)	2.6 16,000 2/28
299-E28-56	7/1948 682.8	^a 1963, ^b 1976	682-532	680-679 – ¹³⁷ Cs 554 – ¹³⁷ Cs 669 – ²³⁸ U 648 – ^{235/238} U	1.4 <1 14 1/19

Table 4-1. Boreholes and Groundwater Monitoring Wells Logged with the SGLS and HRLS During the Investigation of the 216-B-5 Injection Well, 216-B-9 Crib & Tile Field, and Adjacent Sites

Borehole	Date Drilled TOC (ft)	Previous Logging Review	SGLS Interval Logged (Elevation, ft)	Elevation (ft) Radionuclides Detected	Maximum Concentration (pCi/g)
299-E28-57	7/1948 683.5	^a 1963, ^b 1976	681-533	680-679 – ¹³⁷ Cs 673-642 – ¹³⁷ Cs 580 – ¹³⁷ Cs 553 – ¹³⁷ Cs 664-665 – ^{235/238} U 631 – ^{235/238} U	1.3 7,000 <1 <1 2/20 1/15
299-E28-58	7/1948 681.6	^a 1963, ^b 1976	679-533	678-677 – ¹³⁷ Cs 649 – ¹³⁷ Cs 617 – ^{235/238} U	<1 <1 1/18
299-E28-59	7/1948 682.3	^a 1963, ^b 1976	680-538	678 – ¹³⁷ Cs 578 – ¹³⁷ Cs 673 – ²³⁵ U	<1 <1 1
299-E28-60	7/1948 680.7	^a 1963, ^b 1976	680-533	680-676 – ¹³⁷ Cs 571 – ¹³⁷ Cs	<1 <1
299-E28-61	8/1948 685.9	^a 1963, ^b 1976 ^c 1992	684-534	682 – ¹³⁷ Cs 668-657 – ¹³⁷ Cs 600 – ¹³⁷ Cs 663 – ²³⁸ U 649-648 – ^{235/238} U	<1 220 <1 15 1/15
299-E28-62	10/1948 683.9		682-672	682-672 – ¹³⁷ Cs	5,100
299-E28-67	683.5		681-671	679 – ¹³⁷ Cs	<1
299-E28-68	682.9		680-671	680-678 – ¹³⁷ Cs	<1
299-E28-50	680.4		678-668	678-675 – ¹³⁷ Cs 670-668 – ¹³⁷ Cs	4 60
216-B-56 Crib					
299-E28-14	698	^a 1968, ^b 1976 ^b 1979, ^b 1987	696-412	695 – ¹³⁷ Cs 678 – ¹³⁷ Cs 426-415 – ¹³⁷ Cs (intermittent)	<1 <1 <1
Groundwater Wells					
299-E28-2	1/1948 684.2	^a 1958, ^a 1963 ^b 1979	682-374	682 – ¹³⁷ Cs 379-374 – ⁶⁰ Co	<1 <1
299-E28-5	3/1948 676.5	^a 1958, ^a 1963	674-366	674 – ¹³⁷ Cs 415-414 – ¹³⁷ Cs 376-370 – ⁶⁰ Co	<1 <1 <1
299-E28-10	8/1961 681.0	^a 1963, ^b 1979	679-410	679-678 – ¹³⁷ Cs	<1

^a Gross gamma or scintillation probe used prior to 1976

^b Gross gamma system used between 1976 and 1991

^c Radionuclide Logging System (RLS) used after 1990

4.2 Radionuclides Detected

Only ¹³⁷Cs, ⁶⁰Co, and ^{235/238}U were detected while logging in this area. Three-dimensional data plots, which are presented in Figures 11 through 15, provide an enhanced perspective of the contaminant distribution of ¹³⁷Cs, ⁶⁰Co, ²³⁸U, and ²³⁵U. Figures 13 through 15 show the ¹³⁷Cs, ²³⁵U, and ²³⁸U distributions for the 216-B-9 Crib and Tile Field. Even though ²³⁸U and ²³⁵U co-exist, both are

plotted because they were detected at scattered locations near their respective detection limits. These three-dimensional data plots show the 0.5-ft assays recorded by the SGLS or HRLS as spheroids that are colored and sized to show the position and relative concentrations of each radionuclide. In addition, cross sections (Figures 16 through 20) provide two-dimensional perspectives of the distribution of the man-made radionuclides and ^{40}K . These cross sections are discussed in Section 5.0, “Interpretation of Results.” No other man-made radionuclides were detected in the study area.

4.2.1 Cs-137

^{137}Cs was detected in every well and borehole except for borehole 299-E28-73. A three-dimensional data plot, which is presented in Figure 11, provides an enhanced perspective of the contaminant distribution for the entire study area. ^{137}Cs was detected near the ground surface at levels less than 1 pCi/g. In addition to the surface ^{137}Cs contamination and scattered occurrences of ^{137}Cs near the MDL in well 299-E28-3, ^{137}Cs was intercepted near the 216-B-5 Injection Well (Figure 16) and the 216-B-9 Crib and Tile Field (Figures 13, 19, and 20). The maximum ^{137}Cs concentration detected near the 216-B-5 Injection Well was 3,300 pCi/g at an elevation of 418 ft (272-ft log depth). The maximum ^{137}Cs concentration detected near the 216-B-9 Crib was 84,000 pCi/g at an elevation of 646 ft (20-ft log depth).

4.2.2 Co-60

^{60}Co was only detected below the water table at activities ranging from the MDL to 1.1 pCi/g, except for well 299-E28-1, where ^{60}Co was also detected at an elevation just above the groundwater intercept. A three-dimensional data plot of the ^{60}Co subsurface distribution (Figure 12) provides an enhanced perspective of the contaminant distribution. ^{60}Co was detected at elevations between 404 and 365 ft. ^{60}Co was not detected in any borehole above an elevation of 404 ft.

4.2.3 U-235/238

In the study area, anthropogenic uranium (^{235}U and ^{238}U) was only detected at the 216-B-9 Crib and Tile Field. Even though ^{238}U and ^{235}U co-exist, both are plotted because they were detected at scattered locations near their respective detection limits. $^{235/238}\text{U}$ (Figures 14, 15, 19, and 20) were detected at elevations ranging from 617 to 673 ft (approximately 11- to 67-ft log depth). Three-dimensional data plots, which are presented in Figures 14 and 15, illustrate the $^{235/238}\text{U}$ distribution at the 216-B-9 Crib and Tile Field.

5.0 Interpretation of Results

All log data collected from the boreholes and wells in the study area were assembled and correlated in an effort to identify geophysical markers, contaminated zones, and potential contaminant sources. Five cross sections that pass through the waste sites and connect with nearby boreholes were constructed from spectral gamma logs collected in the study area.

C Tech Development Corporation’s Environmental Visualization System (EVS) was used to perform a geostatistical analysis of the data and to create visualizations. Visualizations generated by EVS

were then selected for the report and exported to a graphics program for annotation and final presentation.

A review and comparison of historical logs shown in Table 4-1 with the current logs were conducted to identify changes over time that might affect the current interpretation.

An interpretation regarding the nature and extent of contamination for each waste site that incorporates the cross sections, visualizations, and historical data is presented. This interpretation also presents possible sources of the contamination.

5.1 Geophysical Correlation

The purpose of this analysis was to identify and correlate sedimentary features between boreholes that may influence the migration of contaminants in the vadose zone. The data acquired from 25 boreholes (Table 4-1) were interpreted and correlated with existing geophysical and stratigraphic models for the area. A simplified stratigraphic model based on DOE (1993a) for the 216-B-5 Injection Well (Figure 4) was used as a starting point to identify potential geophysical markers. The spectral gamma-ray logs for the naturally occurring isotopes (^{40}K , ^{238}U , and ^{232}Th) and total gamma logs for each borehole were compared and correlated with those from surrounding boreholes and checked for the presence of man-made radionuclides. After noting any influences of man-made radionuclides and changes in casing thickness on the spectral and total gamma logs, geophysical markers were identified.

Within the study area, five cross sections were constructed from spectral gamma logs. All SGLS log data collected from the boreholes and wells in the study area are shown on Cross Sections A-A' (Figure 16), B-B' (Figure 17), C-C' (Figure 18), D-D' (Figure 19), and E-E' (Figure 20) and correlated with the existing geophysical control in the surrounding area. Figure 3 shows the locations of these cross sections. The cross sections serve multiple purposes. They were constructed such that 1) the nature and extent of measured contamination are portrayed at each major waste site, 2) relationships of contamination between sites (if any) are presented, 3) stratigraphic relationships that may affect contamination profiles can be understood, and 4) relationships between probable migratory pathways and probable sources of contamination are identified.

Both the contaminant profile and contaminant concentration are useful as indications of the proximity of boreholes to a contaminant source. For example, intercepts of contamination at a higher elevation suggest closer proximity to a source. Higher relative concentrations may also suggest closer proximity. By evaluating the contaminant profile in conjunction with stratigraphic correlation based on evaluation of natural gamma emitters, it may be possible to identify likely sources and probable migration pathways.

In the absence of man-made radionuclides, gamma-ray log response is generally proportional to abundance of silt and/or clay that may indicate changes in lithology. The new spectral gamma-ray logs are much more useful to interpret stratigraphy than the older gross gamma-ray logs because of better sensitivity to small changes in radioactivity. A far greater advantage is that ^{40}K and ^{232}Th concentrations can be determined from the spectral data. The larger variations in ^{40}K content (about 4 pCi/g) appear to be correlatable between most boreholes. ^{40}K content and ^{232}Th are probably the most reliable stratigraphic indicators.

Variations in natural radionuclides can be used to identify major changes in Hanford formation lithology. The H1 gravel facies is identified by a relatively low ^{40}K concentration of about 13 pCi/g and lower total gamma reading. The H2 sand facies is identified by a marked increase in apparent ^{40}K concentrations to about 18 pCi/g and an increase in total gamma count rate. In geophysical terms, the base of the H2 generally is defined as a zone of elevated total gamma count rate just above the point where apparent ^{40}K concentrations start to decrease. The H3 generally contains coarser sediment than the H2 and has gamma-ray response similar to H1; it is identified by lower total gamma count rates and ^{40}K concentrations ranging from 12 to 15 pCi/g. Within the H3, Smith (1980) and DOE (1993a) have identified a silt layer (Figure 4). On cross sections A-A', B-B', and C-C' (Figures 16, 17, and 18), this silt layer has been labeled the "H3 Silt". This silt layer is readily identified at elevations ranging between 429 and 454 ft, by a 2- to 4-pCi/g increase in ^{40}K content with a corresponding increase in total gamma count rate and ^{232}Th concentration. This silt layer is apparent in eight of the 11 boreholes that are deep enough to intercept the silt layer, which appears to dip to the northeast.

The influence of stratigraphy upon the subsurface distribution of radionuclides near Hanford's waste sites was recognized at least as early as 1950 (Brown and Ruppert 1950). The purpose of correlating the stratigraphic units was to evaluate and account for their effect on lateral spreading. "Stratification tends to increase spreading of liquids along bedding planes and along contacts between sedimentary units" (Fecht et al. 1977). The Log Data Reports in Appendix A were completed prior to the production of this report, and the stratigraphic interpretation contained in Appendix B describes the compilation of the stratigraphic interpretations supplied in each individual Log Data Report.

5.2 Development of the Visualizations

Visualizations were prepared to illustrate the extent of contamination within the three-dimensional space that constitutes the vadose zone in the vicinity of the study area. Creating the visualizations required developing geostatistical models of the ^{137}Cs , ^{60}Co , and $^{235/238}\text{U}$ contaminant distributions. Visualizations of contamination in the vicinity of the study area include three-dimensional "sphere plots," which show contamination as detected in boreholes relative to the locations of the waste sites and the study area. Because ^{60}Co and $^{235/238}\text{U}$ were detected at low concentrations and at a few locations, their distributions are shown only on the three-dimensional data plots. The ^{137}Cs contaminant models are considered empirical models because they are based on data obtained by measuring the ^{137}Cs concentrations at discrete points in the subsurface and extrapolating those values into the nearby subsurface volume. These contaminant models *are not conceptual models* based on assumed waste disposal and contaminant transport mechanisms. No effort was made to calculate hypothetical distributions using contaminant transport models.

The visualizations are intended to provide the reader with an understanding of how the gamma-emitting contaminants may have been distributed in the vadose zone sediments. The visualizations may also provide an assessment of the extent to which operations may have contributed to contaminant distribution and to define areas of concern for subsequent investigation.

5.2.1 Development of the Interpreted Data Set

The radionuclide concentration values derived from the SGLS and HRLS data reported in the Log Data Reports were placed in data files that defined the position of each data point and the nuclide-

specific concentration for that point. These data files were revised to create an "Interpreted Data Set," and the ^{137}Cs visualizations are based on these revisions. The revisions consist of removing radionuclide concentrations that are not considered reflective of actual formation concentrations.

The interpreted data set reflects interpretations of the radiological contamination based on familiarity with the distribution of contaminants gained from experience with many SGLS logs. Specific data points may be removed from the interpreted data set if they are judged to represent contamination on the outside of the casing resulting from "dragdown" during drilling, internal casing contamination from a variety of sources, or contamination that either appears to be localized to the borehole or that may be from a remote source, such as a buried pipeline. Shape factor analysis, which in certain situations can distinguish contamination in the formation from contamination that is related to the borehole casing (e.g., dragdown of contamination during drilling), was not used because the casing thicknesses were variable and not consistent with the 6-in.-diameter, 0.28-in.-thick casing for which the technique was developed (Wilson 1997). Log run overlaps are eliminated, and SGLS data are replaced with HRLS data where appropriate. The resultant concentration data are collectively referred to as the interpreted data set.

Intervals of apparent ^{137}Cs contamination near the 216-B-5 Injection Well were removed from the SGLS data. The casing in the 216-B-5 Injection Well was perforated below an elevation of 446 ft, providing the means for distributing waste solutions into the surrounding sediments (Smith 1980). All ^{137}Cs occurrences detected by the SGLS above an elevation of 446 ft in wells 299-E28-7, 299-E28-23, 299-E28-24, and 299-E28-25 were removed from the dataset. These occurrences were omitted because the contamination is believed to occur inside one of the casing strings. Above an elevation of 446 ft in wells 299-E28-23, 299-E28-24, and 299-E28-25, the highest reported sediment sample concentration for ^{137}Cs was only 0.0131 pCi/g when the wells were drilled in 1979 and 1980. Figure 16 illustrates that the ^{137}Cs detected by the SGLS in these wells above an elevation of 446 ft ranges from 0.2 to 100 pCi/g. The ^{137}Cs detected above an elevation of 446 ft was probably "dragged-up" during drilling in 1979 or 1980 when these boreholes were drilled. Similarly, the ^{137}Cs detected by the SGLS above an elevation of 446 ft in well 299-E28-7 was also "dragged-up" when the well was deepened in 1979. No nearby waste sites are reported to be potential sources for the contamination observed above an elevation of 446 ft near the 216-B-5 Injection Well, which ceased operating in 1947. The intervals of ^{137}Cs contamination that have been removed from the SGLS data are indicated in Table 5-1. No ^{60}Co or $^{235/238}\text{U}$ concentration data were omitted from the data set for any borehole.

Table 5-1. Summary of the Wells Edited Before Inclusion Into the Interpreted Data Set Used During the Investigation of the 216-B-5 Injection Well and 216-B-9 Crib and Tile Field

Borehole	Date Drilled	Interval Edited (Log Depth)	Comment
299-E28-7	April 1948; deepened in May 1979	0 to 145 ft	The highest ^{137}Cs concentration in a sediment sample was 65.1 pCi/g at 320-ft log depth as reported by Smith (1980).
299-E28-23	July 1979	0 to 243 ft	The highest ^{137}Cs concentration was 51,300 pCi/g at 284-ft log depth as reported by Smith (1980).
299-E28-24	Feb. 1980	0 to 243 ft	The highest ^{137}Cs concentration in a sediment sample was 1,600 pCi/g at 294-ft log depth as reported by Smith (1980).
299-E28-25	Feb. 1980	0 to 210 ft	The highest ^{137}Cs concentration in a sediment sample was 135 pCi/g at 255-ft log depth as reported by Smith (1980).

5.2.2 Visualizations

The distribution of boreholes within the study area was used to develop a three-dimensional geostatistical model at the 216-B-9 Crib and Tile Field and a two-dimensional geostatistical model at the 216-B-5 Injection Well. The kriging algorithms used to extrapolate data are most effective when data points are uniformly distributed; the uncertainty increases with distance from known points. Visualizations are dependent on parameter selection as well as the subsurface data. Thus, many different visualizations are possible based on any one singular data set. The radionuclide concentration data were input to EVS subroutines that created a quadrilateral finite-element grid with kriged nodal values and output these data for viewing. The visualizations were constructed to include the highest and lowest node values. Because nodes were set up at all data sampling points, the extents of the model and the visualizations were governed by the positions of the boreholes. The model does not extrapolate beyond the extent of either the assumed range value or the kriging extent. As a result, both the model and the visualizations can only extend to the maximum depth of the boreholes and the extent of the geostatistical range.

The EVS software is an “expert” system that automatically determines parameter settings for the geostatistical model and for the kriging operation. These settings were used as a starting point for refinement of the model. Parameters were initially calculated by the software and then refined to create the most representative models for the ^{137}Cs distributions.

The kriging software applied an “anisotropy ratio” that allowed the user to adjust the way values are extrapolated. The anisotropy ratio applied a bias to horizontal distances over vertical distances. The program default is 10, which means that vertical distances were multiplied by a factor of 10 before the distance between the grid point and the data point was calculated. A data point 1 ft above or below the grid point will thus appear to be 10 times farther away than a data point 1 ft away at the same level. The effect is to lessen the influence of additional data points in the same borehole. The anisotropy “forces” the kriging algorithm to give more weight to data points at the same level.

The 216-B-9 Crib and Tile Field were visualized by creating solid rectangular three-dimensional surfaces at the locations of the crib center and tile field center. The extrapolation is not affected by the insertion of the waste sites; a borehole directly across a crib still influences the node-point concentration calculation.

The horizontal distribution of boreholes within the study area was not adequate for development of a three-dimensional geostatistical model at the 216-B-5 Injection Well. Therefore, the kriging capability in EVS was only used to extrapolate in two dimensions along A-A' (Figures 3 and 16) at the injection well. EVS was used to model the surfaces defined by the geophysical interpretation of the cross section with the radionuclide concentration data to create the visualization at the 216-B-5 Injection Well.

5.3 Distribution of Man-Made Radionuclides

As noted in Section 4.0, ^{137}Cs , ^{60}Co , and $^{235/238}\text{U}$ were detected by the SGLS in the study area. After considering the relationships between the sites using the historical log data, cross sections, and visualizations, it was determined that the contamination distribution should be summarized and discussed in three areas: 1) the 216-B-5 Injection Well, 2) the 216-B-9 Crib and Tile Field, and 3) a ^{60}Co presence below the groundwater table. Visualizations of ^{137}Cs are presented in Figures 21, 22, and 23. Because ^{60}Co and $^{235/238}\text{U}$ were detected at low concentrations and at a few locations, their distributions are only shown on the sphere plots.

5.3.1 216-B-5 Injection Well

Wells 299-E28-23, 299-E28-24, 299-E28-25, and 299-E28-7 (Figure 3) are located within 75 ft of the 216-B-5 Injection Well. Three-dimensional data plots, which are presented in Figures 11 and 12, include data for these boreholes. ^{137}Cs is the only man-made radionuclide that was detected near the injection well. For reasons previously stated, all ^{137}Cs occurrences detected by the SGLS above an elevation of 446 ft (Figure 16) in wells 299-E28-7, 299-E28-23, 299-E28-24, and 299-E28-25 are believed to occur inside one of the casing strings. Figure 21 is a visualization of the distribution of ^{137}Cs near the injection well, which is consistent with the distribution reported by Smith (1980) as shown on Figure 9. It is important to note that Figure 9 contains data below the water table and Figure 21 does not. The elevation of the water table in 1980 (405 ft) is close to that in 2002 (402 ft), and both water table elevations are still above the 1949 water table elevation (388 ft). Above the present groundwater level and below elevation 446 ft, ^{137}Cs concentrations appear to decrease with distance (Figure 16) and are below the detection limit within 75 ft of the injection well. The highest ^{137}Cs concentrations are below an elevation of 420 ft.

Other than minor surface contamination, the SGLS logs of the two boreholes (299-E28-73 and 299-E28-74, Figure 17) located close to the 241-B-361 Settling Tank did not intercept any gamma-emitting radionuclides. Therefore, subsurface evidence that the tank leaked was not detected. These two boreholes are located approximately 3 ft (1 m) north and south of the tank (Smith 1980).

Brown and Ruppert (1950) suggested the “floating of activity” on the surface of the groundwater near the 216-B-5 Injection Well. Figures 7, 8, and 9 illustrate that the highest radionuclide activities are near the 1948 water table elevation and closest to the injection well. As shown on Figures 7 through 10, flow direction from the injection well was primarily to the southeast (Brown and Ruppert 1950; Smith 1980). The ^{137}Cs concentrations detected in wells 299-E28-14 and 299-E28-1 (Figures 16 and 17) at elevations between 426 and 415 ft probably originated from the injection well and were transported by groundwater to their present location.

The H3 Silt appears to have influenced the distribution of ^{137}Cs (Smith 1980). The top of the H3 Silt at well 299-E28-25 is slightly down-dip from well 299-E28-23, and ^{137}Cs activities in the H3 Silt at

well 299-E28-25 are elevated (Figure 16). ^{137}Cs activities in the H3 Silt are higher at well 299-E28-25 than at 299-E28-23, which is closer to the injection well. Below the H3 Silt, ^{137}Cs activities are higher at well 299-E28-23 than at 299-E28-25. The H3 Silt appears to be absent in well 299-E28-24, and significant ^{137}Cs activities do not occur at the equivalent elevation of the H3 Silt in well 299-E28-24.

^{60}Co was not detected by the SGLS in the vadose zone near the injection well (Figures 12 and 16). Smith (1980) did not report the occurrence of ^{60}Co in the samples acquired during the drilling of wells 299-E28-23, 299-E28-24, and 299-E28-25 and the deepening of well 299-E28-7. Simpson et al. (2001) indicated that less than 0.01 Ci of ^{60}Co were discharged at the 216-B-5 Injection Well.

5.3.2 216-B-9 Crib and Tile Field

^{137}Cs contamination was detected in two intervals, which are related to the elevation of discharge from either the crib or the tile field (Figures 19 and 20). Three-dimensional data plots for the 216-B-9 Crib and Tile Field (Figures 13 through 15) illustrate that ^{137}Cs is the predominant contaminant detected in this area. Near the ground surface, ^{137}Cs contamination is detected with a maximum concentration of approximately 4 pCi/g at elevations ranging from 685 to 680 ft. An interval of ^{137}Cs contamination related to discharges from the tile field ranges in elevation from about 675 to 667 ft. After receiving about 4,000 m³ of waste, the crib became sealed with sludge, and overflow into the tile field began in November 1948 (Brown and Ruppert 1950). The boreholes where ^{137}Cs was detected and is interpreted as having been discharged from the tile field are boreholes 299-E28-55, 299-E28-62, and 299-E28-57 (Figure 19), located on the west side of the tile field. The maximum ^{137}Cs concentration associated with the tile field was approximately 7,000 pCi/g in borehole 299-E28-57. The ^{137}Cs contamination is interpreted as having been discharged from the crib. ^{137}Cs was detected in all of the boreholes at the 216-B-9 Crib and only at borehole 299-E28-57 in the tile field (Figures 19 and 20). The interval of ^{137}Cs related to seepage from the crib has its highest elevation in borehole 299-E28-53 at approximately 673 ft. The maximum ^{137}Cs concentration measured was approximately 84,000 pCi/g in borehole 299-E28-53 at an elevation of 667 ft. The bottom of the crib is at an elevation of 669 ft. In borehole 299-E28-57, ^{137}Cs detected below 663 ft is interpreted as seepage from crib, which has spread along the Hanford H1/H2 boundary. In addition, ^{137}Cs was detected near its MDL at scattered depths and locations at elevations between 615 and 550 ft.

Visualizations of the ^{137}Cs activities at the 216-B-9 Crib and Tile Field are illustrated on Figures 22 and 23. Figure 22 shows the distribution of ^{137}Cs related to the crib and tile field described in the previous paragraph. Figure 23 is an alternative visualization of the ^{137}Cs activities at the 216-B-9 Crib and Tile Field that demonstrates that seepage from the crib and tile field can be explained without the lateral spreading shown on Figure 22. For this visualization (Figure 23) the “Octant Search” method was used to determine which data points were selected for inclusion in the kriging matrix. Figure 23 supports the interpretation in Fecht et al. (1977) that radioactive effluents primarily were discharged to the secondary lateral, immediately south of borehole 299-E28-57. Due to the limited number of boreholes in the area, either interpretation is plausible.

Figures 24 and 25 further describe the ^{137}Cs detected at the 216-B-9 Crib and Tile Field. Zone(s) of soil contaminated with ^{137}Cs (100 pCi/g or greater) are apparent at elevations below the tile field in boreholes north of the crib and at elevations near the base of the crib in boreholes south of the crib (Figure 24). The area of ^{137}Cs contaminated soil appears to dip to the north-northwest, which is

similar to the dip of the Hanford H2. An isopach map of net footage with activities greater than 100 pCi/g is shown on Figure 25. An area with 10 ft or more of contaminated soil (Figure 25) trends from the crib to borehole 299-E28-57. Because the crib sealed with sludge relatively early in its operation, the bulk of the discharges to the soil may have been via the tile field, and the SGLS logging of the crib and tile field indicates that borehole 299-E28-57 is located in the thickest area of contaminated soil (Figure 25). Wastes discharged to the crib and tile field may have migrated down stratigraphic dip toward the north-northwest as well as vertically. The extent of the vadose zone contamination is unknown west of the crib and tile field and south of the crib (Figures 22 through 25).

According to Brown and Ruppert (1950), acid used to clear the crib caused the 299-E28-53 (previously known as 361-B-13) well casing to corrode, and the borehole was filled with sludge and sediments to within 24 ft (7.3 m) of the ground surface. It was concluded that some waste liquids were introduced into the ground at a depth of 150 ft at the 216-B-9 Crib. The maximum ^{137}Cs concentration measured in the study area was approximately 84,000 pCi/g at the bottom of the borehole at a log depth of 25.5 ft.

The gross gamma logging is the best historical record of the gamma contamination around the 216-B-5 Injection Well and the 216-B-9 Crib and Tile Field. Evaluations of previous investigators are summarized in Section 3.6, "Previous Investigations." The gross gamma instrumentation was designed to respond in a consistent manner over the years, making it possible to compare spatial and temporal differences in contaminant profiles. With the limitations of these data well understood, the data have been useful for assessing the general history of the vadose zone contamination. These systems were effective for high activity but were not sensitive to lower radionuclide concentrations (less than approximately 10 pCi/g equivalent ^{137}Cs). Data were presented as plots of the gross count rate in counts per minute (cpm) as a function of depth. Gross gamma logs were visually compared with previous data to determine, in a qualitative manner, if changes had occurred. No additional data processing or analyses were performed on these data.

A comparison of SGLS data to the scintillation probe profiles collected found in Additon et al. (1978) suggests that contaminants from the 216-B-9 Crib and Tile Field did not breakthrough to groundwater. Scintillation probe profiles (reproduced in the Log Data Reports contained in Appendix A) collected in 1963 in boreholes 299-E28-58, 299-E28-59, and 299-E28-60 may have detected gamma activity above background at the north end of the tile field. This gamma activity is not apparent on the profiles collected in 1976, presumably due to radioactive decay. The deepest contamination recognized on any of the scintillation probe profiles occurred on the 1963 profile in borehole 299-E28-58 (reproduced in the Log Data Report contained in Appendix A) at elevations between 540 and 550 ft, which is at least 138 ft above the present groundwater level. The deepest contamination encountered by the SGLS (Figures 18, 19, and 20) was ^{137}Cs at activities near its MDL at elevations of 599 ft and 611 ft near the crib. This contrasts with depths of 553 ft, 561 ft, 578 ft, 581 ft, 586 ft underneath the tile field. The SGLS (Figures 19 and 20) intercepted $^{235/238}\text{U}$ at activities near the MDL at elevations ranging from 620 to 543 ft near the crib versus 618 ft, 631 ft, 647 ft, 664 ft, 669 ft, and 672 ft underneath the tile field. The deepest contamination intercepted by the SGLS is at least 151 ft above the present groundwater level.

5.3.3 Adjacent Waste Sites

The 216-B-59 Trench, 216-B-59B Retention Basin, and UPR-200-E-7, 216-B-56 Crib, and 200-E-112 are the other waste sites located in the study area. Because no boreholes were located near the 216-B-59 Trench, 216-B-59B Retention Basin, and UPR-200-E-7, these waste sites could not be evaluated and will not be discussed. Three groundwater wells (299-E28-2, 299-E28-10, and 299-E28-14) are located near the 216-B-56 Crib and 200-E-112. The 216-B-56 Crib was never used (Fecht et al. 1977), and 200-E-112 encompasses two transfer lines that leaked (WIDS). No contamination was intercepted by the SGLS logging in either 299-E28-2 or 299-E28-10 that can be attributed to 200-E-112. The contamination detected by the SGLS logs in the groundwater wells is discussed in the next section.

5.3.4 ⁶⁰Co Contamination Below Groundwater Level

Only three of the 10 groundwater wells in the study area were logged below the water table. Waste management issues prevented logging below groundwater level in wells not specifically associated with the 200-TW1/TW-2 Operable Unit. These wells are 299-E28-1, 299-E28-2, and 299-E28-5, and the intervals of contamination lie below the water table in the Ringold. ⁶⁰Co activities ranged from an MDL of about 0.2 to 1.1 pCi/g (Figure 12). ⁶⁰Co was detected at elevations between 379 and 365 ft. ⁶⁰Co was not detected in any borehole above elevation 404 ft.

When the gross gamma logs for the groundwater monitoring wells in the study area presented in Additon et al. (1978) and Smith (1980) are interpreted on the basis of the SGLS results, elevated gamma (interpreted as ⁶⁰Co) was observed below groundwater level. Elevated gamma was observed below groundwater level in 1959 as far south as well 299-E28-1. 1963 gross gamma log from wells 299-E28-2, 299-E28-5, and 299-E28-10 (Additon et al. 1978) also indicate elevated gamma below the groundwater level. Elevated gamma was not observed in well 299-E28-14 in 1968. The log collected on 5/4/76 detected gamma activity above background in well 299-E28-14. The elevated gamma in well 299-E28-14 indicates that a radioactive contaminant front passed through well 299-E28-14 between 1968 and 1976 (Smith 1980). Elevated gamma has not been observed in well 299-E28-3. The Log Data Reports in Appendix A detail the intervals of elevated gamma observed on the available gross gamma logs.

The 216-B-5 Injection Well is probably not the source of ⁶⁰Co observed in the study area. Only 0.006 Ci of ⁶⁰Co was reportedly discharged from the injection well (Simpson et al. 2001). Smith (1980) did not report the occurrence of ⁶⁰Co in the samples acquired during the drilling of wells 299-E28-23, 299-E28-24, and 299-E28-25 and the deepening of well 299-E28-7. Figures 7 through 10 indicate that gamma contamination from the 216-B-5 Injection Well that had spread as far as well 299-E28-2 in 1947 was due to short-lived radionuclides. By 1949, elevated contaminant activity was not present at well 299-E28-2. Therefore, the 216-B-5 Injection Well is probably not the source ⁶⁰Co observed in the area. Contamination from the 216-B-9 Crib does not appear to have reached groundwater. On the basis of the historical logs in wells near the 216-B-5 Injection Well and discharge estimates for 200 East waste sites from Simpson et al. (2001), the elevated gamma (interpreted as ⁶⁰Co) detected below the current groundwater level may have originated from the BY Cribs north of the BY Tank Farm as suggested by Smith (1980). Smith (1980) suggested that the gamma activity below groundwater level reached the wells in the study area by flowing along the surface of the basalt, which slopes to the south from the BY Cribs.

5.4 Comparison to Prior Spectral Gamma Logging

A comparison of the SGLS (data acquired for this report) and RLS logs (previously acquired spectral gamma log data) was made to determine if any significant changes in subsurface contaminant profiles have occurred. The boreholes with existing RLS logs are 299-E28-25 and 299-E28-61. Discrepancies in log depth between the SGLS and RLS measurements are typical. The cause is probably depth initialization differences between the top of casing and ground level. SGLS depth measurements are consistently referenced to the top of casing. In order to compare the measurements, the RLS data are adjusted to the more current SGLS data based on the profiles of the respective log data. RLS data are decayed to the date of the SGLS measurements where necessary to make valid comparisons. Figure 26 is the comparison log plot of ^{137}Cs data collected in 1992 by Westinghouse Hanford Co. (WHC) and in 2001 by DOE-GJO (MACTEC-ERS) in well 299-E28-25. The comparison for borehole 299-E28-61 is detailed in the Log Data Report included in Appendix A. Apparent ^{137}Cs concentrations show good agreement between the logging systems when the decayed concentrations are above the SGLS MDL. Other than radioactive decay, no significant changes in contaminant profile appear to have occurred in the boreholes over the time periods between log events (10 years).

5.5 Potential Uncertainties and Inaccuracies

The interpretations discussed above are subject to a relatively high degree of uncertainty because of the number and distribution of boreholes with respect to the waste sites; consequently, the extent of the vadose zone contamination is poorly controlled both vertically and horizontally.

The construction of most boreholes is documented in the form of drilling logs. It is common for the drilling logs to provide varying degrees of detail and description regarding the drilling operations, geologic descriptions of sediments penetrated by the drilling, and explanation of the construction configurations of the "as-built" boreholes. Geologic sample descriptions are subjective and the depth control can vary by as much as 5 ft. The drilling logs provide information regarding when and how the boreholes were drilled and document the occurrences of radiological contamination that were encountered during drilling.

Some of the cased boreholes are open at the bottom and may contain sediment or contaminated material that migrated down the inside of the borehole casing. As a result, the gamma rays emitted from these sediments and/or materials are not attenuated by the casing, but a casing attenuation factor is applied to the log data during processing. Therefore, the reported apparent concentrations may be slightly higher at the bottoms of the boreholes.

6.0 Conclusions

Twenty-five boreholes were logged with the SGLS in the area of surrounding the 216-B-5 Injection Well and 216-B-9 Crib and Tile Field. Gamma-emitting radionuclide concentration data were generated for naturally occurring and man-made radionuclides at 0.5-ft intervals and one deep borehole was logged at 1-ft intervals. Logging results were used to create a baseline data set for this collection of waste sites. Log Data Reports and log plots were prepared and published separately for each individual borehole. The Log Data Reports provide a history of boreholes and place the SGLS

log data into an appropriate format to be used for waste site environmental activities that may include monitoring.

Empirical ^{137}Cs , ^{60}Co , ^{235}U , and ^{238}U contamination distribution models were created. These cross sections and models were used to create visualizations of the contamination distribution that were discussed in this report. A review of historical information was conducted to integrate with current information when interpreting the data. The information relating to the contamination distribution beneath the study area can be used to locate additional characterization boreholes, to implement a monitoring program, to provide input for risk assessment calculations, and for planning site environmental and closure activities.

^{137}Cs , ^{60}Co , ^{235}U , and ^{238}U were detected while logging in this study area. The two major waste sites (216-B-5 Injection Well and 216-B-9 Crib and Tile Field) in the study area contained sufficient boreholes such that an evaluation could be made. ^{137}Cs was the predominant contaminant detected at these waste sites. The maximum ^{137}Cs concentration detected near the 216-B-5 Injection Well was 3,300 pCi/g, and the maximum ^{137}Cs concentration detected near the 216-B-9 Crib was 84,000 pCi/g. ^{137}Cs was detected in every well and borehole except for 299-E28-73. Near the ground surface ^{137}Cs was detected at levels less than 1 pCi/g. Aside from the surface ^{137}Cs contamination and scattered intercepts of ^{137}Cs near the MDL in well 299-E28-3, ^{137}Cs was detected only near the 216-B-5 Injection Well and the 216-B-9 Crib and Tile Field. ^{60}Co was detected below the water table at activities ranging from the MDL to 1.1 pCi/g. ^{60}Co was detected at elevations between 404 and 365 ft. $^{235/238}\text{U}$ was only detected at the 216-B-9 Crib and Tile Field at activities near the MDL.

Near the 216-B-5 Injection Well, ^{137}Cs concentrations detected above an elevation of 446 ft in wells 299-E28-7, 299-E28-23, 299-E28-24, and 299-E28-25 are believed to occur inside one of the casing strings. The 216-B-5 Injection Well was perforated below an elevation of 446 ft. The ^{137}Cs above an elevation of 446 ft was probably “dragged-up” during drilling in 1979 or 1980 when these boreholes were first drilled or later deepened. Reported ^{137}Cs activities in sediment samples collected during the drilling of these wells were below the SGLS MDL for ^{137}Cs above an elevation of 446 ft.

The distribution of ^{137}Cs near the injection well, as determined from the SGLS logging data, appears consistent with the distribution reported by Smith (1980). Above the present groundwater level, ^{137}Cs concentrations appear to decrease with distance and are below the detection limit within 75 ft of the injection well. The highest ^{137}Cs concentrations are below an elevation of 420 ft. The ^{137}Cs concentrations detected in wells 299-E28-14 and 299-E28-1 at elevations between 426 and 415 ft probably originated from the injection well and were transported by groundwater to their present location. The H3 Silt appears to have influenced the distribution of ^{137}Cs near the injection well. ^{137}Cs activities in the H3 Silt are higher at well 299-E28-25 than at 299-E28-23, which is closer to the injection well, and the SGLS generally detected the highest activities in well 299-E28-23. The logging of two boreholes (299-E28-73 and 299-E28-74) located close to the 241-B-361 Settling Tank did not detect any gamma-emitting radionuclides that would indicate that the tank had leaked.

The ^{137}Cs activities detected at the 216-B-9 Crib and Tile Field were mapped. The area of ^{137}Cs contaminated soil appears to dip to the north-northwest. An area with 10 ft or more of contaminated soil trends from the crib to borehole 299-E28-57. Borehole 299-E28-57 is located in the thickest area of contaminated soil. Wastes discharged to the crib and tile field migrated vertically as well as down stratigraphic dip toward the north-northwest. The maximum extent of the vadose zone contamination is unknown west of the crib and tile field and south of the crib.

SGLS logging combined with historical log information collected in 1963 suggest that contaminant breakthrough to the groundwater in the vicinity of the 216-B-9 Crib and Tile Field did not occur. The contamination profiles for the 216-B-9 Crib and Tile Field indicate that significant site-related contamination generally is not detected below 60 ft from the ground surface.

^{60}Co detected below the groundwater is probably the result of contamination from a distant source such as the BY Cribs (Smith 1980), which may have contaminated the groundwater prior to 1963. On the basis of the historical logs, SGLS logs, and discharge estimates for 200 East waste sites from Simpson et al. (2001), the 216-B-5 Injection Well is probably not the source of the ^{60}Co observed in the study area. Historical logs indicate that a radioactive contaminant front (interpreted as ^{60}Co based on the SGLS logs) passed through well 299-E28-14 between 1968 and 1976.

A comparison of the profiles of historical gross gamma logs and current SGLS logs, as well as, a more direct comparison of more recent RLS spectral logs with the SGLS data, suggest contamination profiles and concentrations at the waste sites are not changing other than by radioactive decay.

Although questions remain about the true nature and extent of the ^{137}Cs , ^{60}Co , and uranium contamination, a spectral gamma ray characterization baseline has been established for the study area. Future monitoring can be conducted to determine contaminant movement, direction, rate, and potential presence of additional sources.

7.0 Recommendations

The vadose zone characterization of the study area was conducted to establish a baseline value for gamma radionuclide activities in vadose zone sediments surrounding the waste sites. This baseline can be used for comparisons with future logging data to develop a monitoring program that will determine if changes have occurred and to assess the rate and potential causes of the changes. The data from this characterization project can also be correlated and compared with information other than concentration data, such as moisture data. In addition, these data help support modeling efforts, retrieval operations, RI/FS investigations, and closure activities.

Results of this spectral gamma ray baseline characterization have identified several additional areas where future characterization efforts should be considered. The westward extent of the contamination associated with 216-B-9 Crib and Tile Field is undefined. Depending upon the level of characterization required for mitigation or remedial action, additional boreholes are recommended to the west of the 216-B-9 Crib and Tile Field. A borehole located northwest of borehole 299-E28-57 is recommended to further assess the extent of radiological contamination. A borehole is recommended northwest of borehole 299-E28-53 to assess the effect of the open borehole as a pathway for vadose zone contaminants to the deep vadose zone. Because acid was used to clear the crib, the well casing corroded, and crib sediments washed into the casing. The casing is filled with sludge and sediments to within 24 ft (7.3 m) of the ground surface and some waste liquids were introduced into the ground at a depth of 150 ft (Brown and Ruppert 1950).

The SGLS should be used to log the interval below the groundwater intercept in the wells near the 216-B-5 Injection Well. Logging this 40-ft interval in the groundwater is essential to fully characterize the area surrounding the 216-B-5 Injection Well, which is a representative site for the

200-TW-2 Tank Waste Group Operable Unit (DOE 2000). Both Brown and Ruppert (1950) and Smith (1980) constructed detailed maps and geologic cross-sections showing the distribution of gamma-emitting radionuclides in the aquifer. Logging the groundwater within the vicinity of the 216-B-5 Injection Well will provide data that are fundamental to determining mobility of ^{137}Cs and other radionuclides in groundwater under field conditions and for direct comparison to data collected over the past 50 years (Brown and Ruppert 1950; Smith 1980).

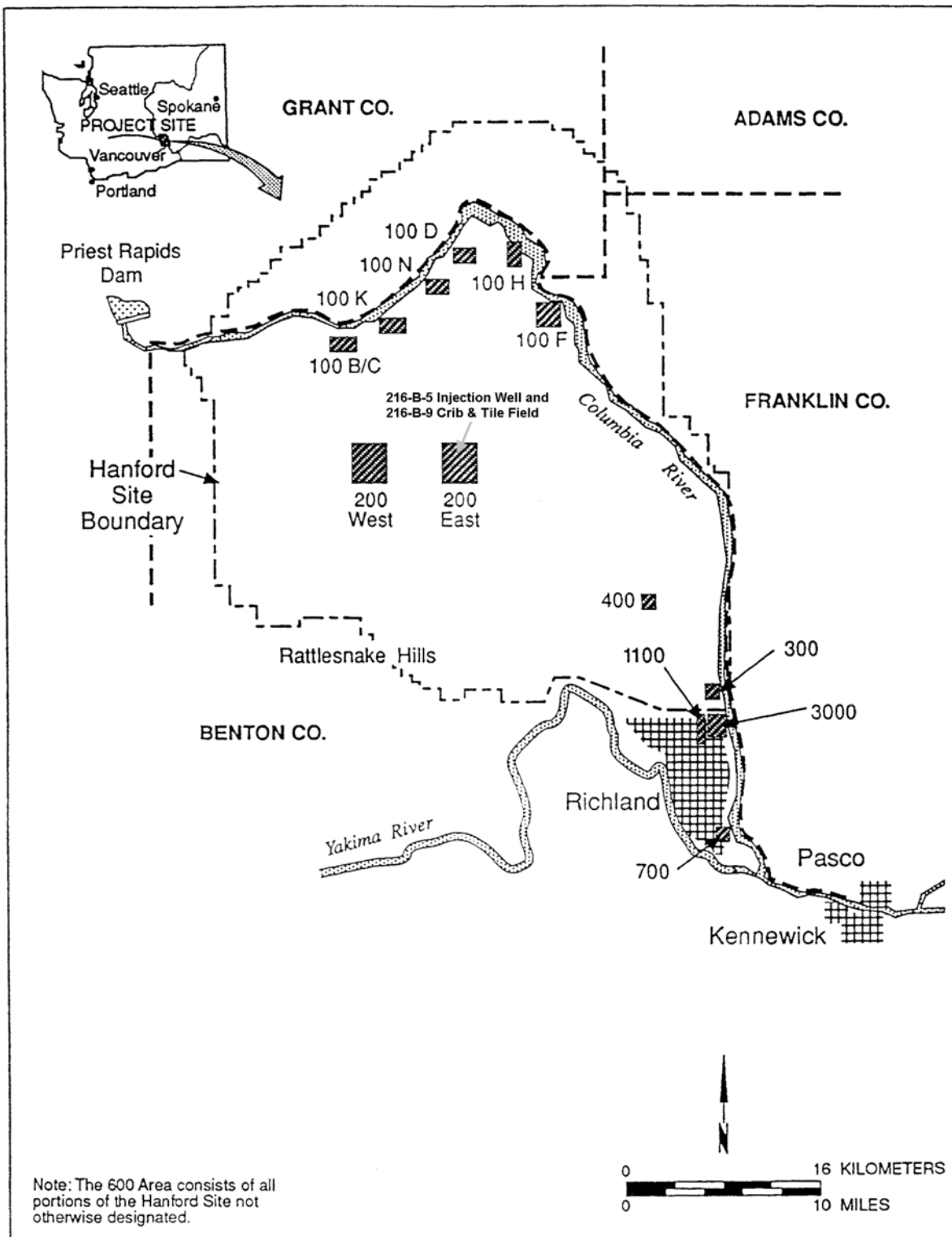
Any additional vadose zone characterization boreholes should include sampling and laboratory analysis for radionuclides and chemical contaminants that do not emit gamma radiation (e.g., ^{90}Sr and ^{99}Tc , ^{241}Am , ^{239}Pu).

Historical logging performed in this area is poorly documented. Additional work is recommended to collect, catalog, digitize, analyze, and assess historical gross gamma logging results for this area. Limited work on collecting historical logs has been performed and presented in various publications that present only a fraction of the logs. Thus, a limited collection of logs has been subjected to a limited amount of analysis. It is recommended that this geophysical characterization work is continued and expanded to include all available logging results.

Other borehole geophysical methods, such as neutron moisture, neutron capture, passive neutron and gamma-density logging, are recommended for development and implementation at the Hanford Site to provide better characterization data. These techniques should become part of the overall vadose zone characterization activities in order to provide data that can be used to validate modeling efforts. Because moisture movement/flux provides the most likely driving force for the migration of radionuclides, it is especially recommended that all the boreholes are logged with an effective moisture logging sonde.

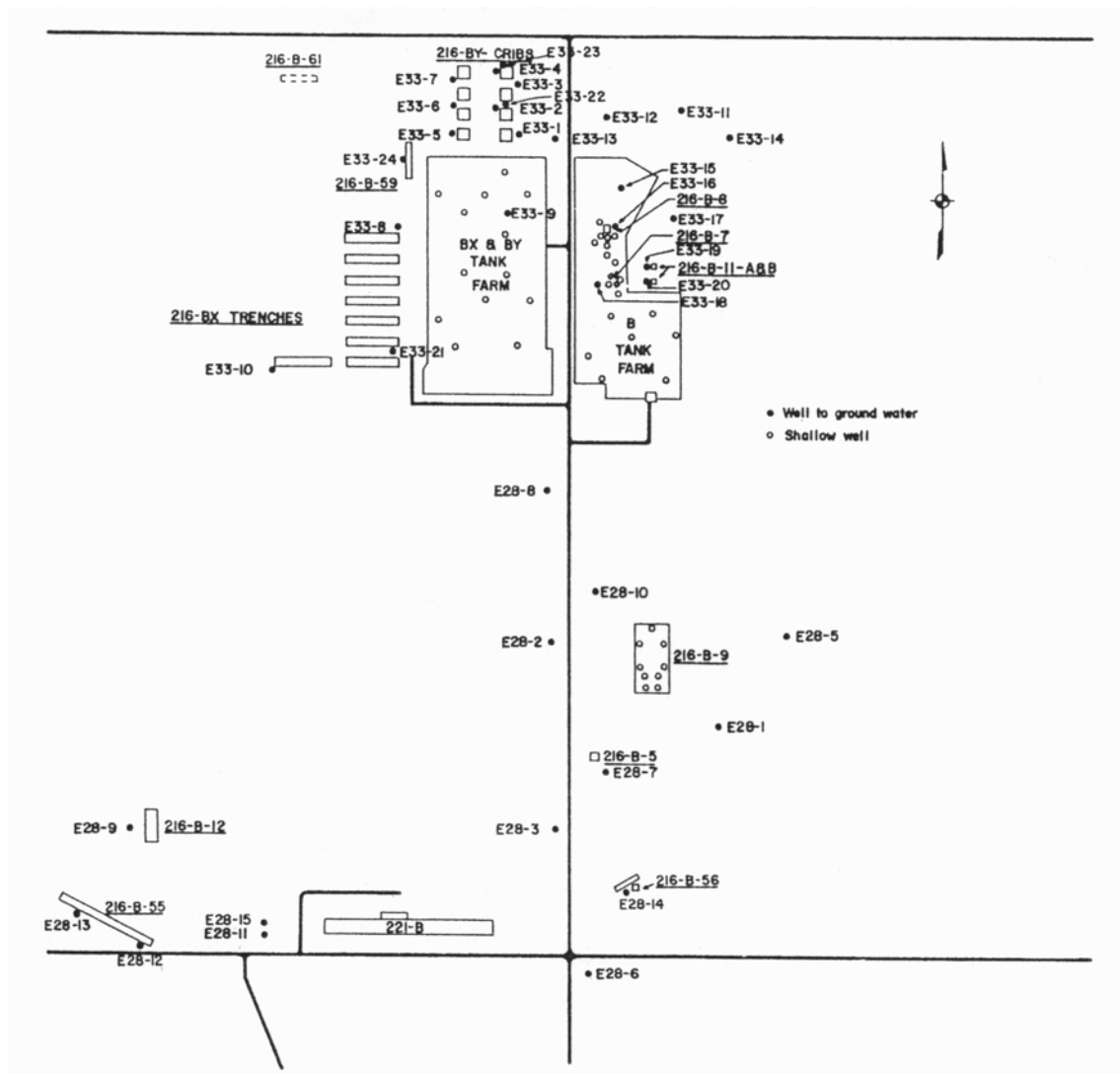
Figures

The following section presents the figures cited in this report in the order in which they were presented.



modified from DOE (1993b)

Figure 1. Hanford Site and Area Designations



from Tillson and McGhan (1969)

Figure 2. Map of B Plant Waste Disposal Sites Showing the Locations of the 216-B-5 Injection Well and 216-B-9 Crib & Tile Field

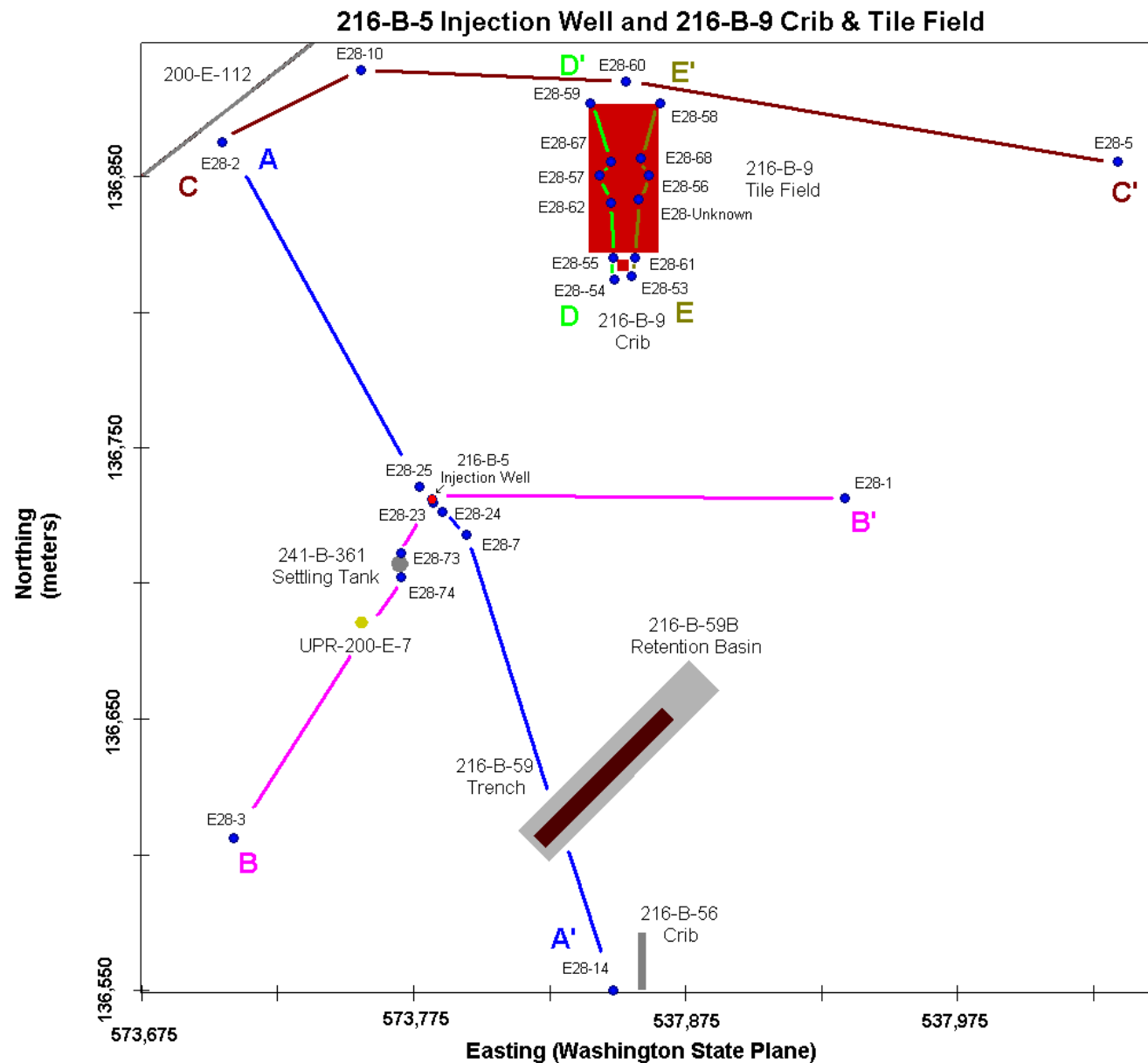
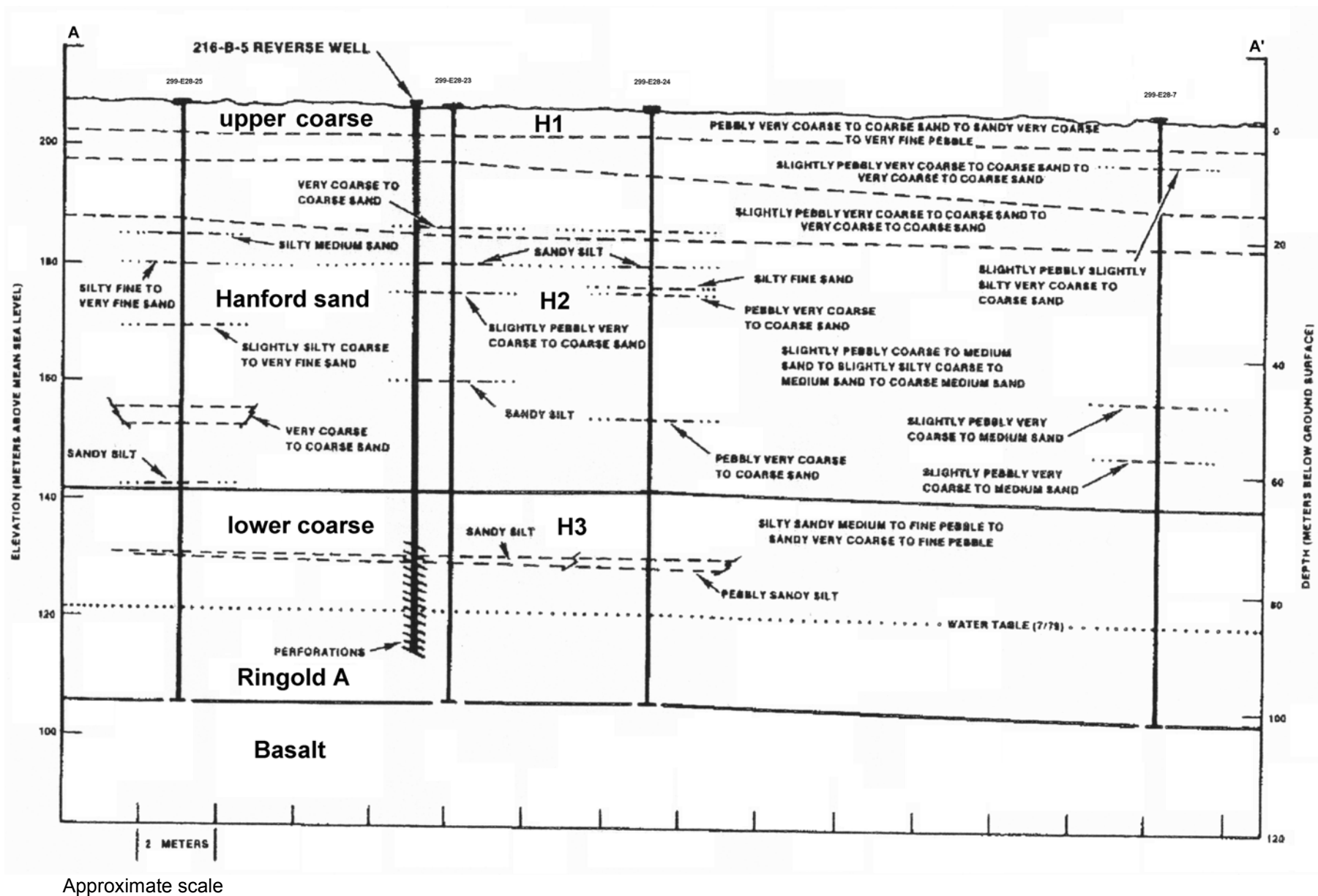


Figure 3. Map of the 216-B-5 Injection Well, 216-B-9 Crib & Tile Field, and Adjacent Waste Sites, Boreholes, and Cross Sections



modified from DOE (1993a)

Figure 4. General Stratigraphy of the 216-B-5 Injection Well and 216-B-9 Crib & Tile Field



Figure 5. View of the Ground Surface at the 216-B-5 Injection Well from the East

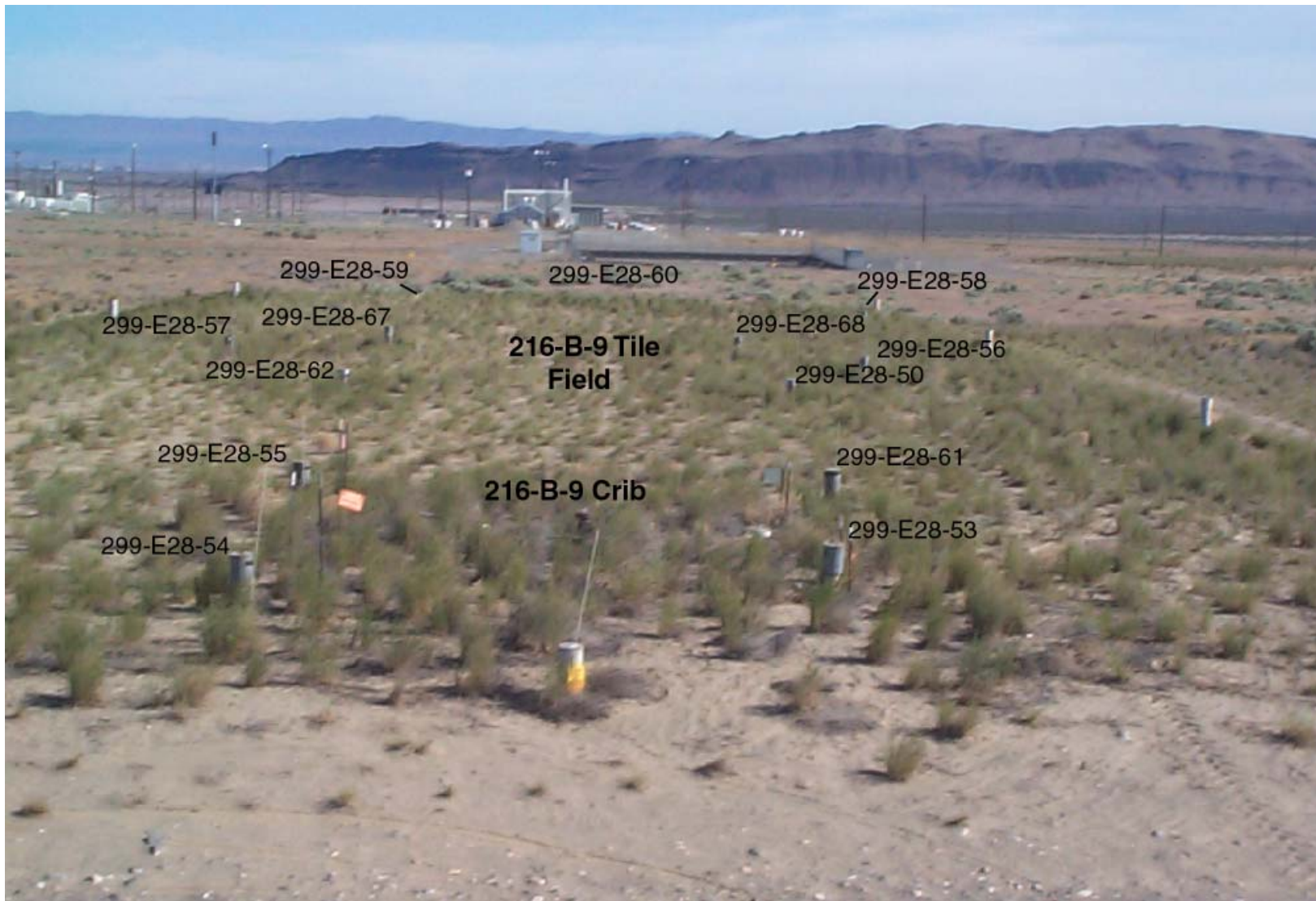
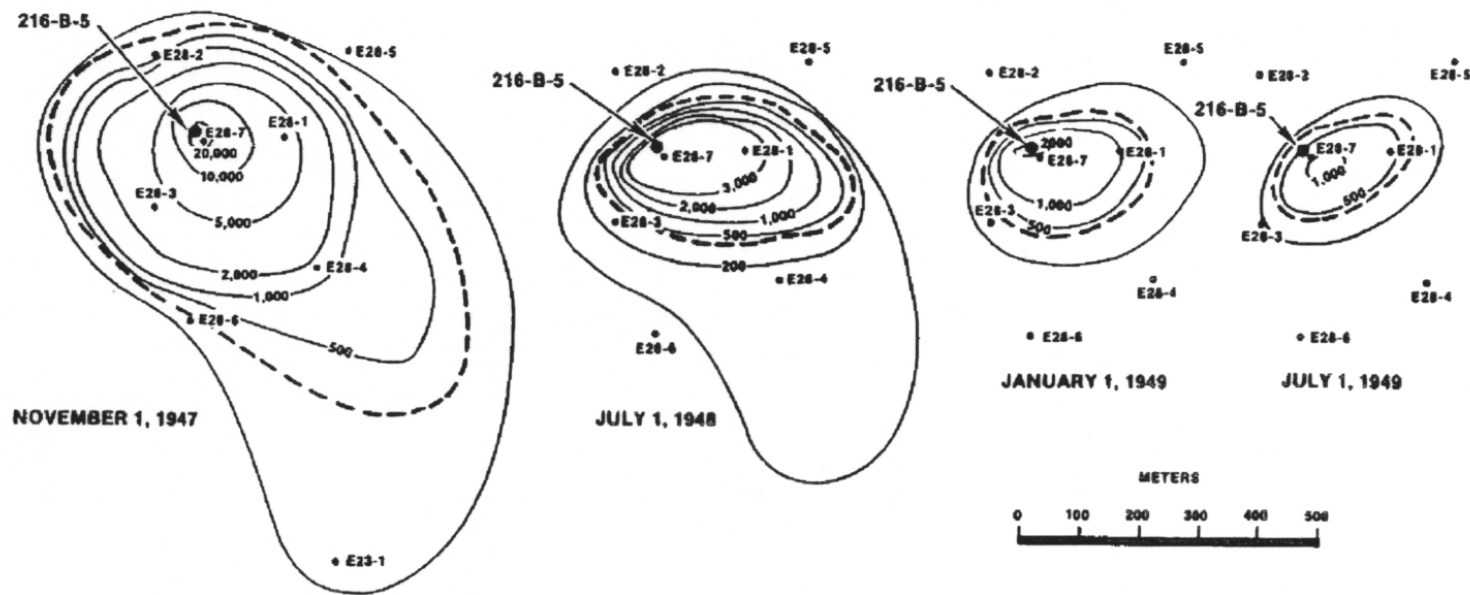
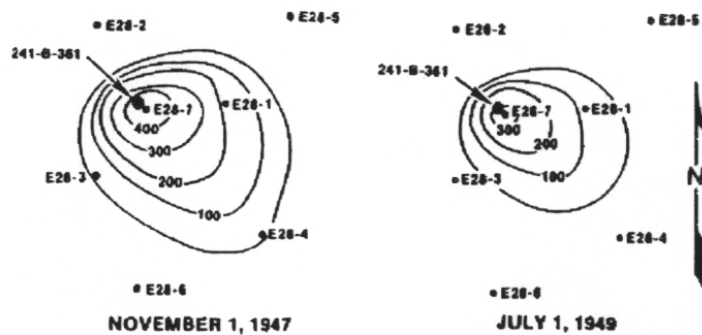


Figure 6. View of the Ground Surface at the 216-B-9 Crib and Tile Field from the South

FISSION PRODUCTS CONTAMINATION



ALPHA CONTAMINATION



EXPLANATION

CONTOUR INTERVAL AS INDICATED. ACTIVITY MEASURED IN pCi FISSION PRODUCTS PER LITER OF WATER, AND IN DIS/MIN/LITER FOR URANIUM. SIGNIFICANT LEVEL OF ACTIVITY CHOSEN AT 20 pCi/LITER AND 10 DIS/MIN/LITER FOR FISSION PRODUCTS AND URANIUM RESPECTIVELY.

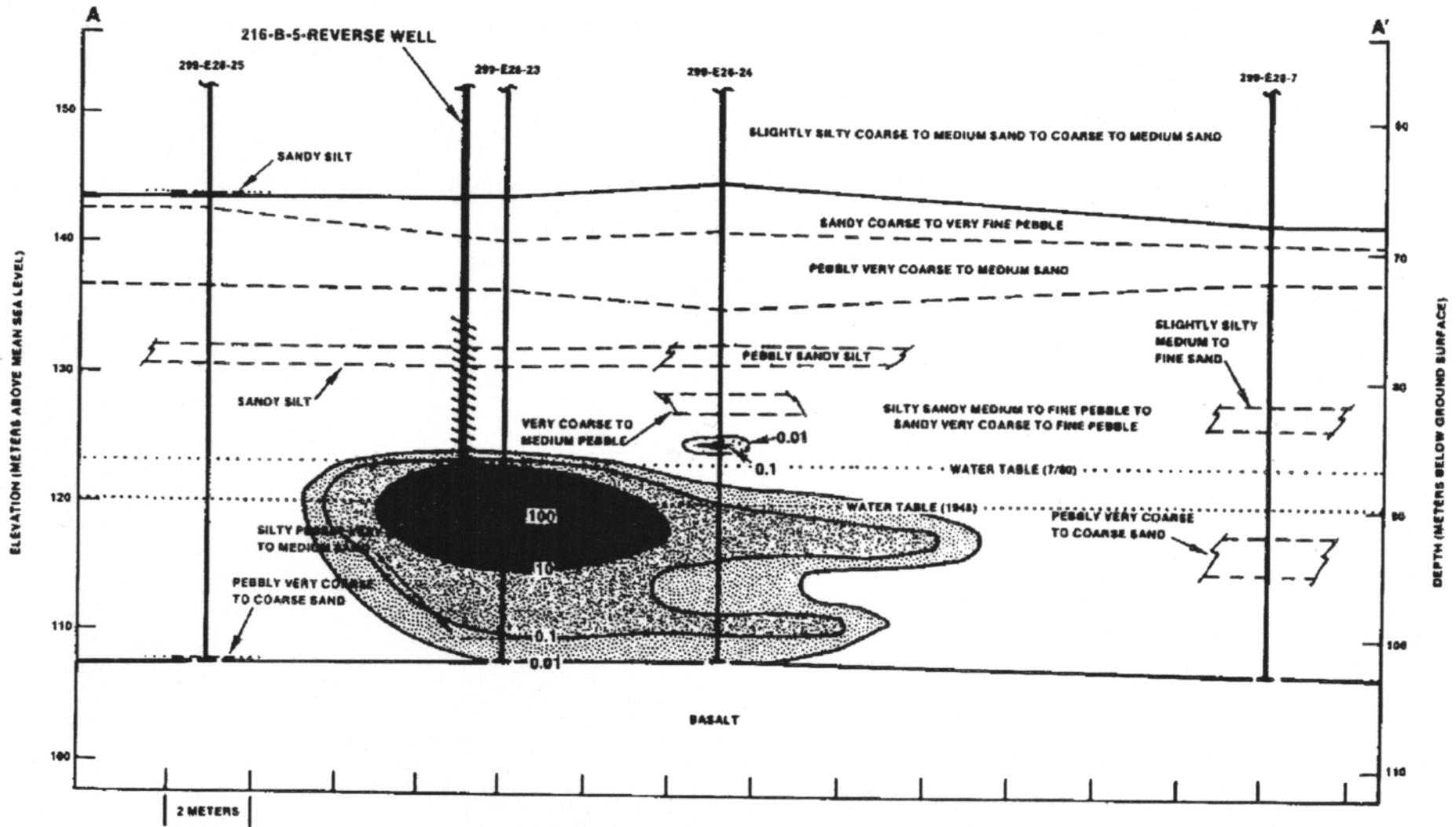
● WELLS TO WATER

Approximate scale

from Smith (1980)

Figure 7. Distribution of Radionuclides in Groundwater in the Vicinity of the 216-B-5 Injection Well

PLUTONIUM - 239,240
(nCi/g)

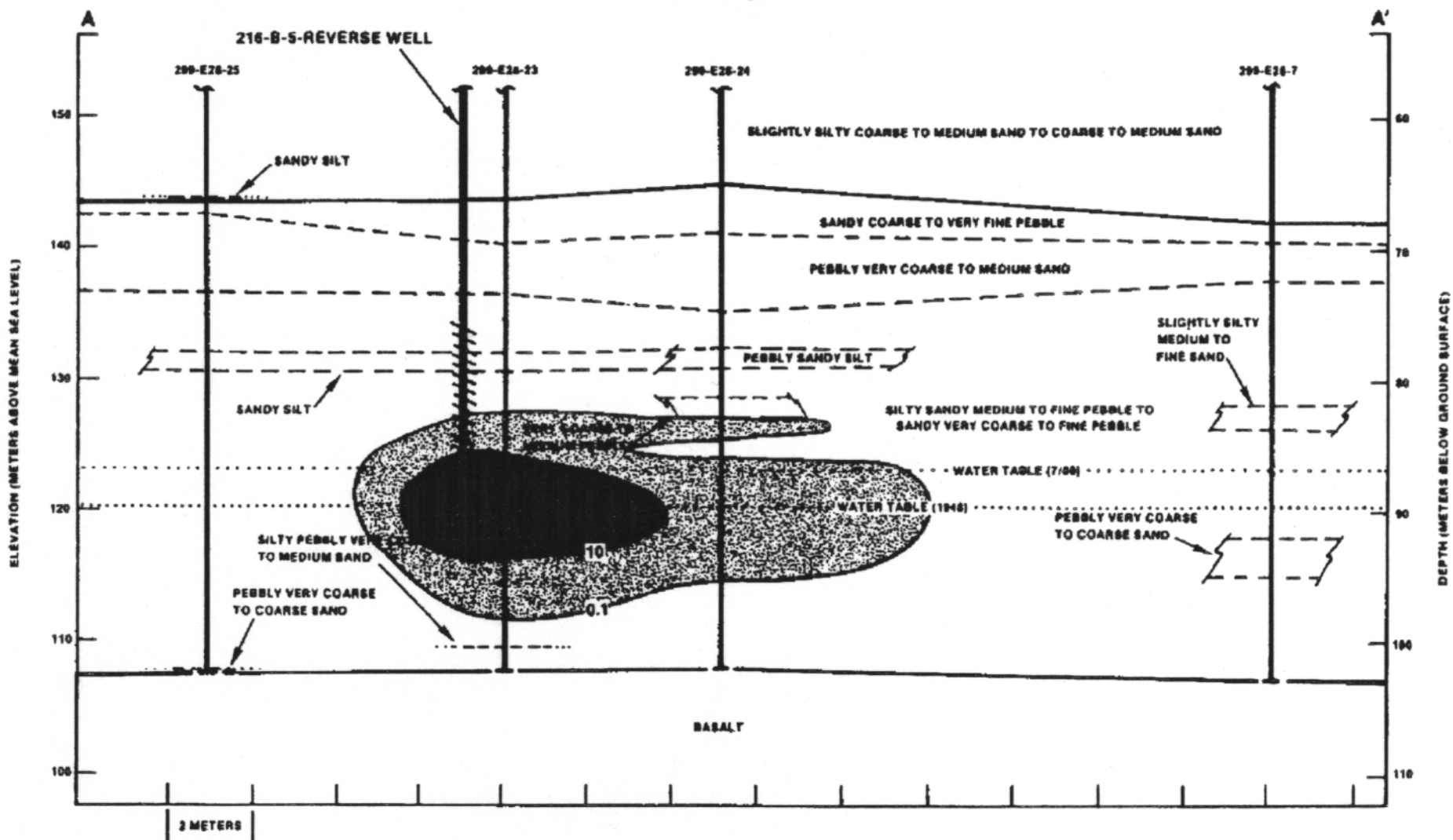


Approximate scale

from Smith (1980)

Figure 8. Distribution of $^{239-240}\text{Pu}$ near the 216-B-5 Injection Well

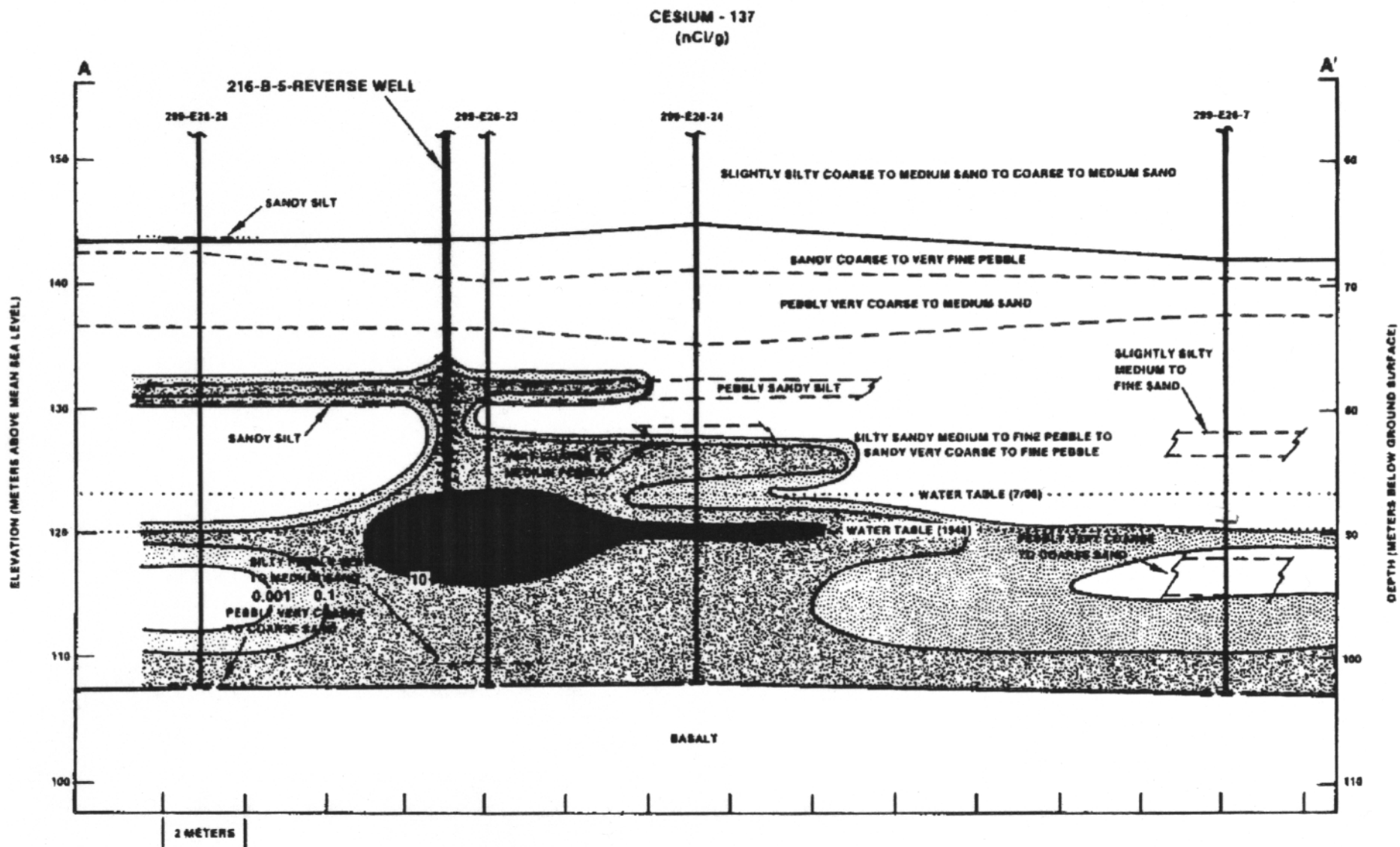
STRONTIUM - 90
(nCi/g)



Approximate scale

from Smith (1980)

Figure 9. Distribution of ^{90}Sr near the 216-B-5 Injection Well



Approximate scale

from Smith (1980)

Figure 10. Distribution of ¹³⁷Cs near the 216-B-5 Injection Well

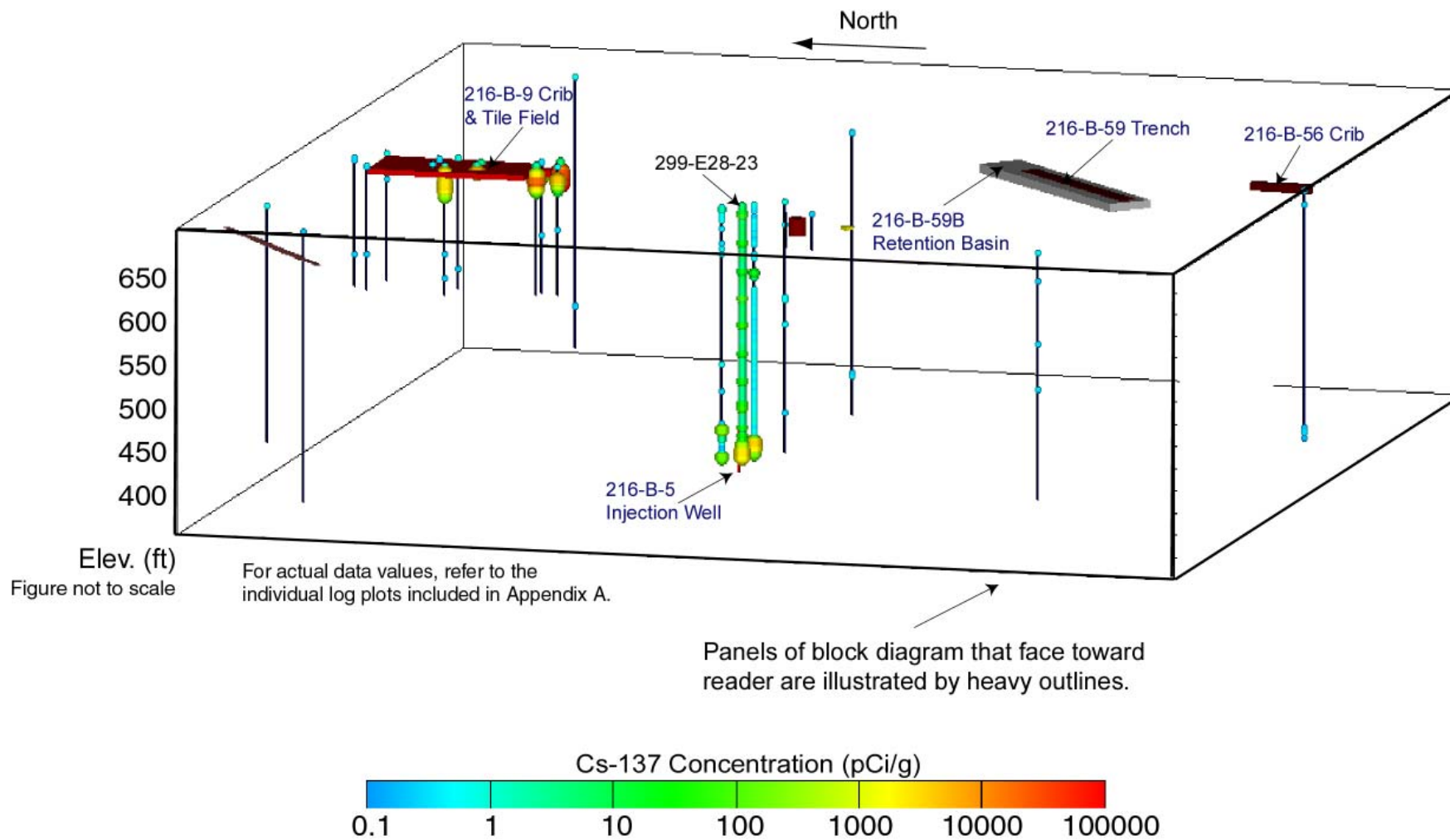


Figure 11. Visualization of the ^{137}Cs Data Acquired near the 216-B-5 Injection Well and 216-B-9 Crib & Tile Field

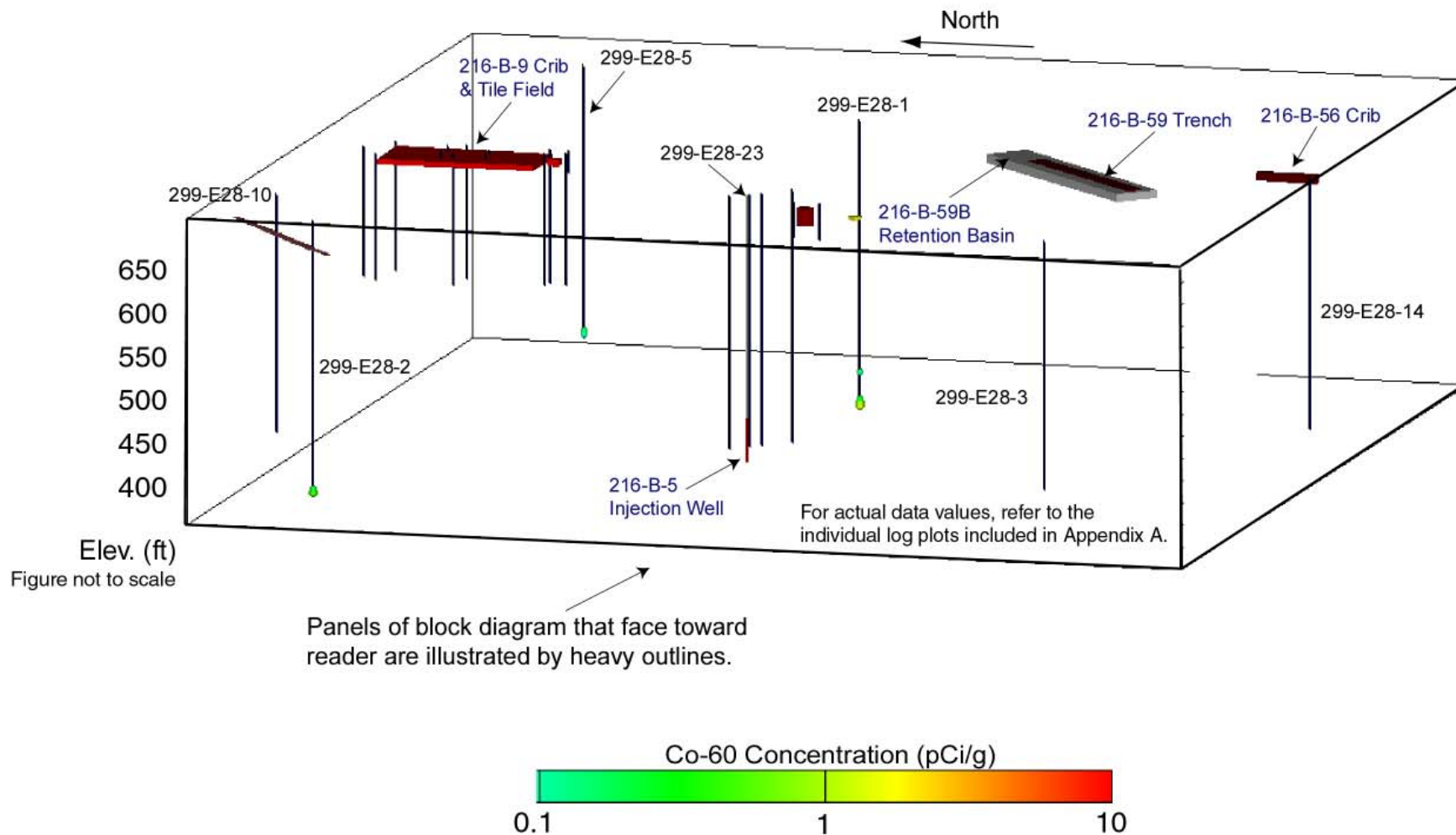


Figure 12. Visualization of the ^{60}Co Data Acquired near the 216-B-5 Injection Well and 216-B-9 Crib & Tile Field

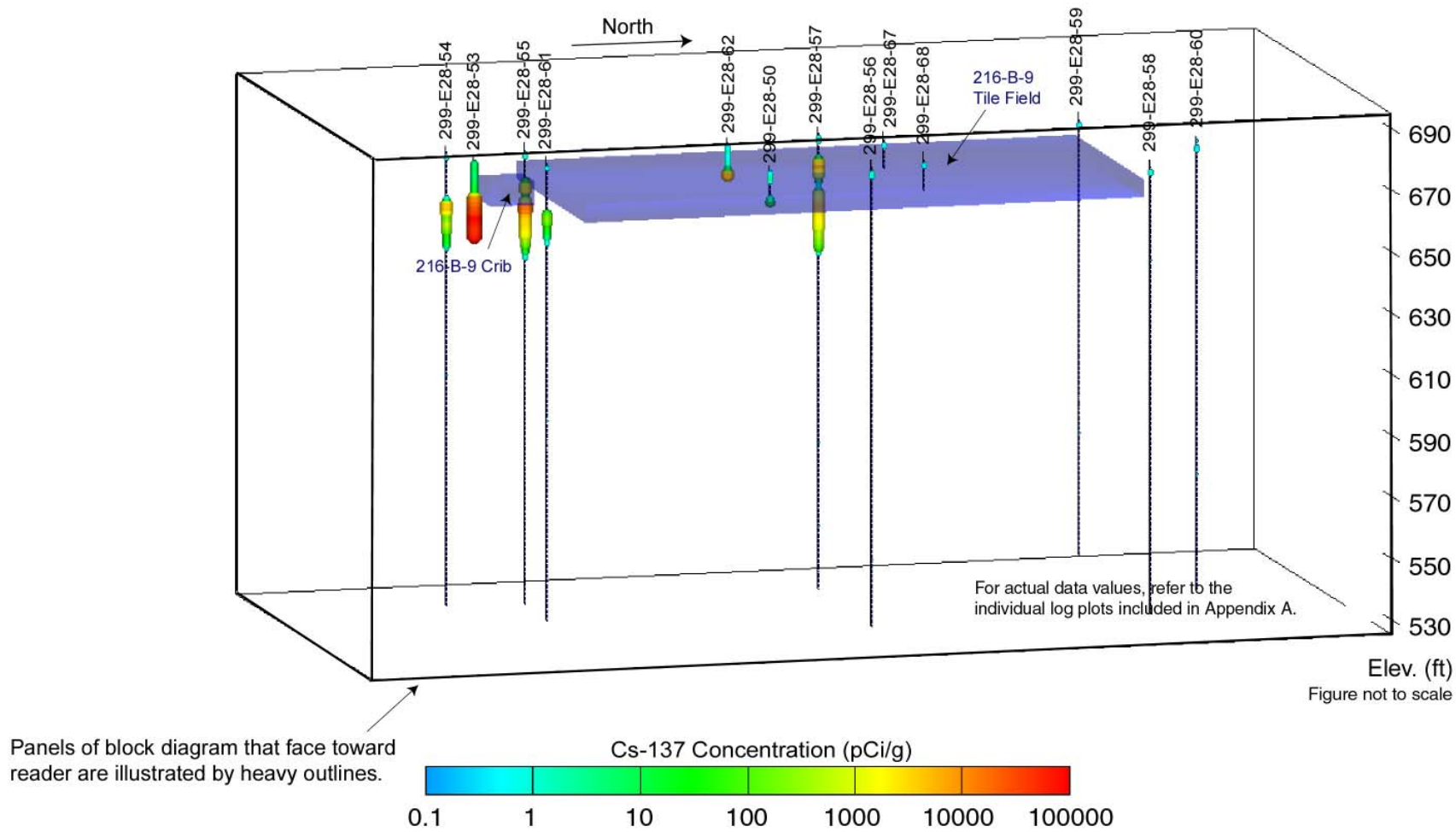


Figure 13. Visualization of the ^{137}Cs Data Acquired at the 216-B-9 Crib and Tile Field

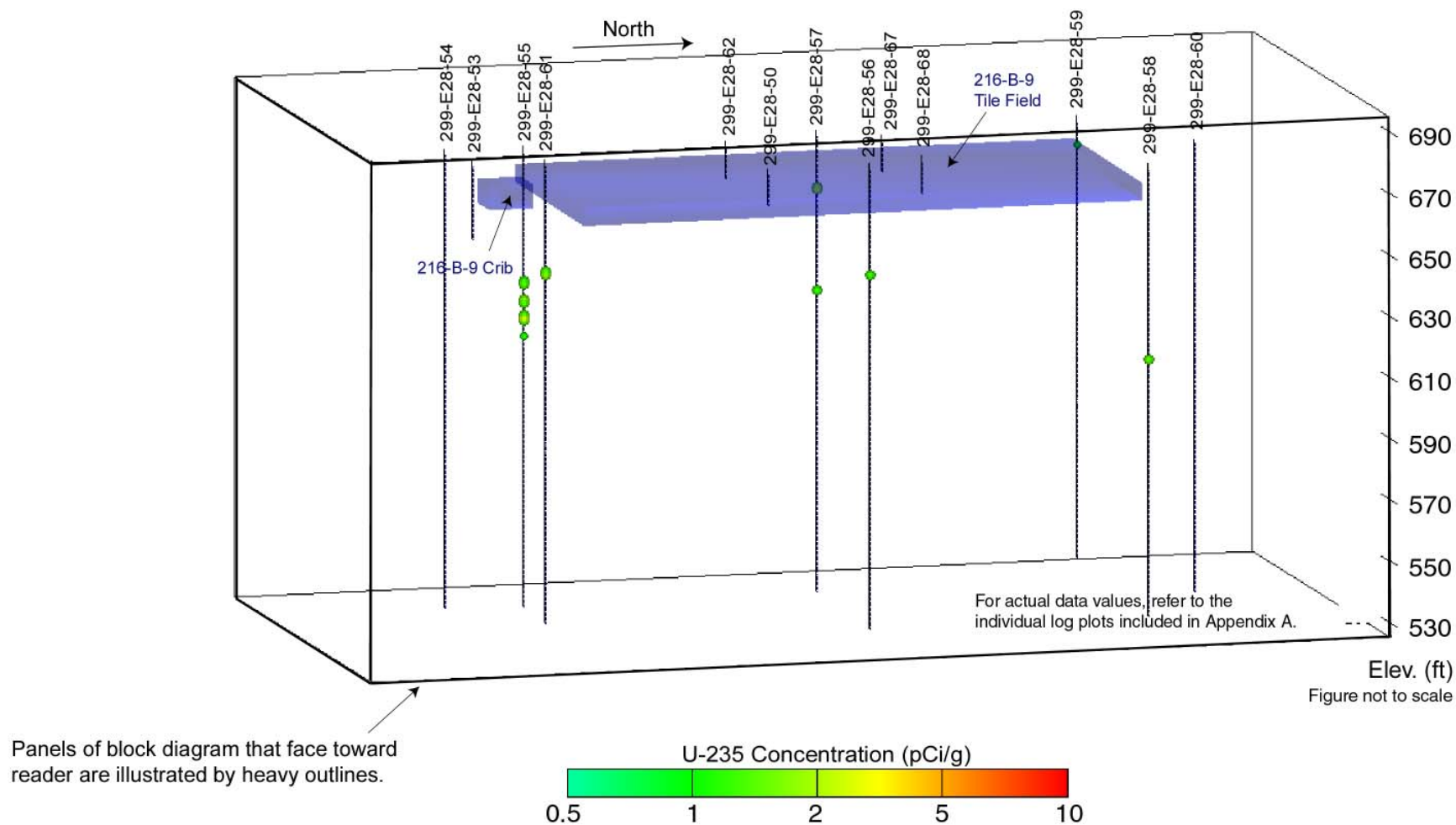


Figure 14. Visualization of the ^{235}U (186 keV) Data Acquired at the 216-B-9 Crib and Tile Field

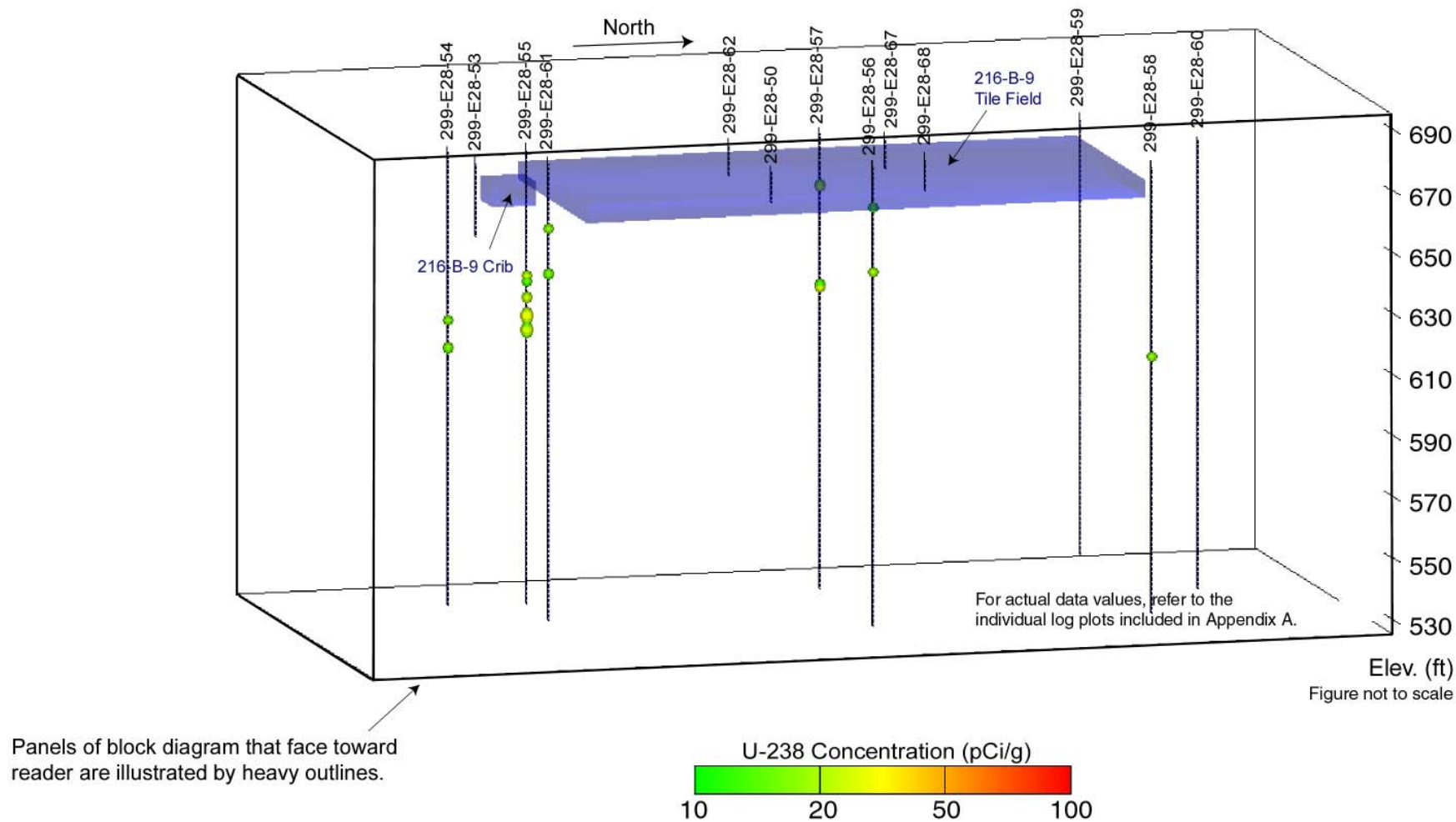


Figure 15. Visualization of the ^{238}U (1001 keV) Data Acquired at the 216-B-9 Crib and Tile Field

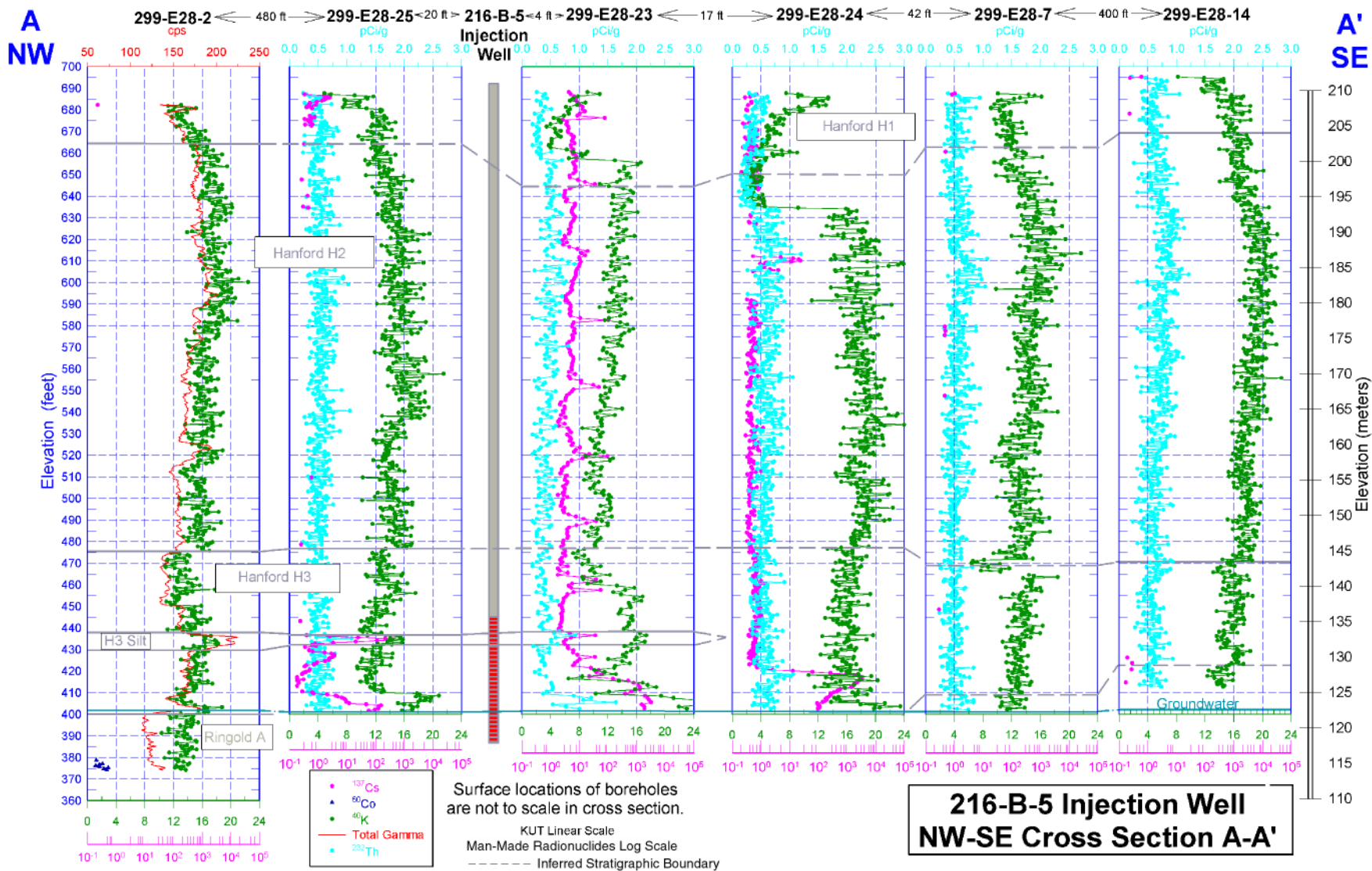


Figure 16. Northwest-Southeast Cross Section A-A' Showing Contamination and Interpreted Stratigraphy at the 216-B-5 Injection Well

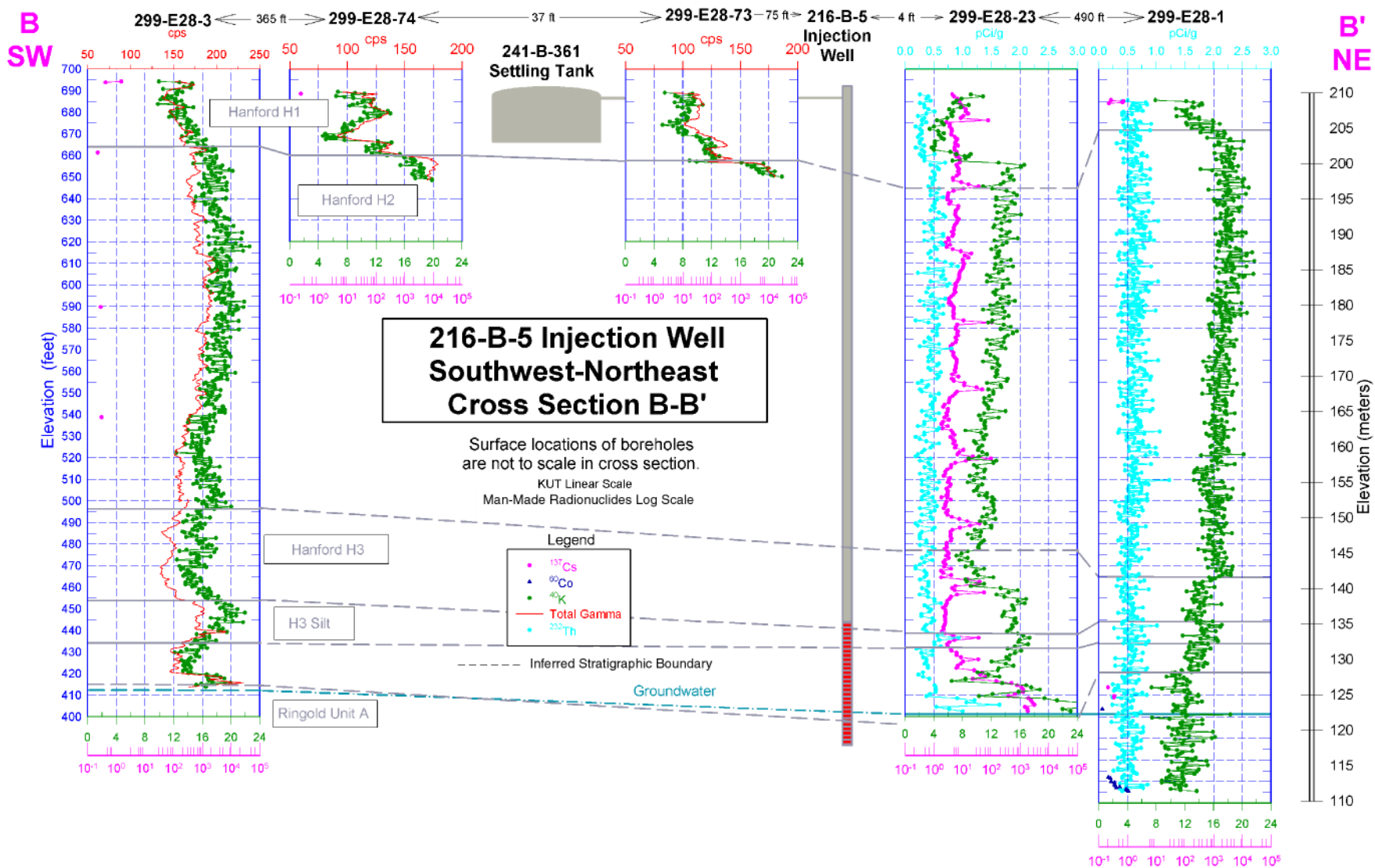
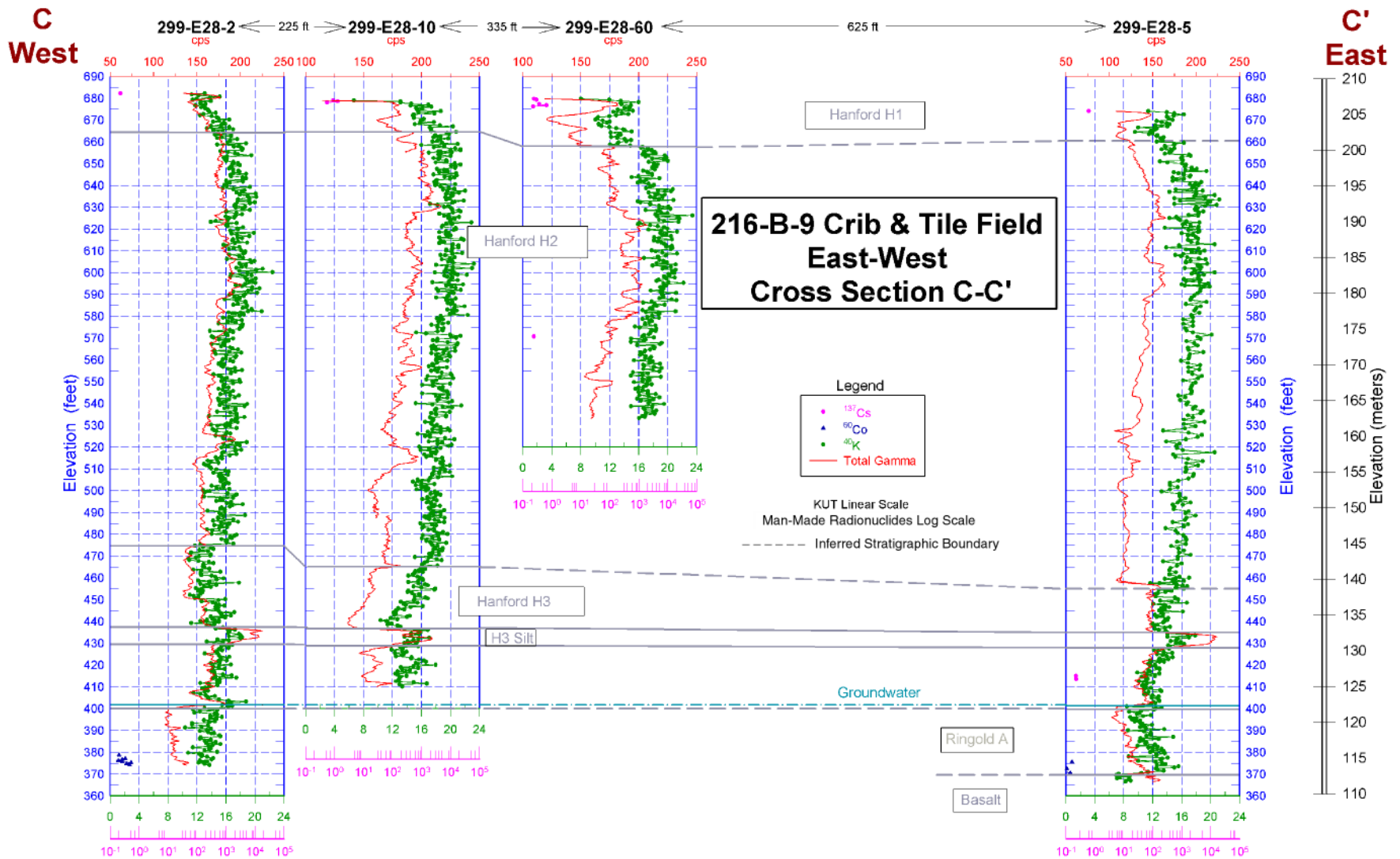


Figure 17. Northeast-Southwest Cross Section B-B' Showing Contamination and Interpreted Stratigraphy at the 216-B-5 Injection Well



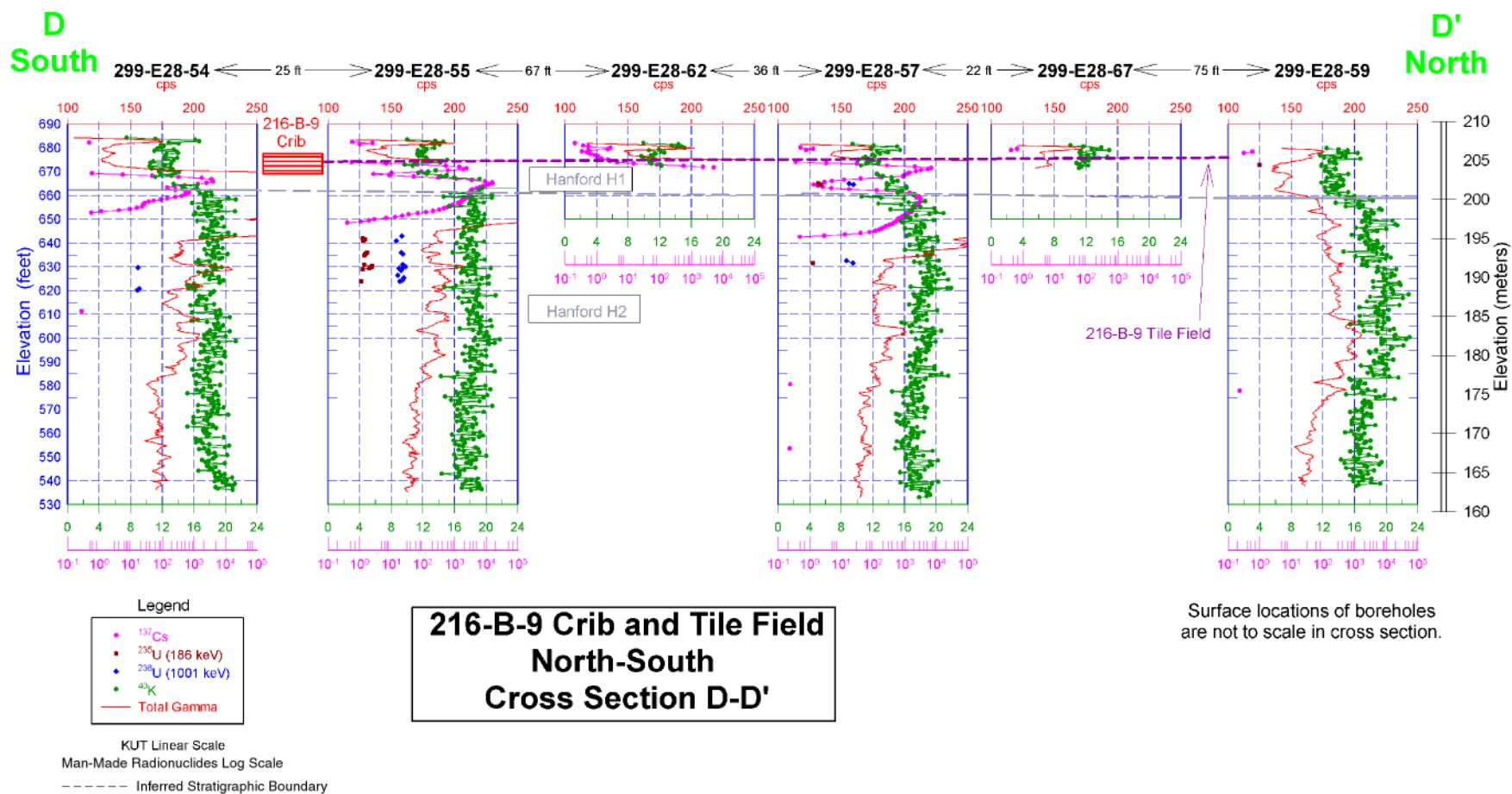


Figure 19. North-South Cross Section D-D' Showing Contamination and Interpreted Stratigraphy at the 216-B-9 Crib and Tile Field

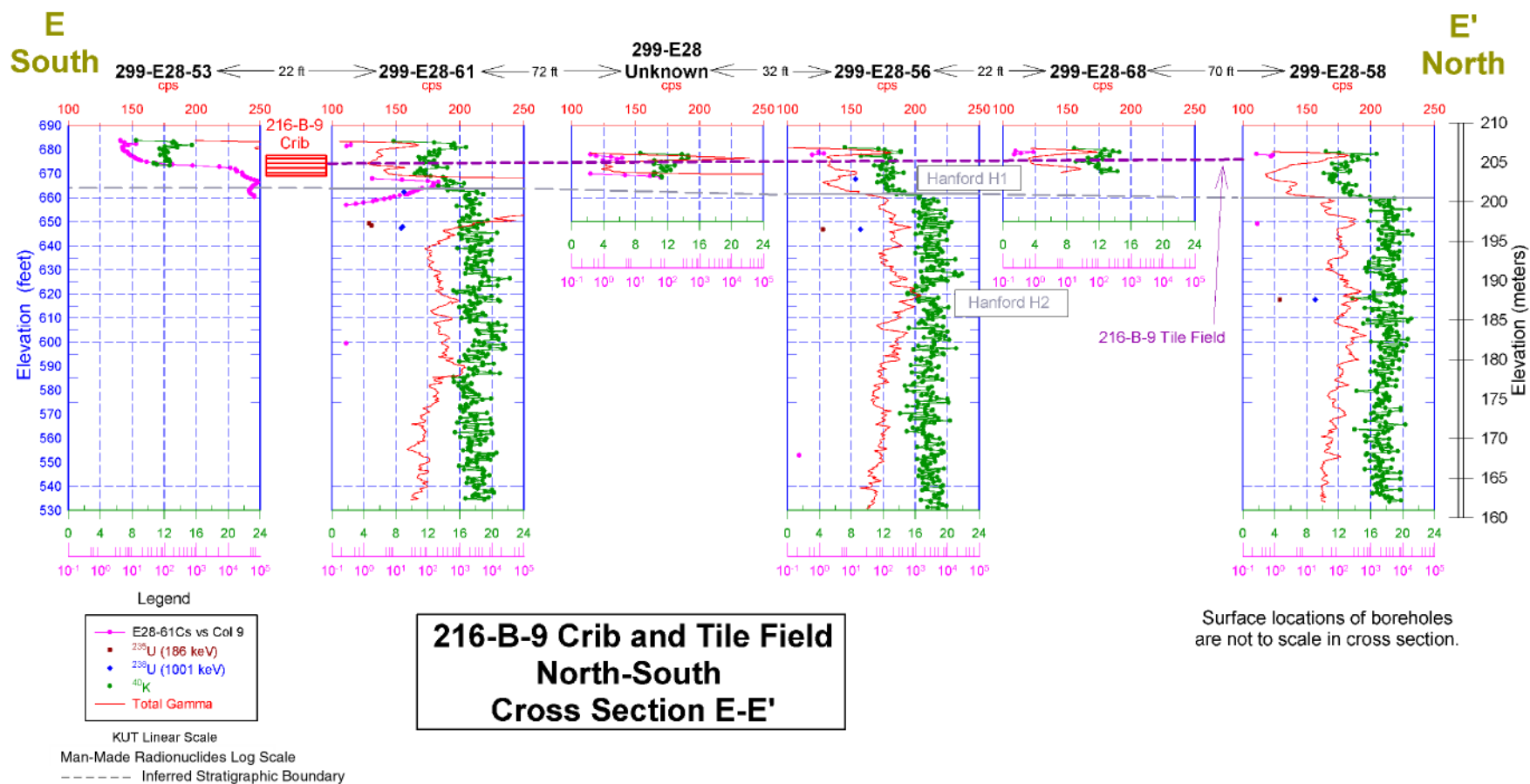


Figure 20. North-South Cross Section E-E' Showing Contamination and Interpreted Stratigraphy at the 216-B-9 Crib and Tile Field

For actual data values, refer to the individual log plots included in Appendix A.

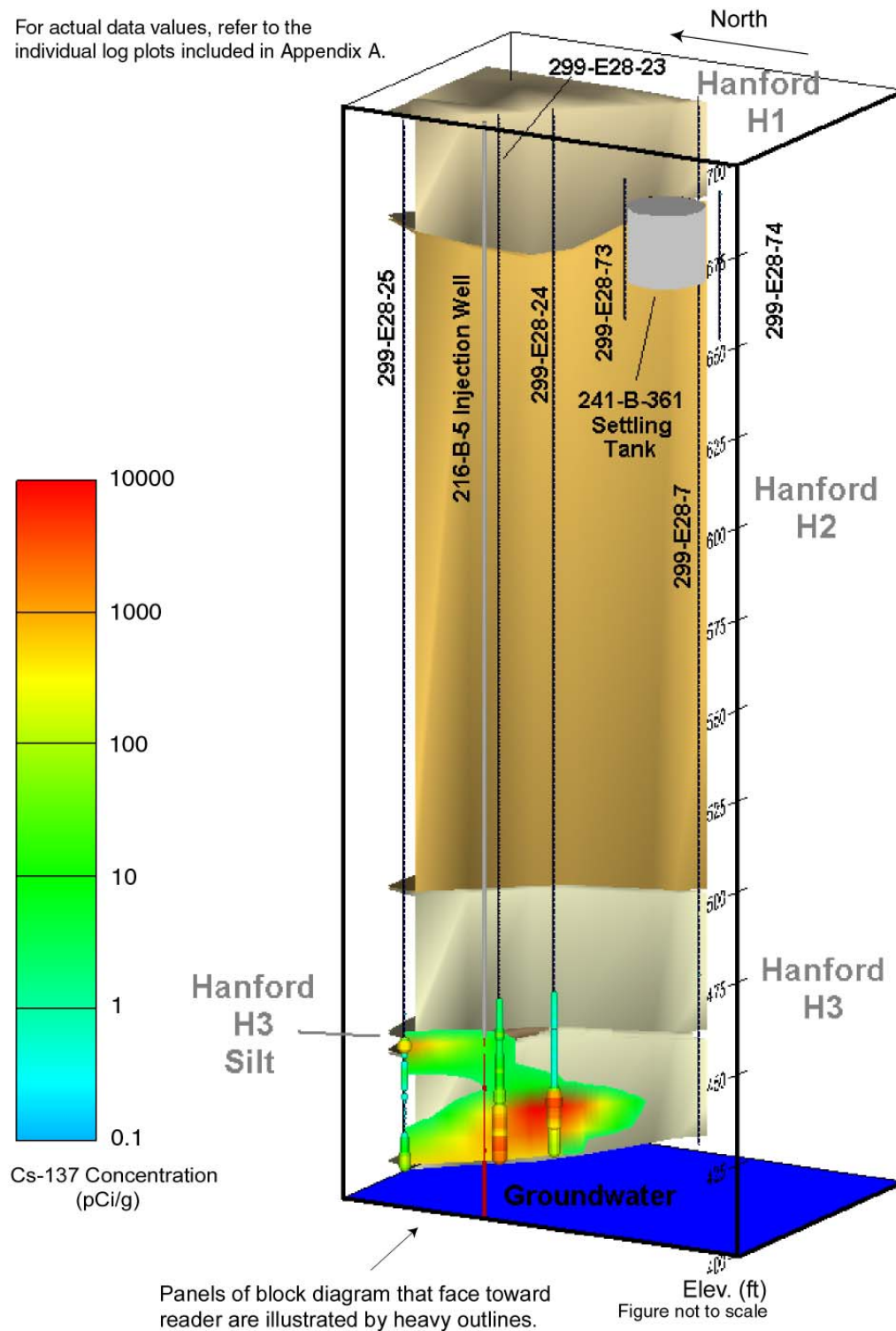


Figure 21. Visualization of the ^{137}Cs Distribution at the 216-B-5 Injection Well

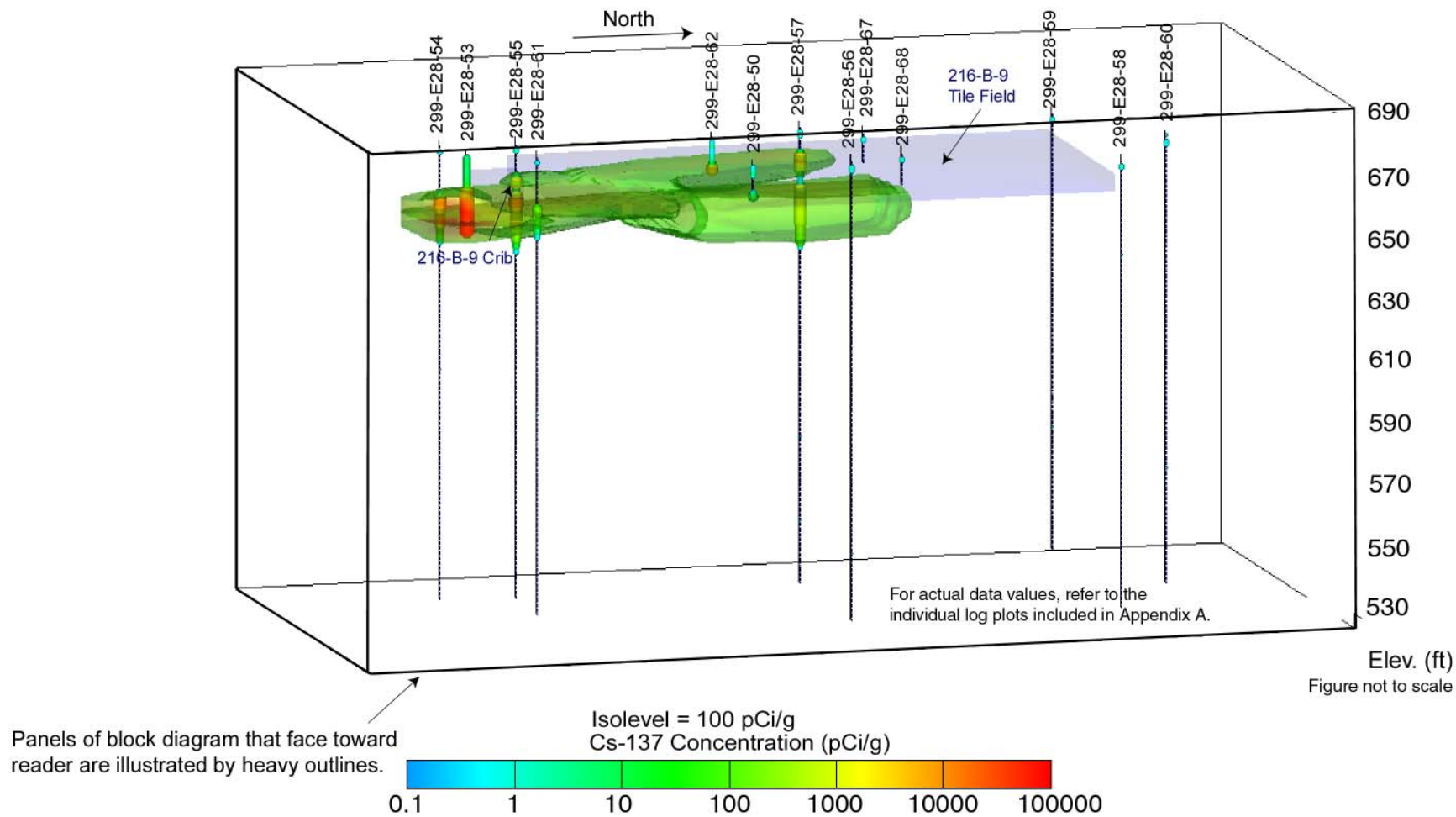


Figure 22. Visualization of the ^{137}Cs Distribution at the 216-B-9 Crib and Tile Field

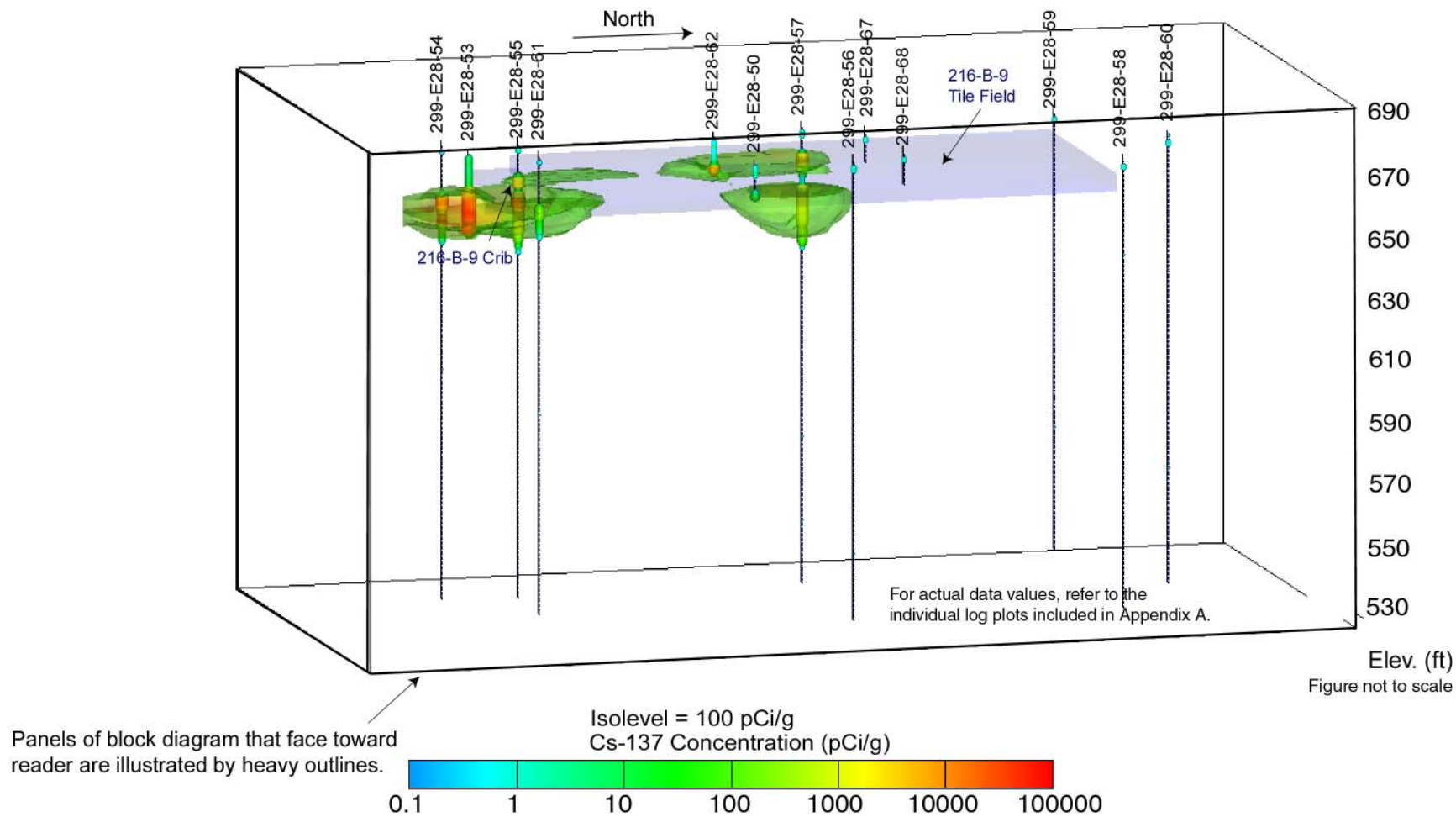


Figure 23. Alternative Visualization of the ^{137}Cs Distribution at the 216-B-9 Crib and Tile Field

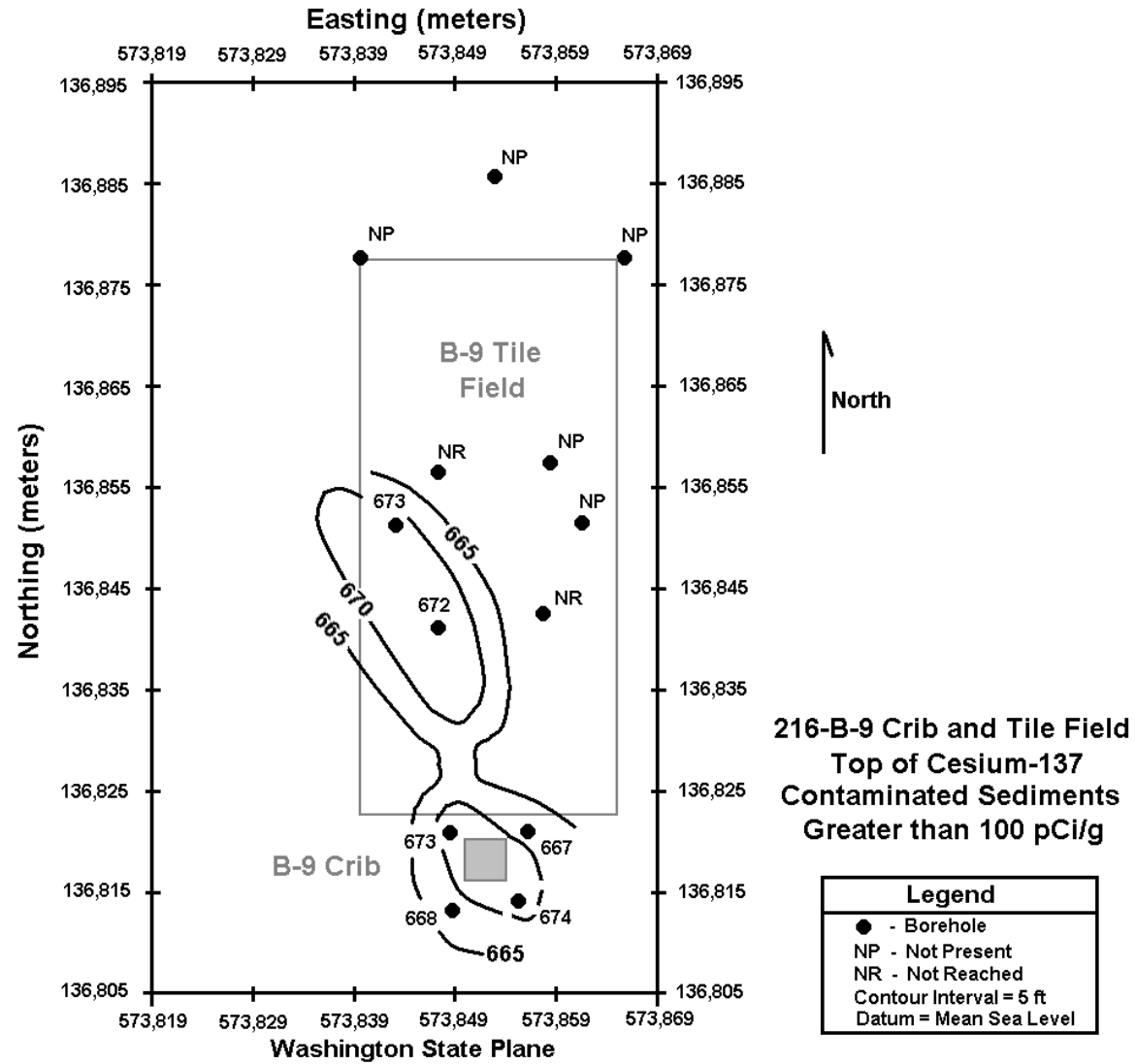


Figure 24. Elevation of the Top of the Zone of Sediments with 100 pCi/g of ^{137}Cs Activity or Greater at the 216-B-9 Crib and Tile Field

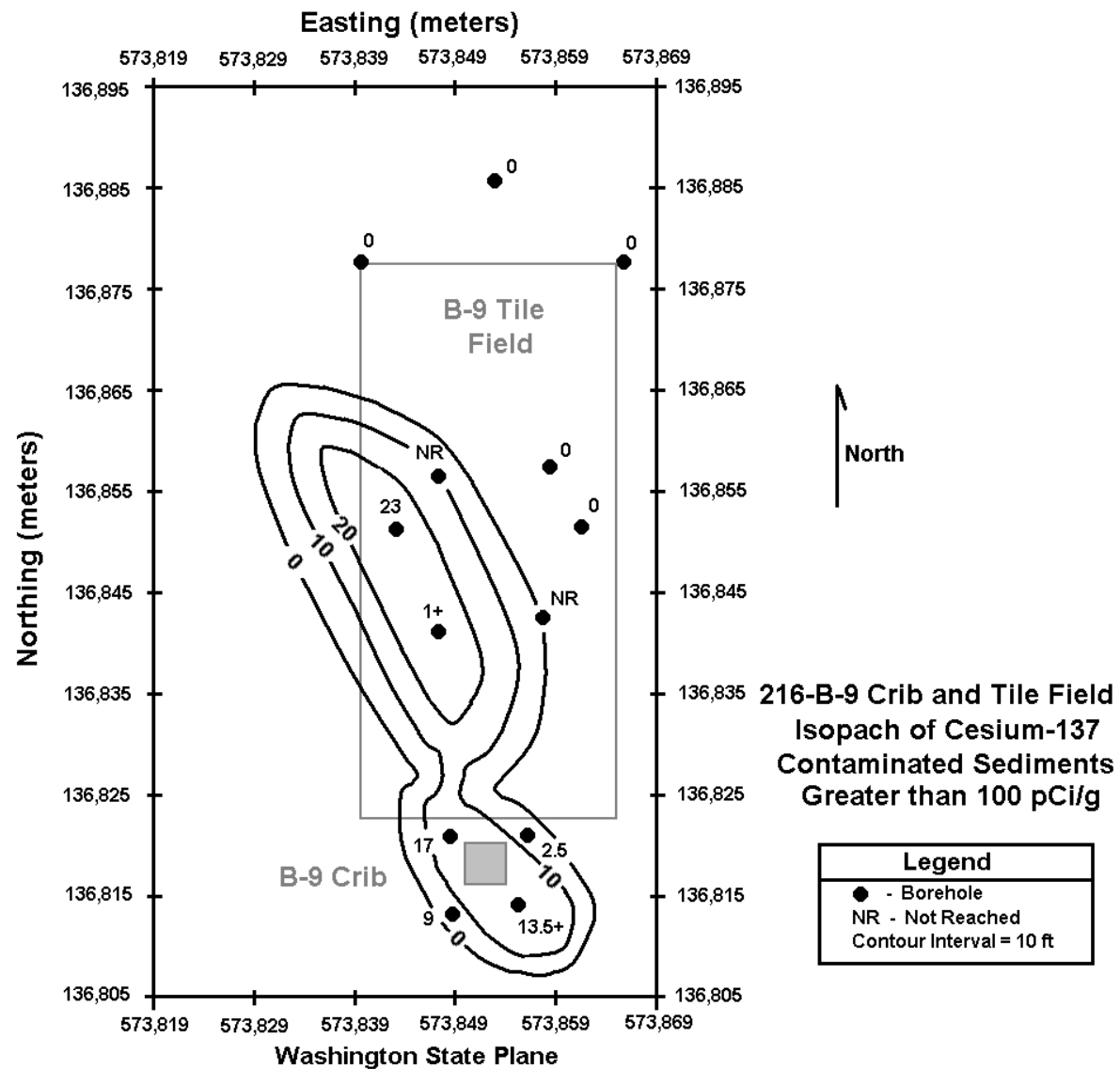


Figure 25. Isopach of Net Thickness of Sediments Containing 100 pCi/g of ¹³⁷Cs Activity or Greater at the 216-B-9 Crib and Tile Field

299-E28-25 (A6801)
 RLS Data Compared to SGLS Data
¹³⁷Cesium Decayed to 10/29/2001

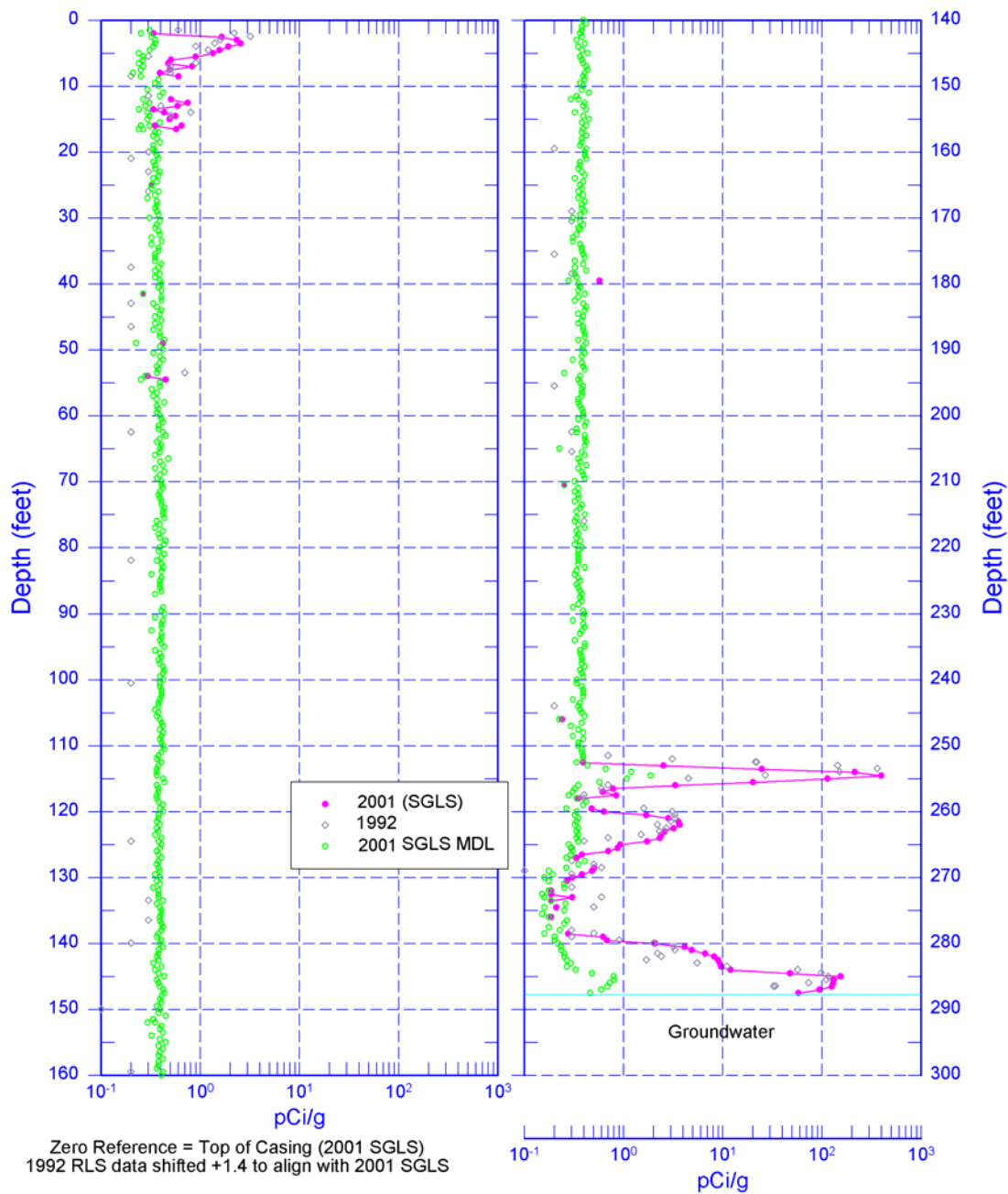


Figure 26. Borehole 299-E28-25 SGLS/RLS Comparison Plot

References

Additon, M.K., K.R. Fecht, T.L. Jones, and G.V. Last, 1978. *Scintillation Probe Profiles from 200 East Area Crib Monitoring Wells*, RHO-LD-28, Rockwell International, Richland, Washington.

Baker, U.R., B.N. Bjornstad, A.J. Busacca, K.R. Fecht, E.P. Kiver, U.L. Moody, J.G. Rigby, O.F. Stradling, and A.M. Tallman, 1991. "Quaternary Geology of the Columbia Plateau" in Morrison, R.B. (ed.), *Quaternary Non-Glacial Geology: Conterminous U.S.*, Boulder, Colorado, GSA, the Geology of North America, Vol. K-2.

Bergeron, M.P., E.J. Freeman, and S.K. Wurstner, 2001. *Addendum to Composite Analysis for Low-Level Waste Disposal in the 200 Area Plateau of the Hanford Site*, PNNL-11800 Addendum 1, Pacific Northwest National Laboratory, Richland, Washington.

Bjornstad, B.N., G.V. Last, G.A. Smith, K.A. Lindsey, K.R. Fecht, S.P. Reidel, D.G. Horton, and B.A. Williams, 2002. *Proposed Standardized Stratigraphic Nomenclature for Post-Ringold Sediments Within the Central Pasco Basin*, 2nd draft, Pacific Northwest National Laboratory, Richland, Washington.

Brodeur, J.R., R.K. Price, R.D. Wilson, and C.J. Koizumi, 1993. *Results for Spectral Gamma-Ray Logging of Selected Boreholes for the 200 Aggregate Area Management Study*, WHC-SD-EN-TI-021, Westinghouse Hanford Company, Richland, Washington.

Brown, R.E., and H.G. Ruppert, 1950. *Underground Waste Disposal at Hanford Works*, HW-17088, General Electric Hanford Company, Richland, Washington.

Caggiano, J.A., 1996. *Assessment Groundwater Monitoring Plan for Single Shell Tank Waste Management Area B-BX-BY*, WHC-SD-ENV-AP-002, prepared by Westinghouse Hanford Company for the U.S. Department of Energy, Richland, Washington.

Delaney, C.D., K.A. Lindsey, and S.P. Reidel, 1991. *Geology and Hydrology of the Hanford Site: A Standardized Text for Use in Westinghouse Hanford Company Documents and Reports*, WHC-SD-ER-TI-0003, Westinghouse Hanford Company, Richland, Washington.

Fecht, K.R., G.V. Last, and K.R. Price, 1977. *Evaluation of Scintillation Probe Profiles from 200 Area Crib Monitoring Wells*, ARH-ST-156, Atlantic Richfield Hanford Company, Richland, Washington.

Fecht, K.R., K.A. Lindsey, B.N. Bjornstad, D.G. Horton, G.V. Last, and S.P. Reidel, 1999. *Clastic Injection Dikes of the Pasco Basin and Vicinity, Geologic Atlas Series*, prepared for the U.S. Department of Energy Office of Environmental Restoration, BHI-01103, Rev. 0, Richland, Washington, July.

Glover, D.W., 1985. *Crustal Structure of the Columbia Basin, Washington, from Borehole and Refraction Data*, M.S. thesis, University of Washington (Seattle).

Hartman, M.J., L.F. Morasch, and W.D. Webber (eds.), 2002. *Hanford Site Groundwater Monitoring for Fiscal Year 2001*, PNNL-13788, Pacific Northwest National Laboratory, Richland, Washington, March.

Hooper, P.R., and V.E. Camp, 1981. "Deformation of the Southeast Part of the Columbia Plateau" in *Geology*, v. 9, p. 323-328.

Hooper, P.R., and R.M. Conrey, 1989. "A Model for the Tectonic Setting of the Columbia River Basalt Eruptions," in Reidel, S.P., and P.R. Hooper (ed.), *Volcanism and Tectonism in the Columbia River Flood-Basalt Province*, Boulder, Colorado, Geological Society of America Special Paper 239, pp. 293-306.

Koizumi, C.J., 2002. *Hanford Geophysical Logging Project, 2001 Recalibration of Logging Systems for Characterization of Subsurface Contamination at the Hanford Site*, GJO-2002-328-TAR, prepared by MACTEC-ERS, Grand Junction Office, Grand Junction, Colorado.

Lindsey, K.A., 1991. *Revised Stratigraphy for the Ringold Formation, Hanford Site, South-Central Washington*, WHC-SD-EN-EE-004, Rev. 0, Westinghouse Hanford Company, Richland, Washington.

_____, 1996. *The Miocene to Pliocene Ringold Formation and Associated Deposits of the Ancestral Columbia River System, South-Central Washington and North-Central Oregon*, Washington Division of Geology and Earth Resources Open-File Report 96-8.

Lindsey, K.A., and A.G. Law, 1993. Westinghouse Hanford Company Internal Memo, Subject: "Geohydrologic Setting, Flow and Transport Parameters for the Single Shell Tank Farms," 81231-93-060, Westinghouse Hanford Company, Richland, Washington.

Lindsey, K.A., B.N. Bjornstad, J.W. Lindberg, and K.M. Hoffman, 1992. *Geologic Setting of the 200 East Area: An Update*, WHC-SD-EN-TI-012, Rev. 0, Westinghouse Hanford Company, Richland, Washington.

Lindsey, K.A., S.P. Reidel, K.R. Fecht, J.L. Slate, A.G. Law, and A.M. Tallman, 1994. "Geohydrologic Setting of the Hanford Site, South-Central Washington," in *Geologic Field Trips of the Pacific Northwest: 1994 Geological Society of America Annual Meeting*, edited by D.A. Swanson and R.A. Haugerud, Dept. of Geological Sciences, University of Washington, Seattle, Washington, pp. 1C-1 to 1C-16.

Lindsey, K.A., S.E. Kos, and K.D. Reynolds, 2000. *Vadose Zone Geology of Boreholes 299-W22-50 and 299-W23-19 S-SX Waste Management Area, Hanford Site, South-Central, Washington*, RPP-6149, Rev. 0, prepared for CH2M Hill Hanford Group, Richland, Washington, April.

Maxfield, H.L., 1979. *200 Areas Waste Sites Handbook*, RHO-CD-673, 3 vols., Rockwell Hanford Operations, Richland, Washington.

Narbutovskih, S.M., 1998. *Results of Phase I Groundwater Quality Assessment for Single-Shell Tank Waste Management Areas B-BX-BY at the Hanford Site*, PNNL-11826, Pacific Northwest National Laboratory, Richland, Washington.

_____, 2000. *Groundwater Quality Assessment Plan for Single Shell Waste Management Area B-BX-BY at the Hanford Site*, PNNL-13022, Pacific Northwest National Laboratory, Richland Washington.

Raymond, J.R., and V.L. McGhan, 1964. *Scintillation Probe Results 200 Area Waste Disposal Site Monitoring Wells*, HW-84577, General Electric Hanford Atomic Products Operation, Richland, Washington.

Reidel, S.P., 1984. "The Saddle Mountains -- The Evolution of an Anticline in the Yakima Fold Belt," in *American Journal of Science*, Vol. 284, No. 8, pp. 942-978.

Reidel, S.P., and K.R. Fecht, 1981. "Wanapum and Saddle Mountains Basalt in the Cold Creek Syncline Area" in *Subsurface Geology of the Cold Creek Syncline*, RHO-BWI-ST-14, Rockwell Hanford Operations, Richland, Washington.

Reidel, S.P., K.R. Fecht, M.C. Hagood, and T.L. Tolan, 1989. "The Geologic Evolution of the Central Columbia Plateau," in *Volcanism and Tectonism in the Columbia River Flood-Basalt Province*, Special Paper 239, edited by S.P. Reidel and P.R. Hooper, Geological Society of America, Boulder, Colorado, pp. 247-264.

Reidel, S.P., N.P. Campbell, K.R. Fecht, and K.A. Lindsey, 1994. *Late Cenozoic Structure and Stratigraphy of South-Central Washington*, Washington Division of Geology and Earth Resources Bulletin 80, pp. 159-180.

Reidel, S.P., K.A. Lindsey, and K.R. Fecht, 1992. *Field Trip Guide to the Hanford Site*, WHC-MR-0391, Westinghouse Hanford Company, Richland, Washington.

Rockwell Hanford Operations (Rockwell), 1979. *Geologic Studies of the Columbia Plateau: A Status Report*, RHO-BWI-ST-4, Rockwell Hanford Operations, Richland, Washington.

Routson, R.C., 1973. *A Review of studies on Soil-Waste Relationships on the Hanford reservation from 1944 to 1967*, BNWL-1464, Battelle Pacific Northwest Laboratory, Richland, Washington.

Simpson, B.C., R.A. Corbin, and S.F. Agnew, 2001. *Hanford Soil Inventory Model*, BHI-01496, Rev. 0, Bechtel Hanford, Inc., Richland, Washington.

Slate, J.L., 1996. "Buried Carbonate Paleosols Developed in Pliocene-Pleistocene Deposits of the Pasco Basin, South-Central Washington, USA," in *Quaternary International*, Vol. 34-36, pp. 191-196.

Smith, R.M., 1980. *216-B-5 Reverse Well Characterization Study*, RHO-ST-37, Rockwell Hanford Operations, Richland, Washington.

Tillson, D.D., and V.L. McGhan, 1969. *Changes in Scintillation Probe Findings -- 1963 to 1968, 200 Area Waste Disposal Site Monitoring Wells*, BNWL-CC-2255, Battelle Pacific Northwest Laboratory, Richland, Washington.

U.S. Department of Energy (DOE), 1988. *Consultation Draft Characterization Plan*, DOE/RW-0164, Vol. 1-9, Office of Civilian Radioactive Waste Management, U.S. Department of Energy, Washington, D.C.

_____, 1993a. *B Plant Source Aggregate Area Management Study Report*, DOE/RL-92-05, Rev. 0, U.S. Department of Energy, Richland, Washington.

U.S. Department of Energy (DOE), 1993b. *Phase I Remedial Investigation Report for 200-BP-1 Operable Unit*, Vols. 1 and 2, DOE/RL-92-70, Rev. 0, prepared by Westinghouse Hanford Company for the U.S. Department of Energy, Richland Operations Office, Richland, Washington.

_____, 1998. Report to Congress, *Treatment and Immobilization of Hanford Radioactive Tank Waste*, U.S. Department of Energy, July.

_____, 2000. *200-TW-1 Scavenged Waste Group Operable Unit and 200-TW-2 Tank Waste Group Operable Unit RI/FS Work Plan*, DOE/RL-2000-38, Draft A, Richland Operations Office, Richland, Washington.

_____, 2001a. *Hanford Geophysical Logging Project, High Resolution Passive Spectral Gamma-Ray Logging Procedures*, MAC-HGLP 1.6.5, Rev. 0, prepared by MACTEC-ERS, Grand Junction Office, Grand Junction, Colorado.

_____, 2001b. *Hanford Geophysical Logging Project, Project Management Plan*, MAC-HGLP 1.6.2, Rev. 0, prepared by MACTEC-ERS, Grand Junction Office, Grand Junction, Colorado.

_____, 2001c. *Hanford 200 Areas Spectral Gamma Vadose Zone Characterization Project, Hanford 200 Areas Vadose Zone Characterization Plan*, MAC-HGLP 1.7.1, Rev. 0, Grand Junction Office, Grand Junction, Colorado.

_____, 2002a. *Hanford 200 Areas Spectral Gamma Vadose Zone Characterization Project*, Project Documents Online: <http://www.gjo.doe.gov/programs/hanf/htfvz.html>

_____, 2002b. *Hanford Geophysical Logging Project, Data Analysis Manual*, GJO-HGLP 1.6.3, Rev. 0, Grand Junction Office, Grand Junction, Colorado.

Williams, B.A., B.N. Bjornstad, R. Schalla, W.D. Webber, 2000. *Revised Hydrogeology for the Suprabasalt Aquifer System, 200-East Area and Vicinity, Hanford Site, Washington*, PNNL-12261, Pacific Northwest National Laboratory, Richland, Washington.

Wilson, R.D., 1997. *Hanford Tank Farms Vadose Zone, Spectrum Shape-Analysis Techniques Applied to the Hanford Tank Farms Spectral Gamma Logs*, GJO-96-13-TAR, GJO-HAN-7, prepared by MACTEC-ERS for the Grand Junction Office, Grand Junction, Colorado, May.

Wood, M.I. (Fluor Hanford, Inc.), T.E. Jones (CH2M Hill Hanford Group, Inc.), R. Schalla, B.N. Bjornstad, S.M. Narbutovskih (PNNL), 2000. *Subsurface Conditions Description of the B- BX-BY Waste Management Area*, HNF-5507, CH2M Hill Hanford Group, Inc., Richland, Washington.

Appendix A
Spectral Gamma-Ray Logs for Boreholes and Wells
in the Vicinity of the 216-B-5 Injection Well, 216-B-9 Crib
& Tile Field, and Adjacent Waste Sites

(included on accompanying CD-ROM)

Appendix B
Spreadsheet Listing Boreholes and Wells Used in this Study of the
216-B-5 Injection Well, 216-B-9 Crib & Tile Field, and Adjacent
Waste Sites and Log Depths of the Main Geologic Units Identified
on the Spectral Gamma-Ray Logs

Table B-1. Spreadsheet Listing of Boreholes and Wells Used in this study of the 216-B-5 Injection Well, 216-B-9 Crib and Tile Field, and Adjacent Waste Sites and Log Depths of the Main Geologic Units Identified on the Spectral Gamma-Ray Logs

Well Name	Reference Elevation	Stickup	H2	H3	H3 Silt	Ringold A	Top of Basalt	Total Depth
299-E28-1	688.5	2.8	17	223	244	267	NR ¹	325.0
299-E28-10	681.0	1.9	17	216	245	284 est ²	313	325.0
299-E28-14	698.0	2.9	30	227	NP ³	277 est	351 est	352.0
299-E28-2	684.2	1.7	20	209	246	284	324	325.0
299-E28-23	689.5	1.33	44	213	251	286 est	NR	331.0
299-E28-24	689.6	1.75	44	213	NP	287 est	NR	329.0
299-E28-25	689.1	1.42	27	213	253	286 est	330	331.0
299-E28-3	696.2	1.7	32	200	242	282	335 est	327.0
299-E28-5	676.5	2.3	17	223	243	275	307	327.0
299-E28-53	686.3	2.5	?	NR				152.0
299-E28-54	686.2	2.5	24	NR				150.0
299-E28-55	685.9	2.5	24 est	NR				150.0
299-E28-56	682.8	2	22	NR				150.0
299-E28-57	683.5	1.9	22.5	NR				150.0
299-E28-58	681.6	2.5	21.5	NR				150.0
299-E28-59	682.3	2.1	23	NR				150.0
299-E28-60	680.7	0.8	23	NR				150.0
299-E28-61	685.9	2.5	23	NR				150.0
299-E28-62	683.9	1.9	NR					9.0
299-E28-67	683.5	2.5	NR					13.1
299-E28-68	682.9	2.3	NR					13.1
299-E28-7	690.0	2.1	26	218	NP	282	333	342.0
299-E28-73	689.0	0	32	NR				40.0
299-E28-74	689.4	0	32	NR				40.0
299-E28-50	680.4	1.9	NR					13.1

¹ Not reached

² Estimate

³ Not present